Tailor-made antioxidative nanocrystals: production and in vitro efficacy

Inaugural-Dissertation

to obtain the academic degree

Doctor rerum naturalium (Dr. rer. nat.)

submitted to the Department of Biology, Chemistry and Pharmacy

of Freie Universität Berlin

by

Run Chen

from Hunan, China

July 2013

The enclosed doctoral research work was performed during the period from October 2010 to July 2013 under the supervision of Prof. Dr. Cornelia M. Keck and co-supervision of Prof. Dr. Rainer H. Müller in the Institute of Pharmacy, Freie Universität Berlin, Department of Pharmaceutical Technology, Biopharmaceutics & NutriCosmetics.

1st reviewer: Prof. Dr. Rainer H. Müller

2nd reviewer: Prof. Dr. Cornelia M. Keck

Date of defence: 28. August 2013

To my parents and my wife

Table of contents

1. Introduction

(partly submitted to *Household and Personal Care today - H&PC today, 2013)*

1.1. Introduction: delivery problems in dermal application

Poorly soluble plant actives such as resveratrol, rutin, apigenin etc. are of high interest for delivery to the skin in consumer care and cosmetics, but their penetration into the skin is very low (Kitagawa, Tanaka et al. 2009). Therefore they have no sufficient dermal "bioactivity". The problem is that these molecules are poorly soluble in water and simultaneously in oils. Therefore – in contrast to e.g. coenzyme Q10 – they cannot be dissolved in the oil phase of dermal creams. Application of a suspension of powdered active in a gel or the water phase of a lotion does not solve the problem. The saturation solubility Cs is too low, this results in a very low concentration gradient between dermal formulation as "donor compartment" and the skin as "acceptor compartment" (Fig. 1 - 1 upper). The present regulatory trend is requiring more and more proofs of dermal effects, to substantiate claims for a dermal product. Therefore it is not sufficient anymore just to admix an active to a product, it should be added in a technical form that it develops sufficient dermal bioactivity in the skin. Therefore smart delivery systems to make problematic actives in the skin are an increasing demand of the industry.

A meanwhile "old" delivery system are the liposomes which can incorporate lipid soluble actives in their phospholipid double layer, but they are not suitable for actives poorly soluble in water and simultaneously in lipids. A popular approach was for some time to use polymeric micro- or nanoparticles to incorporate these actives by using organic solvents in the production process. The polymer particle powders or aqueous suspensions can be admixed easily to a dermal product. However incorporation of a poorly soluble active even worsens the situation. The poorly water soluble actives is firmly encaged in the polymer matrix, diffusion through the water phase into the skin is even retarded compared with the naked crystals of actives (e.g. mi-

cronized active) (Fig. 1 - 1 lower). A delivery technology is clearly required which enhances the solubility of actives.

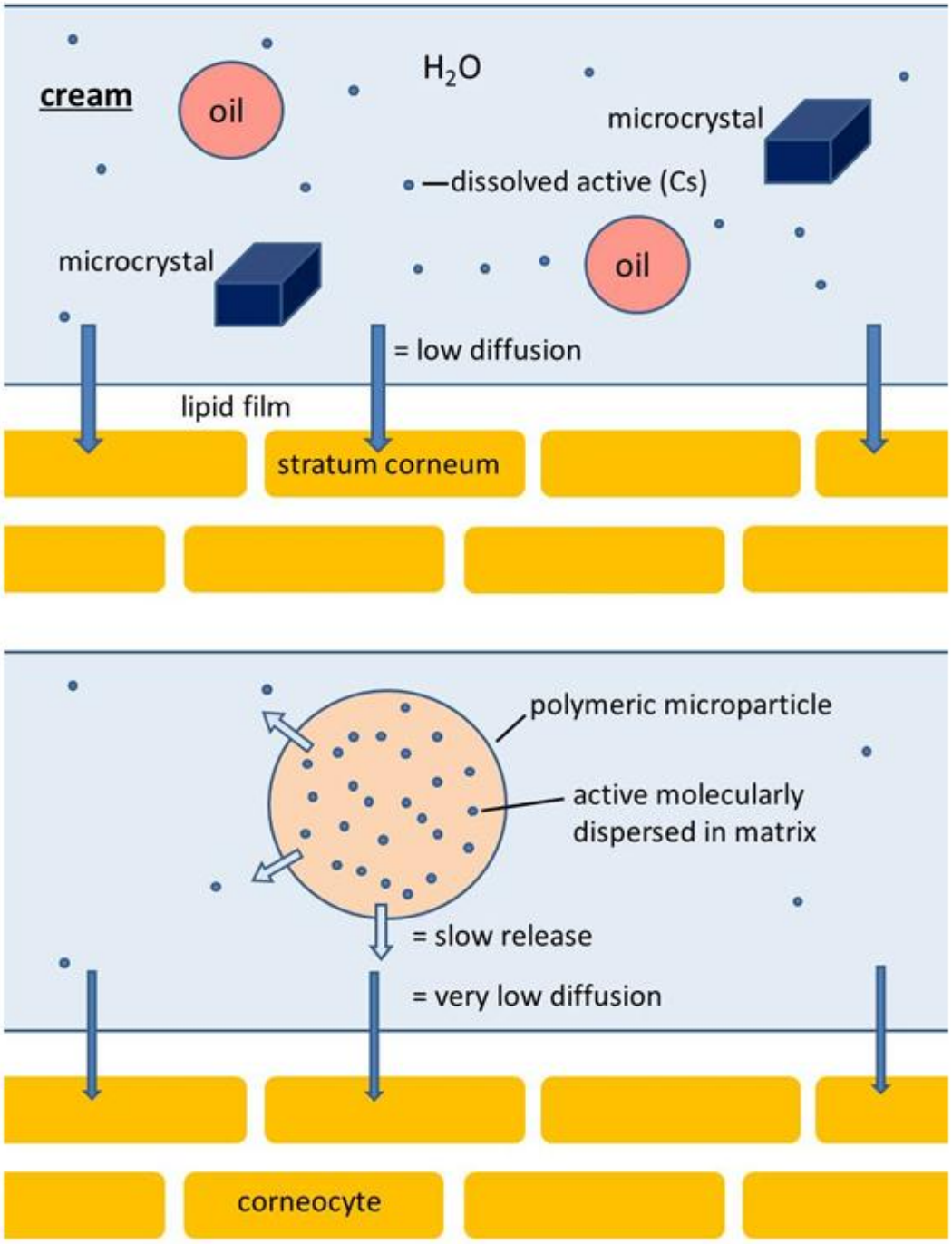

Figure 1 - 1 Microcrystals of a poorly soluble active have a low solubility Cs, thus a low concentration gradient to skin and low diffusion into skin (upper). Incorporation into a polymer matrix encloses the active like in a safe for money, thus even reducing skin penetration (lower) (submitted to *Household and Personal Care today - H&PC today*, 2013)

Solubility enhancing technologies are solubilization in micelles or cyclodextrins (CDs). However many of the current actives do not have a sufficient solubilization ability, and do not fit into the space of the CDs. In addition the problem occurs, that actives are firmly incorporated in micelles (gold fish test by G. Levy 1965) or not released from CDs (too high binding constant). A delivery technology would be ideal which creates an active diffusion pressure into the skin, and provides fast new dissolved molecules from a depot, which replaces the molecules in the dermal formulation which are penetrated into the skin. Such a delivery technology is crystals below about 1 µm in size, the submicroncrystal and the nanocrystals.

1.2. Submicroncrystals & nanocrystals - definitions & properties

"Micronized powders" are technically employed to increase the dissolution velocity of actives. They possess a mean diameter roughly about 5 µm, with a size distribution ranging up to 10/20 µm. The increased dissolution velocity is due to the larger surface area compared to powders of "normal" size (rather 50-100 µm mean diameter). However these powders show no increased "saturation solubility" Cs!

Physicochemical properties change when reducing the size of materials below 1 µm (= 1000 nm), which means generating crystals with a mean size > 100 nm to < 1000 nm (= "submicroncrystals") or "nanocrystals" being 100 nm or below (≤ 100 nm). The saturation solubility Cs increases exponentially with decreasing size. This kinetic saturation solubility $Cs_{kinetic}$ can be 10-100 times higher than the thermodynamic saturation solubility $Cs_{thermodynamic}$. A supersaturated system is generated. In addition the dissolution velocity dc/dt increases as well, due to the further increase in surface area A and in addition to the increase in Cs (dc/dt proportional A and Cs, Noyes-Whitney equation (Noyes and Whitney 1897). An additional benefit for dermal delivery is the increased adhesion of such fine-sized materials to surfaces in general; the skin is such

a surface. In summary the beneficial properties for dermal delivery of poorly soluble actives are:

1. increased saturation solubility,

2. increased dissolution velocity,

3. increased adhesiveness to skin.

Both crystal types are in the nanometer range, however according to the regulations of the European Union (European Union 2011) and the US Food & Drug Administration (FDA) (U.S. Food and Drug Administration 2011) only the crystals ≤ 100 nm are nanoproducts. In the future consumer care and cosmetic products containing these nanocrystals need to be clearly labeled as nanoproducts. However, many companies do not want to have products to be labeled with "nano", because in the public perception there is increasing concern about potential "nanotoxicity" (Müller, Gohla et al. 2011). The solution is the use of submicroncrystals. Due to their size below 1 µm they have still the benefit of improved physicochemical properties, without being nanoparticles according to the regulations. They have a high safety profile, because they belong to the well tolerated class ("green light") of the nanotoxicological classification system (NCS) (Keck, Kobierski et al. 2012; Keck and Müller 2013). The NCS classifies materials in the physical size dimension of the nanometer range (1 nm to 1000 nm), i.e. submicronparticles (< 100 nm to < 1000 nm, class I (= green) and class II) and nanoparticles (≤ 100 nm, class III and IV (= red)). However, generally in pharmaceutical field, based on the size unit drug nanocrystals which have size below 1000 nm can all be regarded as nanocrystals (Junghanns and Müller 2008) as the other parts in this thesis used.

1.3. Overview of production methods of submicroncrystals & nanocrystals

Many kinds of technologies have been developed in these years to produce drug submicroncrystals/nanocrystals. Most of them can be divided into three groups: bottom-up technologies, top-down technologies, and the combinational technologies. Bottom-up technologies can be basically described as "via humida paratum", which construct nanocrystals by precipitation and controlled crystal growth, from dissolved molecules to nanoparticles. The brief process can be concluded as dissolving drug in a solvent and extracting the solvent by an anti-solvent after proper emulsification. The solvent and anti-solvent of targeted drug have to be miscible with each other. Precipitation is a cost-effective approach and requires only low-cost equipment. However, it also involves some problems, e.g. residual of organic solvents, difficulty to scale up and the possible change of the crystalline state during storage, which make bottom-up technologies not very applicable (Lindfors, Skantze et al. 2006).

Recently, the most frequently used methods for producing nanocrystals are top-down technologies which mainly include wet bead milling (WBM) and high pressure homogenization (HPH). At present all nanocrystals products on the market are produced by these top-down technologies. The milling chamber of WBM equipment holds beads, drug and stabilizer-contained dispersing medium all together. When the beads are moving, the generated shear force and the collision between beads can break drug particles into nano-dimension. The process is efficient. However, it also involves some disadvantages. WBM is a low energy process and thus requires long production time. Hazards are the erosion of the pearl during milling and the microbial contamination by the beads that might impair the product quality. A large problem is always the separation of the beads from the final product and the scale up (Merisko-Liversidge, Liversidge et al. 2003).

HPH is a high energy inputting process which can be applied by two kinds of equipment: microfluidizers and piston-gap homogenizers. Microfluidization uses pressure to generate a jet stream with ultra-high speed to pass through a "Y" or "Z" interaction chamber, the collision and shear forces break particles into the nano-dimension (Müller and Akkar 2004). Piston-gap homogenization uses pressure to force a suspension to pass through a tiny gap thus to obtain extremely high speed there. According to the law of Bernoulli, the high speed flow will have corresponding low static pressure in a closed system. When it decreases to below the vapor pressure of the liquid, bubbles are generated in the gap. After the liquid passed through the gap, the speed and static pressure return to normal, thus the bubbles implode and bring intensive shock waves in a local area, namely cavitation (Keck and Müller 2006), then the generated force can break particles.

Combinational technologies comprise a pre-treatment followed by a high energy step which can be not only HPH. The nanocrystals produced by combinational technologies also can be called the second generation nanocrystals (Müller and Keck 2008). Compared to the traditional nanocrystals (first generation nanocrystals), the second generation of nanocrystals is produced either by combinational technologies including a pre-treatment step and a subsequent high energy input step (e.g. HPH) (Müller, Becker et al. 1999), or using different types of dispersing medium. Many advantages were shown for the second generation of nanocrystals. Examples are a faster production (H42 technology) (Möschwitzer and Müller 2006), smaller nanocrystals (H96 technology, H69 technology) (Kipp, Wong et al. 2006; Möschwitzer and Lemke 2008) improved physical stability (CT technology) (Petersen 2008) or a faster way to formulate final products (Nanopure® technology) (Krause, Mäder et al. 2001).

Among the combinational technologies of the second generation of nanocrystals, only the CT technology (Al Shaal, Müller et al. 2010) is a combinational technology of two top-down approaches, e.g. WBM followed by HPH. All other approaches, i.e. H42,

H96 and H69, are the combinations of a top-down and a bottom-up process (Müller, Becker et al. 1999; Möschwitzer and Lemke 2008; Müller, Shegokar et al. 2011).

Because the WBM in CT possesses some disadvantages, e.g. long running time, difficulty in separation of beads and samples, introduction of impurities and macrobiotics a method to overcome these flaws is desired. In that sense, to avoid the disadvantage of WBM, the exchange of the WBM pre-treatment step by another pre-treatment might be sensible.

An alternative pre-treatment step to WBM might be high speed stirring using rotor/stator systems. High speed stirring (e.g. the use of Ultra Turrax systems) is a common method for the dispersion of powders or the production of emulsions (Ayoub, Ahmed et al. 2011; Gao, Ren et al. 2013). The advantages are e.g. large batch volume and high shear force and no separation step, when compared to WBM. Moreover, high speed stirring is a fast and cost efficient process with a simple and fast cleaning step (Kohler, Santana et al. 2010). However, typically the shear forces created are not high enough to break crystals down to the smaller micrometer or nanometer range. Thus, typically high speed stirring is only used to disperse powder into a liquid, i.e. to destroy agglomerates and to diminish large particles (Scalia, Salama et al. 2012) and required further step to break the intact particles. In 2011 a new combinational technology – ARTcrystals (Keck 2011), which is also a part of the thesis, introduced a high speed stirrer system (http://www.miccra.com) with improved rotor/stator geometry and thus improved shear forces followed by low energy high pressure homogenization.

1.4. The commercial use of submicroncrystals & nanocrystals

Based on those technologies, the properties of crystals below 1000 nm were first exploited to improve the oral delivery of poorly soluble drugs. In the year 2000 the first pharmaceutical product Rapamune was introduced to the market (Junghanns and Müller 2008). Leading technology in pharma is the NanoCrystals™ by the company ALZA in the USA (previously Nanosystems/Elan). The competitive product was nanosized crystals by SkyePharma PLC (UK), the DissoCubes®. These two are considered as the first generation technology, the crystals are produced by wet bead milling or by high pressure homogenization, respectively (Müller, Böhm et al. 1999; Müller, Böhm et al. 1999; Merisko-Liversidge, Liversidge et al. 2003).

The above mentioned second generation is the smartCrystal® technology, developed by the company PharmaSol Berlin. This technology covers various processes to tailor-make differently sized crystals, both submicron- and nanocrystals (≤ 100 nm), for details (Möschwitzer and Müller 2006; Möschwitzer and Müller 2006; Möschwitzer and Lemke 2008). The pharmaceutical rights belong still to the US company Abbvie (previously Abbott), the rights for non-pharma including dermal application to PharmaSol. The smartCrystals are the first ones - and are by now the only ones - applied dermally, i.e.in cosmetic products. For reasons of differentiation to the crystals specific for other application routes, the term smartCrystal is used for the dermal application. In addition, they are especially produced providing optimized performance in dermal product using a combination of bead milling and a subsequent step of HPH (Petersen 2008).

1.5. Incorporation into dermal products

smartCrystals are contained in the aqueous phase of dermal consumer care and cosmetic products, e.g. water of gels and water phase of o/w creams and lotions. Incorporation is very easy. Nanocrystals concentrates are available on the market and can be simply admixed to dermal formulations. The dermal formulation is produced with slightly reduced water content, e.g. 2% of total formulation. Then the smartCrystal concentrate is admixed at room temperature by slight stirring. In general, the concentrates are diluted by a factor up to 50 (e.g. 2 g concentrate + 98 g cream).

Concentrates are provided by the company Dr. Rimpler GmbH in Wedemark/Germany, examples of actives are rutin (INCI: Rutin Submicron Crystals) and hesperidin (INCI: smartCrystal-lemon extract). They contain 5% active, diluted by a factor 50 this results in a product concentration of 0.1%. Typically it is recommended to have a concentration in the product being a multiple (e.g. 5-10 x) of the saturation solubility to ensure a sufficient nanocrystal depot. Other actives are available on request, development of company specific exclusive actives is also possible on request.

1.6. Mechanism of action on the skin

Some dermal carriers claim to deliver actives by penetration of the carriers into the skin, e.g. transfersomes (Cevc 1996), or carriers having a very small size (<< 50 nm) to promote penetration of active, e.g. polymeric dendrimer nanoparticles (Haag, Sunder et al. 2000). Problems are that carrier penetration is very limited (= limitedly effective), and small particles as “nano” might become less accepted by the consumer in future. These problems are clearly circumvented by the smartCrystals. They deliver actives to the skin solely by simple physical principles. And physics is reproducible, thus it is a reliable delivery system.

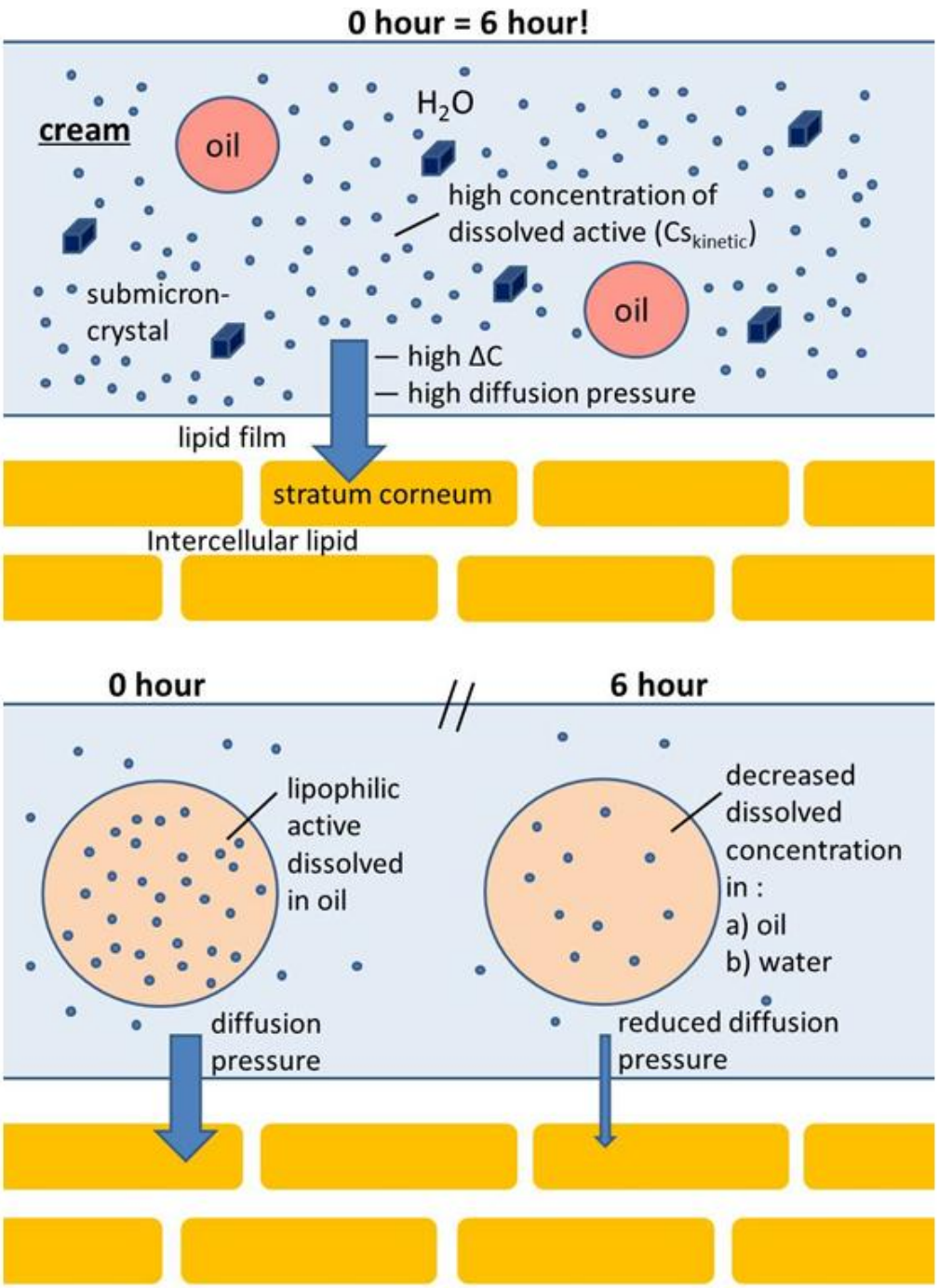

Figure 1 - 2 Principle of action of smartCrystals in a cream via supersaturation $Cs_{kinetic}$, increased diffusion gradient ΔC and nanocrystal depot, providing constant zero order flow (upper) versus low concentration gradient and decreasing 1st order diffusion into skin from a solution formulation (lower) (submitted to *Household and Personal Care today - H&PC today*, 2013)

The smartCrystals are dispersed in the water phase of an o/w emulsion, in the water phase they create a supersaturation. The water phase contains dissolved molecules and

in addition nanocrystals as depot. The kinetic saturation solubility $Cs_{kinetic}$ is a multiple higher than the thermodynamic solubility, thus a higher concentration gradient is generated. This increases the diffusive flow of the lipophilic actives into the skin (Fig. 1 - 2, upper). Molecules diffused into the skin are immediately replaced in the water phase by molecules dissolving from the nanocrystals acting as depot. This ensures a constant flow of zero order kinetic. In dermal formulations with only dissolved active, only a flow of first order kinetics occurs (formulation is getting depleted from active, flow assumed as rate-controlling factor (Fig. 1 - 2, lower).

1.7. Neuroprotective effect

Many publications have described the neuroprotective effect of flavonoids (Bei, Zang et al. 2009; Gopinath, Prakash et al. 2011; Abbasi, Nassiri-Asl et al. 2012; Dajas, Andres et al. 2013). This effect is mainly attributed to the antioxidative and anti-inflammatory effect. The compounds having the structure of flavone and flavonol possess the ability to scavenge the free radicals and chelate the metal ions (Dajas, Andres et al. 2013). In addition, they can modulate the activities of enzymes to keep the homeostasis to fight against the neurodegeneration. The anti-inflammatory effect, on the other hand, can directly level up the survival of the neurons.

Although the potent compounds are so promising, the poor solubility is the hurdle to utilize them in practice. As the BCS II drugs, the compounds are difficult to exist molecularly in the therapeutic site which is full of aqueous solution. They can be dissolved in some organic solvents, but the neurons are so sensible that they cannot bear any toxicity from the solvent. Delivering the compounds efficiently is a tough task for pharmaceutical research. Nanocrystals provide a reasonable solution. Not only the increased concentration in aqueous solution, but also the potential direct endocytosis due to the small size of the nanocrystals (Fig. 1 - 3) can contribute to the delivery.

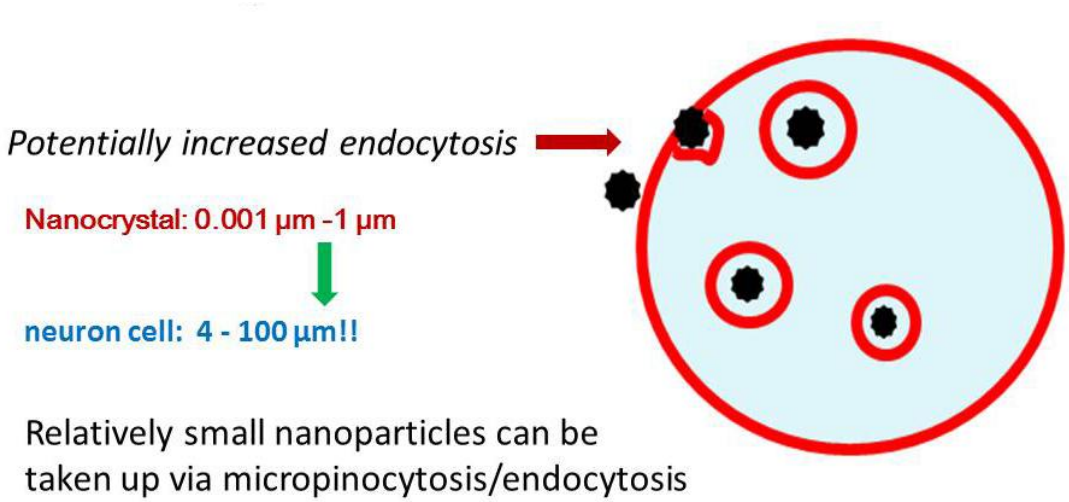

Figure 1 - 3 Endocytosis of neuron cell to nanocrystals

Owning to the delightful property of nanocrystals, the better in vivo efficacy can be expected as proven (Wang, Sun et al. 2009). However, the particles size as an important factor has not been detailed investigated yet. Theoretically, although all of the particles are smaller than 1 µm, different size may have different performance. Smaller size shall have better absorption because of the further increased solubility and endocytosis. What should be noticed is that API with smaller particle size may also need to be more precisely controlled in dosage form since the variation of a dosage form may cause more significant change in the therapy.

1.8. In vitro and in vivo performance

Primarily data were collected from compounds with antioxidant activity. e.g. rutin, hesperidin and hesperetin, but in principle the observed increased penetration into the skin and increased bioactivity apply to all poorly soluble actives, cosmetic and pharmaceutical ones. Then anti-oxidative capacity was analyzed in vitro in cell cultures, investigating submicron-sized smartCrystals of decreasing size. The antioxidant effect increased with decreasing size (Fig. 1 - 4). Interestingly it was found that too high concentrations were cell damaging, i.e. it is important to select the appropriate dose (hormesis effect).

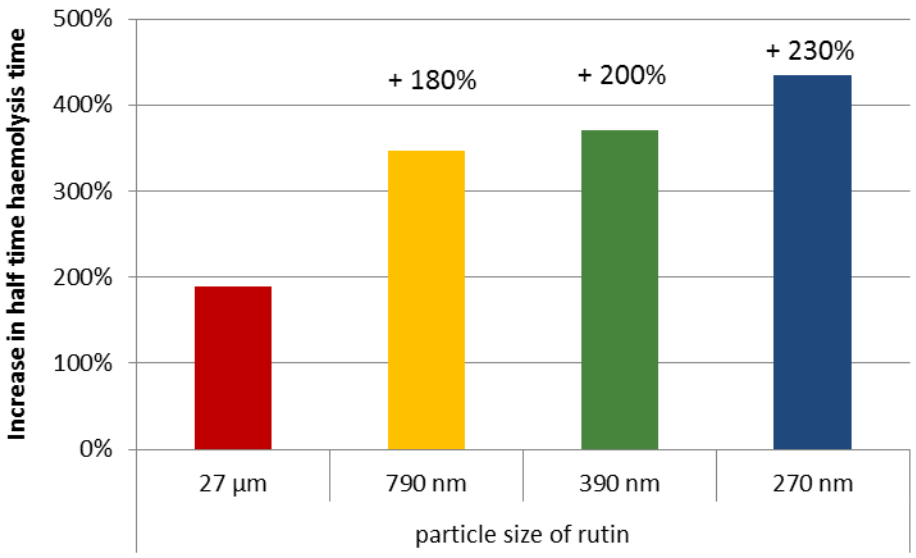

Figure 1 - 4 Antioxidative capacity (AOC) of rutin smartCrystals of decreasing size, measured in red blood cells using the KRL Test (submitted to *Household and Personal Care today - H&PC today*, 2013)

In vitro dermal effects were studied in human. Instead analyzing the penetrated concentration, the biological effect was measured being the much more relevant than concentration data in skin layers. To assess the antioxidative effect in the skin, the increase in the sun protection factor (SPF) was measured after exposure of untreated and smartCrystals treated human skin to UV irradiation. For this study, the poorly soluble rutin was made water-soluble by chemical coupling of a glucose molecule. Dermal formulations were investigated containing 5% of the water soluble rutin derivative and alternatively 0.001% rutin dissolved from a smartCrystals depot. Despite the 1/500 concentration, the rutin smartCrystals formulation lead to a 2 x increase in SPF compared to the formulation with the water soluble rutin derivative (Petersen 2008) (Fig. 1 - 5). Based on this data, the smartCrystals technology acts as a "bio-booster" for poorly soluble actives.

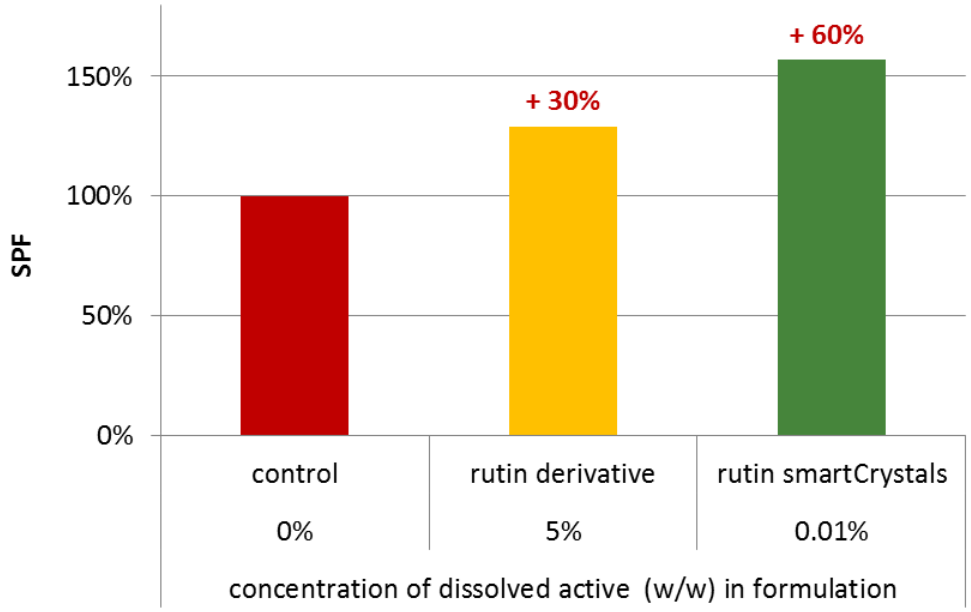

Figure 1 - 5 Human study: Increase in the SPF on skin after application of a dermal formulation with water-soluble rutin-glucoside compared to a formulation with 0.01% dissolved rutin from a smartCrystal depot (after (Müller, Keck et al. 2008))

The increase in bioactivity is explained by four effects:

1. Increased diffusion pressure into skin due to increased concentration gradient ΔC;

2. Fast dissolution velocity from nanocrystal depot (= considered as rate limiting step for absorption);

3. Better skin penetration of the more lipophilic original molecule rutin than the water-soluble, highly hydrophilic rutin derivative (likes to stay in hydrophilic environment of dermal formulation than going into more hydrophobic skin);

4. Higher affinity of the lipophilic rutin to the relevant cell compartments.

Apart from the anti-oxidant effect, providing ultraviolet (UV) protection and reducing UV-related aging signs, the appearance of the skin is important, i.e. number and depth of wrinkles and skin complexion. The eye lifting serum by IPAM (cf. below), con-

taining apart from rutin smartCrystals® also Argireline® and Eyeseryl®, was investigated in a human study. The increase in skin roughness was investigated by laser profilometry using a PRIMOS system (GF Messtechnik GmbH, Teltow, Germany). The regular application of the test product decreased significantly the skin roughness, having statistically proven a positive correlation ($r > 0.8$) with the applied dose (Sinambela, Löffler et al. 2013). Skin complexion was analyzed using a VISIA Complexion Analysis system (Canfield Imaging Systems, Fairfield, New Jersey). Analysis of melanin related brown spots was performed before treatment and after 4 and 8 weeks of application of the product. Melanin formation is one of the aging signs. 4 weeks of treatment were enough to obtain a suppressive effect of rutin on the melanin production. The brown spots were reduced due to the antioxidant activity of rutin (Sinambela, Löffler et al. 2012).

1.9. First commercial products

The first commercial products with "rutin submicron" were JUVEDICAL Age-decoder Face Cream and JUVEDICAL Age-decoder Face Fluid, introduced to the market in 2007. In 2009 la prairie introduced platinum rare containing smartCrystal-Lemon Extract, platinum rare being one of the expensive exclusive high-end cosmetic products (50 ml about 1000 € = US$ 1,400). The next products with rutin submicron were within the line "Edelweiss" the "Wrinkle Fighter" (company Audorasan/Germany, http://www.audorasan.de/) and within the line "ageLine® wo/man one" the product "eye lifting serum" (Institute for Preventive and Aesthetic Medicine - IPAM Germany, http://www.ipam.eu/). In the INCI nomenclature on the product packaging, the smartCrystals INCI names can be used, alternatively the ingredients of the smartCrystals concentrates be listed e.g. in case of smartCrystal-Lemon Extract the three ingredients hesperidin as active, Poloxamer 188 as stabilizer of the suspension, Euxyl® PE 9010 as preservative and glycerol.

1.10. Summary

The submicron crystals (smartCrystals) are a formulation solution for poorly soluble consumer care and cosmetic actives. They are based on simple, but very effective physical principles of increase in kinetic saturation solubility (stable supersaturation), increased diffusion pressure into skin and fast dissolution from a crystal depot in the dermal formulation. No "fancy" unrealistic penetration of carriers themselves into the skin is required. Skin "penetration", which can even appear frightening to consumers, is avoided.

The crystals are in the nanometer range, and fully benefit from the optimized physico-chemical properties of the nanodimension. However, they are above the magic threshold of 100 nm, i.e. they do not need to be regulatorily labeled as nano products. This is important for the public perception, which potentially might turn negative about nano in the future. In addition, they are safe as indicated by their classification into the "green" class I of the nanotoxicological classification system (NCS).

The technology can be considered as "universal", because any active can be reduced in size to the submicron range. It opens the perspective to introduce new molecule classes to the market, because molecules can be made active, which were not active before, e.g. as micronized powders. This leads to new dermal products. The technology can be applied to purified compounds, but also to complex composed plant extracts! And very important: the pre-requisite for market products is fulfilled: commercial suppliers are available providing cosmetic actives from the shelf (e.g. rutin, hesperidin, apigenin, resveratrol etc.), but also customer specific tailor-made actives on request.

Except this, in pharmaceutical research, nanocrystals still can be regarded as the drug crystals smaller than 1000 nm. Expect the dermal application, the nanocrystals of flavonoids can be also expected as promising in treatment of neurologic diseases. The

good AOC of the APIs can be enhanced by the form of nanocrystals and utilized in improving the defected nervous system.

2. Aims of thesis

As introduced above, flavonoids have potent antioxidative effect. Many publications have proven that by processing them into nanocrystals, the increased bioavailability can be expected. However, there are still many works to do: establishment of a guideline to produce nanocrystals with expected size, proof of the size influence on the in vitro performance of nanocrystals, improvement of the production process, industrialization of the production of nanocrystals and further evidence of the superiority of nanocrystals in AOC. Therefore, to develop the production process and to find the new application of the nanocrystals are the general targets of the thesis.

The aims of the thesis include:

The first aim: Understanding the influencing factors in more depth for production of flavonoid nanocrystals using high pressure homogenization.

Intensive research about preparing drug nanocrystals by HPH has been reported concerning different drugs and stabilizers. Smaller size is always preferable because it can bring higher solubility and size tunability. To realize this aim, four structurally similar flavonoids were chosen as candidates, using piston-gap homogenization as preparation method, to find which factors can influence the final size of nanocrystals, to investigate how they work, and to summarize a general conception of their ability, thereby guide the production to obtain smaller size in an efficient way.

The second aim: Production of the tailor-made quercetin nanocrystals with different sizes and investigation of the influencing factors in in vitro cell culture test.

In theory, the solubility increases with the decrease of the size of nanocrystal, especially the nanocrystal smaller than 100 nm will exponentially increase the dissolution pressure and rate (Müller, Gohla et al. 2011). The more powerful properties brought by the smaller size would also bring the strengthened performance in vitro and in vivo, regardless positive or negative. However, the influence of the size has not been inves-

tigated. Actually, from the hypothesis, the performance in cell culture test could also be size-dependent, one reason is the increased solubility in cell culture medium, the other is the potential enhanced cellular uptake of ultrafine particles through endocytosis (Lu, Wu et al. 2009; He, Hu et al. 2010). However, compared to finding a method to produce the smallest nanocrystals, very few studies have been done to differentiate the nanocrystals with different sizes, and to investigate the performance in cell culture tests. Therefore, this aim is to produce tailor-made quercetin nanocrystals with a series of sizes, and to investigate the in vitro performance of the products in human neuroblastoma cells SH-SY5Y, with or without toxins.

The third aim: Establishment of a new method for the production of nanocrystals on industrial scale.

Technology innovation never ends. As the introduction part has referred, recently, the main groups of nanocrystals production technologies include bottom-up, top-down and combinational technologies. For industry, cost-control is always an important concern in production. How to produce the product with same quality but lower cost is one of the research directions in process development. This aim is to establish a new combinational method to produce nanocrystals in an industrially feasible and cost-effective way.

The fourth aim: Large scale production and reproducibility of nanocrystals for cosmetic use.

As a mature technology, smartCrystals can be used in large scale production. However, the reproducibility should also be taken into account for ensuring the identical quality, including the contents of materials and the size as the key factors of nanocrystals of different batches. This aim is to apply the smartCrystals technology to hesperidin nanocrystals production for cosmetic use and to investigate the reproducibility and the feasibility.

The fifth aim: Antioxidative capacity (AOC) test of the obtained hesperidin, rutin and quercetin nanocrystals.

Flavonoids have a very high antioxidative capacity, but the applications are limited because of the poor solubility. Applying them in the form of nanocrystals can enhance the solubility, thus the bioavailability. Size should be an essential factor because of the better solubility with smaller size. This aim is to test the AOC of hesperidin, rutin and quercetin nanocrystals and to compare themselves and with the respective bulk powder suspensions using a new measurement - the KRL Test, therefore to confirm the superiority of the nanocrystals.

3. Materials and methods

3.1. Materials

3.1.1. Active pharmaceutical ingredients

All of the used active pharmaceutical ingredients (APIs) belong to flavonoids which are a group of molecules having the same flavone backbone (2-phenyl-1,4-benzopyrone) in their chemical structure (Fig. 3 - 1). When a –OH group replaces the –H in 3C on the flavone backbone, it forms the structure of flavonol (Fig. 3 - 2) which is the backbone of another subgroup of flavonoids. Flavonoids from natural plants have been massively investigated these years and many functions have been discovered such as anti-inflammatory (Garcia-Lafuente, Guillamon et al. 2009; Verri, Vicentini et al. 2012), anti-oxidating (Bors and Saran 1987; Rice-Evans 2001; Heim, Tagliaferro et al. 2002), anti-aging (Yan, Wu et al. 2009), anti-cancer (Chowdhury, Sharma et al. 2002; Cragg and Newman 2005) and neuroprotective effect (Zhang, Cheang et al. 2011).

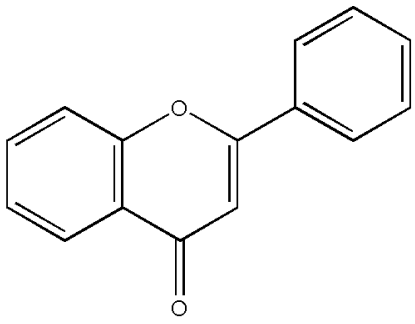

Figure 3 - 1 Molecular structure of the flavone backbone

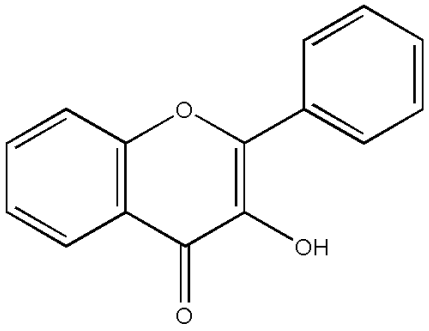

Figure 3 - 2 Molecular structure of the flavonol backbone

Since they possess so many merits that pharmaceutical, cosmetic and nutritional industry all devote much to try to utilize them in commercial products. However, most of them belong to the BCS (Biopharmaceutical classification system) class II, which contains poorly soluble and well permeable drugs. This situation hinders the application of them in final therapeutic use, which also makes them become the good candidates to use nanocrystals technology to increase the solubility, thus facilitate the practical usage.

3.1.1.1. Apigenin

Apigenin (Fig. 3 - 3), 5,7-dihydroxy-2-(4-hydroxyphenyl)-4H-1-benzopyran-4-one, has an –OH group at 5C, 7C and 4C' of flavone backbone. It commonly exists in the plants parsley and celery(Wang and Huang 2013).

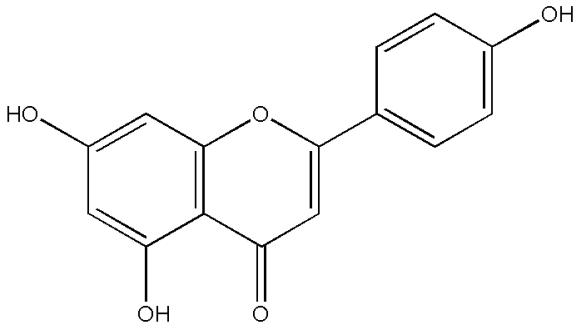

Figure 3 - 3 Molecular structure of apigenin

Apigenin powder was purchased from Exquim, S.A. (Spain) and used in the comparative study of different flavonoids in nanocrystals production.

3.1.1.2. Hesperetin

Hesperetin (Fig. 3 - 6),
(S)-2,3-dihydro-5,7-dihydroxy-2-(3-hydroxy-4-methoxyphenyl)-4H-1-benzopyran-4-one, has an –OH group at 5C, 7C, 5'C and a $–OCH_3$ group at 4'C of flavone backbone. It mainly exists in citrus fruits (Kanaze, Kokkalou et al. 2004)

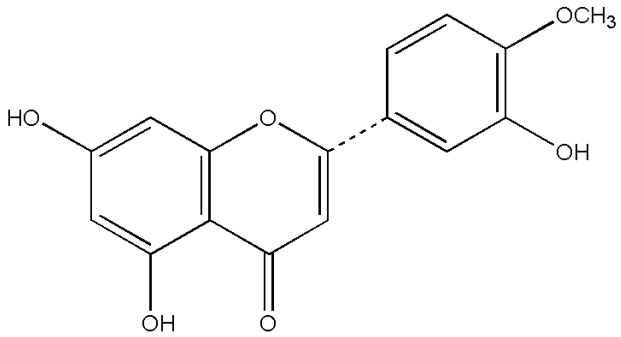

Figure 3 - 4 Molecular structure of hesperetin

Hesperetin powder was purchased from Exquim, S.A. (Spain) and used in the comparative study of different flavonoids in nanocrystals production.

3.1.1.3. Quercetin

Quercetin (Fig. 3 - 5),
2-(3,4-dihydroxyphenyl)-3,5,7-trihydroxy-4H-1-benzopyran-4-one, has a –OH group at 5C, 7C, 4'C and 5'C at the backbone of flavonol. It is one kind of flavonoids which have been proven as a potent antioxidant (Boots, Haenen et al. 2008; Zhang, Swarts et al. 2011). Quercetin is widely distributed in many fruits, vegetables, leaves and grains (Suhaj 2006).

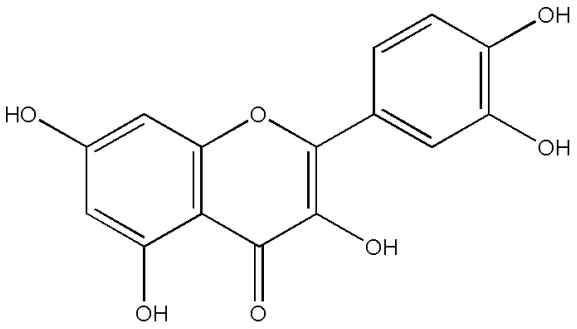

Figure 3 - 5 Molecular structure of quercetin

The quercetin bulk powder was purchased from Sigma–Aldrich Chemie GmbH (Germany), used in in the comparative study of different flavonoids in nanocrystals production and in neuroprotective study.

3.1.1.4. Rutin

Rutin (Fig. 3 - 6), 2-(3,4-dihydroxyphenyl)-5,7-dihydroxy-3-{[(2S,3R,4S,5S,6R)-3,4,5-trihydroxy-6-({[(2R,3R,4R,5R,6S)-3,4,5-trihydroxy-6-methyloxan-2-yl]oxy}methyl)oxan-2-yl]oxy}-4H-chromen-4-one, is also called quercetin-3-O-rutinoside which is the glycoside of quercetin in 3O position. It is also dispersed widely in citrus fruits (Davis 1947).

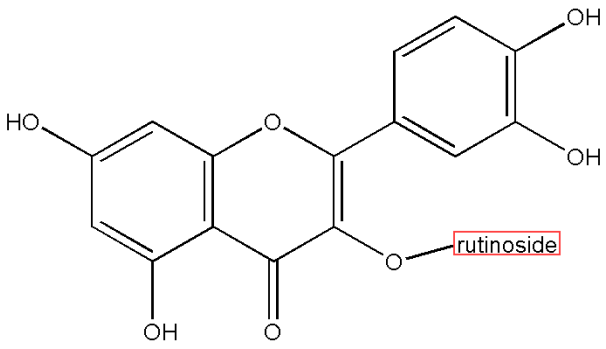

Figure 3 - 6 Molecular structure of quercetin

The rutin bulk powder was purchased from Exquim, S.A. (Spain), used in in the comparative study of different flavonoids in nanocrystals production and as the model drug to develop new production method.

3.1.1.5. Hesperidin

Hesperidin (Fig. 3 - 7), (2S)-5-hydroxy-2-(3-hydroxy-4-methoxyphenyl)-7-[(2S,3R,4S,5S,6R)-3,4,5-trihydroxy-6-[[(2R,3R,4R,5R,6S)-3,4,5-trihydroxy-6-methyloxan-2-yl]oxymethyl]oxan-2-yl]oxy-2,3-dihydrochromen-4-one, is a glycoside of hesperetin in 7O position. It is also abundant in citrus fruits (Kanaze, Gabrieli et al. 2003).

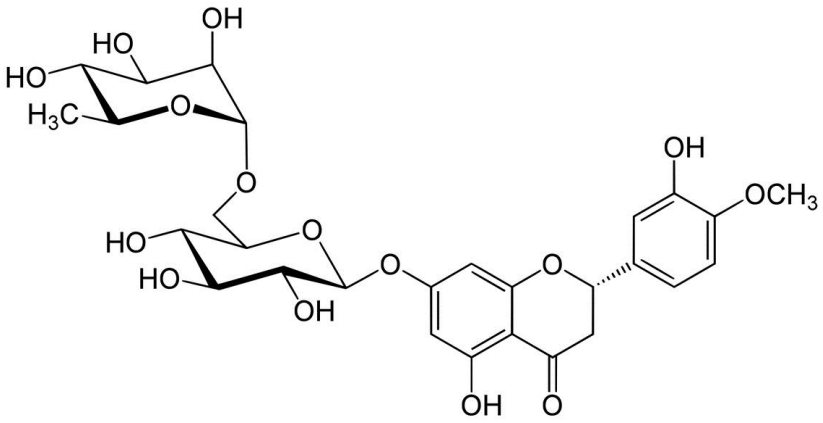

Figure 3 - 7 Molecular structure of hesperidin (from www.wikipedia.com)

Hesperidin was purchased from DENK Ingredients GmbH (Germany) and used in large scale production with smartCrystals technology to investigate the reproducibility.

3.1.2. Surfactants

Surfactants are essential for the stability of poorly soluble particles in aqueous medium. Normally used surfactants include ionic and non-ionic surfactants. The stabilizing effect of ionic surfactant is mainly attributed to the electrostatic repulsion based on

DLVO (Derjaguin, Landau, Verwey, Overbeek) theory (Rosen 2004), while the non-ionic surfactant functions by steric effect.

3.1.2.1. Plantacare® 2000 UP

Plantacare® 2000 UP was bestowed by BASF (Germany). UP means unpreserved. The INCI name is decyl glucoside. It appears as cloudy, viscous, aqueous solution of a C8-C16 fatty alcohol polyglycoside. It is a nonionic surfactant with excellent foaming capacity and good dermatological compatibility and may be monomeric or polymeric (Belsito, Hill et al. 2011).

3.1.2.2. Poloxamer 188

Poloxamer 188 (Kolliphor® P 188) was bestowed by BASF (Germany). It is a white, fine powder with melting point about 50 ℃. It is very soluble in water and alcohol with an average molecular weight from 7680 to 9510. It is also a non-ionic surfactant which is widely used in pharmaceutical products and regards as safe that can be used in injective applications. Poloxamer 188 was ordered as Kolliphor® P 188 from BASF AG (Germany)

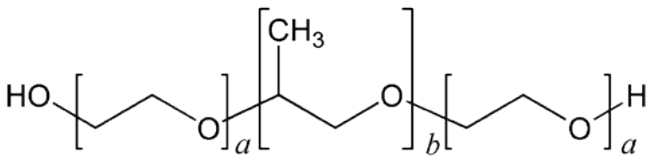

Figure 3 - 8 Chemical structure of Poloxamer 188 (a = 80, b = 27) (Rowe, Sheskey et al. 2009)

3.1.2.3. Tween® 80

Tween® 80 (Polysorbate 80) is a viscous, water-soluble yellow liquid. Low toxicity makes it very popular in food and pharm products as a non-ionic surfactant and it is

also permitted to be used in injectable preparations. Tween® 80 was purchased from AMRESCO LLC (USA).

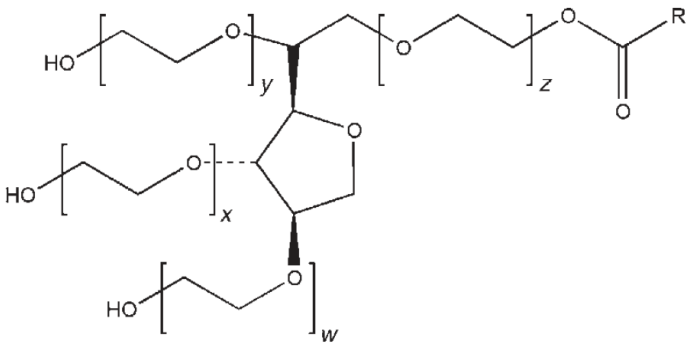

Figure 3 - 9 Chemical structure of Tween® 80 (w + x + y + z + w = 20, R = fatty acid) (Rowe, Sheskey et al. 2009)

3.1.2.4. Sodium dodecyl sulfate

Sodium dodecyl sulfate (SDS) was the only one used anionic surfactant in this thesis. It shows as white, fine powder. Some researcher argued that the combinational use of non-ionic and ionic surfactants could increase the stabilizing effect (Merisko-Liversidge, Liversidge et al. 2003). SDS was purchased from Fluka Chemie GmbH (Germany).

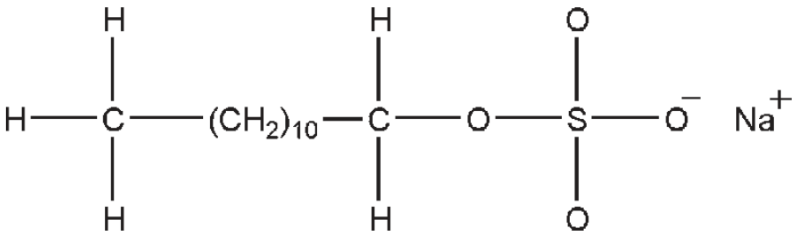

Figure 3 - 10 Chemical structure of sodium dodecyl sulfate (Rowe, Sheskey et al. 2009)

3.1.3. Reagents and tested substances in cell culture test

In cell culture test with human neuroblastoma cells SH-SY5Y, Dulbecco's Modified Eagle's Medium (DMEM), fetal bovine serum (FBS), phosphate buffered saline (PBS), Trypsin-EDTA were purchased from Biochrom AG (Germany). Toxins of 3-hydroxykynurenine (3-HK), 6-hydroxydopamine (6-OHDA), (±)salsolinol (SAL), were obtained from Sigma-Aldrich Co. LLC (USA).

3.1.4. Other materials

3.1.4.1. Cellulose acetate membrane

Cellulose acetate membrane with 0.2 μm pore size (sterile, individual, Minisart®) was purchase from Sartorius Stedim Biotech GmbH, Germany)

3.1.4.2. Dimethyl sulfoxide

Dimethyl sulfoxide (DMSO) was purchased from Merck KGaA (Germany). It was used in preparation of quercetin DMSO solution in cell culture test.

3.1.4.3. Glycerin 87%

Glycerin 87% (w/w) was purchased from LS Labor – Service GmbH (Germany). It was used as a penetrating agent and osmotic regulator in the study.

3.1.4.4. Preservative

Euxyl® PE9010, as the preservative for cosmetics, was bought from Schülke & Mayr GmbH (Germany) and used in the product from large scale production.

3.1.4.5. Water

Purified water produced by Milli-Q system from Millipore GmbH (Germany) was used during production. Sterile water for injection purchased from B. Braun Melsungen AG (Germany) was used in the preparation of the samples for in vitro cell culture test.

3.2. Methods

3.2.1. High speed rotor/stator shear force dispersion

High speed rotor/stator stirring is the main method to pre-treat the raw powder suspension. The bulk powder can be diminished by shear-force. In this thesis, the traditional method (low speed + open system) and the new method (high speed + closed system) were both used.

As the low speed and open system, an Ultra Turrax T25 (Janke and Kunkel GmbH, Germany) was used with 8000 rpm. The reason of using the relatively low speed rotary is to avoid the generation of foam due to the surfactants. Because the dispersion with Ultra Turrax T25 was conducted in a glass beaker, the speed also cannot be too high in case the instability of the beaker, thus breakage.

As the high speed and closed system, Miccra D-27 rotor/stator dispersion system (ART Prozess- & Labortechnik GmbH & Co. KG, Germany) was applied. It worked under a cooling system which made the sample temperature under 10 ℃ during the process. The stirring speed can achieve up to 36,000 rpm.

3.2.2. High pressure homogenization

In this thesis, two types of piston-gap homogenizers were used: APV Micron LAB 40 (APV Deutschland GmbH, Germany) on lab scale with discontinuous production in

40 ml batches and AVESTIN EmulsiFlex-C50 (Avestin, Canada) on large scale with continuous production in 18 kg batch. The principle of these two homogenizer is the same by propelling suspension to pass through a narrow gap, thus generate shock-waves to break particles (cf. 1.3). It is a high energy- and short time-consuming process.

3.2.3. Wet bead milling

In the following investigated combinational technology, a bead mill Bühler PML-2 (Bühler, Switzerland) was used as the main step to produce nanocrystals. In the 1050 ml milling chamber, 75% volume of Yttria stabilised zirkonia milling beads of size 0.4–0.6 mm (Hosokawa Alpine, Germany) were used as milling medium. Continuous mode with 2000 rpm of rotator speed and 10% of pump capacity was applied. During the production, the milling chamber was kept at 5 ℃. Under high speed stirring, a great number of small beads move fast, and conflict to each other to break particles between them. It is a low energy- and long time-consuming process.

3.2.4. Photon correlation spectroscopy

Photon correlation spectroscopy (PCS) or dynamic light scattering (DLS), is a technique used to measure the movement of particles (diffusion) by the Brownian motion of surrounding molecules and subsequent size distribution of an ensemble collection of particles in dispersion by detecting the changing scattering light intensity at different angles. A Zetasizer Nano ZS (Malvern Instruments, UK) with optimized measurement method mode and 25 ℃ environment temperature was applied in particle size characterization. Mean particle size of measured sample was given as z-average, which is an intensity-weighted mean diameter of the bulk population. Polydispersity index (PdI) calculated from a cumulants analysis of the DLS measured intensity autocorrelation function is used to describe the width of the particle size distribution.

3.2.5. Laser diffractometry

The PCS instrument was sensitive only in the 0.6 nm to 6 μm size range. For detecting larger particles in the sample, laser diffractometry (LD) was applied. Mastersizer 2000 (Malvern Instruments, UK) operating together with the Hydro S sample dispersion unit was utilized to conduct LD. Volume-weighted diameters including d(v)10%, d(v)50%, d(v)90%, d(v)95% and d(v)99% yielded by LD had been chosen as characterization parameters. d(v)10% value means 10% particles in tested samples are smaller than the given value, the same as the others. All parameters were analyzed using the Mie theory with respective optical parameters. The real refractive indices and imaginary indice of apigenin, hesperetin, hesperidin, quercetin, and rutin are 1.59 and 0.01 (Al Shaal, Müller et al. 2010), 1.59 and 0.01 (Mishra, Al Shaal et al. 2009), 1.57 and 0.01 (Petersen 2008), 1.59 and 0.01 (Kakran, Shegokar et al. 2012) (Kakran, Shegokar et al. 2012) and 1.593 and 0.01 (Keck 2010), respectively.

3.2.6. Optical microscopy

Optical microscopy (Ortophlan, Leitz, Germany) was performed to analyze the morphology of the particles, distinguish the different particles directly, with or without aggregation. Magnifications of 160-fold, which was for aggregation determination, and 1000-fold, which was for particles observation, were applied.

3.2.7. Zeta potential

The surface charge of particles can contribute as electrostatic force to the stability of nanosuspension system, which is also correlated with physicochemical properties of actives. Zeta potential (ZP) is a parameter of surface charges which is the charge value on the hydrodynamic shear surface of the particle. Zetasizer Nano ZS (Malvern Instruments, UK) was utilized to measure zeta potential under field

strength of 20 V/cm. Purified water with 50 μS/cm conductivity adjusted by 0.9% NaCl solution was used as dispersing medium for a fixed testing environment. The values of zeta potential were obtained by calculating electrophoretic mobility of the particles and using the Helmholtz–Smoluchowski equation which has already built in the Malvern Zetasizer software.

3.2.8. High performance liquid chromatography

HPLC system for hesperidin: KromaSystem 2000 (Kontron Instruments GmbH, Germany) with a solvent delivery pump equipped with a 20 μl loop and a rheodyne sample injector. Column: Eurospher 100-5 C18 (250 × 4 mm, 5 μm). Mobile phase: acetic buffer (pH 4.8) : acetonitrile = 75:25. Flow rate: 1 ml/min. Temperature: 25 ℃. UV Detector: a diode array detector (DAD-Kontron Instrument HPLC 540). Detect wavelength: 285 nm. Retention time: about 7 min.

HPLC system for quercetin: KromaSystem 2000 (Kontron Instruments GmbH, Germany) with a solvent delivery pump equipped with a 20 μl loop and a rheodyne sample injector. Column: Eurospher 100-5 C18 (250 × 4 mm, 5 μm). Mobile phase: K2HPO4 buffer : acetonitrile = 50:50. Flow rate: 0.5 ml/min. Temperature: 37 ℃. UV Detector: a diode array detector (DAD-Kontron Instrument HPLC 540). Detect wavelength: 258 nm. Retention time: about 7 min.

3.2.9. Powder X-ray diffraction

Powder X-ray diffraction (PXRD) was conducted at room temperature by a Philips X-ray Generator PW 1830 (Philips, Netherlands) on the bulk powders of apigenin, hesperetin, quercetin and rutin for investigating the influencing factors during the production of the nanocrystals. The diffraction angle range was between 0.6 °-40 ° with a step size of 0.04 ° per 2 seconds. The diffraction pattern was measured at a voltage of 40 kV and a current of 25 mA.

3.2.10. Cell culture test

Human neuroblastoma cell line SH-SY5Y was obtained from the Deutsche Sammlung von Mikroorganismen und Zellkulturen (DMSZ), Germany. SH-SY5Y cell cultures were grown in Dulbecco's Modifed Eagle's Medium (DMEM) supplemented with 15% FBS. All cells were maintained at 37 ℃ in a humidified 5% CO_2/air atmosphere. The cells were transferred to low serum media (1% FBS) 2 hours prior to the treatment. Cells were weekly passaged (Trypsin-EDTA, Germany). Cell number was measured using a CASY cell counter (Schärfe System, Germany). Tests were carried out in white 96-well microplates, and the density of 5 x 104 (SH-SY5Y) cells per well was used in the screening experiment. Cells were incubated 24 h before the quercetin nanocrystals were added, and the drug remained in contact with the cells for 24 h.

3.2.11. KRL Test

A novel commercial test called KRL Test (Spiral patent) was utilized. KRL is the abbreviation of three French words "Kit Radicaux Libres", that means "Free Radicals Kit". This abbreviation is adopted as the name of the method. The KRL Test allows the dynamic evaluation of the overall antioxidant defense potential of an individual. Whole blood and erythrocytes are submitted to an oxidant stress and free radical-induced hemolysis is recorded by optical density decay with the KRL reader. As inside the body, both extracellular and intracellular antioxidant defense contributes in maintaining the cell integrity until hemolysis. The resistance of whole blood and red blood cells to free radical attack is expressed as the time that is required to reach 50% of maximal hemolysis (half-hemolysis time, T1/2 in minutes).

The tested sample and the standard oxidant stress were applied in the erythrocytes culture at the same time. The KRL reader read the level of the hemolysis with the time passing based on the change of spectral absorption. When the hemolysis achieved the half level of the total hemolysis, the time point was recorded. The overall

antiradical efficiency (or the prooxidant action) is then expressed as the percentage of the compound-mediated T1/2 increase (or decrease) as compared to control (% variation of control blood T1/2).

3.2.12. pH measurement

The pH value was determined by pH meter DocuMeterpH (Sartorius AG, Germany) at room temperature.

3.2.13. Dry residue test

Approximate 2 g final product of each batch was loaded in a dry evaporating dish. The mass of the empty dish (m_{empty}) and the filled dish (m_{before}) were both recorded. After being placed in an oven at 102 ℃ for 2 h, the mass of the dish (m_{after}) was recorded again and the dry residue was calculated using the following equation:

$$dry\ residue\ \% = \frac{m_{after} - m_{empty}}{m_{before} - m_{empty}} \times 100\%$$

3.2.14. Sterilization

The samples for in vitro cell test were all produced in sterile condition. Before production, all parts which would contact samples were sterilized by autoclaving (EFS-S-A S2000, MMM-Group, Germany). The working place was disinfected by spraying 70% isopropanol.

4. Flavonoid nanocrystals - influencing factors

4.1. Preparation of flavonoid nanocrystals

4.1.1. Formulation

Four flavonoid nanocrystals (apigenin, hesperetin, quercetin, and rutin) were produced. Poloxamer 188 (0.2%, w/w) was chosen as the stabilizer because it is universally accepted by pharmaceutical preparations and regulations and has good stabilizing ability. To investigate the influence of surfactant, Plantacare® 2000 UP and Tween® 80 were also used. Glycerol (2.5%, w/w) was added after high pressure homogenization production into the sample as an ingredient for dermal application. The different flavonoid nanosuspensions had same composition ratio (2%, w/w), which made them comparable. Concentration influence was also investigated in rutin and quercetin nanocrystals. Therefore, 1/10 substance concentration formulation with respective 1/10 stabilizer concentration was applied. The formulations involved in this study are displayed in Tab.4 - 1.

Table 4 - 1 Formulations applied in this study (w/w)

Formulation	Apigenin	Hesperetin	Quercetin	Rutin	Poloxamer 188	Tween® 80	Plantacare® 2000 UP	Glycerol	Water	Total
1	2.00%	-	-	-	0.20%	-	-	2.50%	95.30%	100.00%
2	-	2.00%	-	-	0.20%	-	-	2.50%	95.30%	100.00%
3	-	-	2.00%	-	0.20%	-	-	2.50%	95.30%	100.00%
4	-	-	-	2.00%	0.20%	-	-	2.50%	95.30%	100.00%
5	-	-	0.20%	-	0.02%	-	-	2.50%	97.28%	100.00%
6	-	-	-	0.20%	0.02%	-	-	2.50%	97.28%	100.00%
7	-	-	-	2.00%	-	0.20%	-	2.50%	95.30%	100.00%
8	-	-	-	2.00%	-	-	0.20%	2.50%	95.30%	100.00%

4.1.2. Production method

Classic high pressure homogenization was applied in nanocrystals production (Keck and Müller 2006). Homogenizer Micron LAB 40 (APV Deutschland GmbH, Germany) in discontinuous mode with batch weight of 40 g was used as the homogenization equipment. The mixture of flavonoid bulk powder and stabilizer solution was subjected to high speed stirring via Ultra Turrax T25 with 8000 rpm for 2 min followed by two cycles at 250 bar, two cycles at 500 bar, two cycles at 750 bar and one cycle at 1000 bar as pre-milling step, and twenty cycles at 1500 bar as main-milling step. Samples were drawn after/during pre-milling and after 1, 5, 10, 15 and 20 homogenization cycles in main-milling step. In the study of concentration influence, samples were also taken after the different cycles in pre-milling.

4.2. Result and discussion

4.2.1. Influence of dispersion method on PCS measurement

To fix a certain method of dispersion sample in PCS measurement to ensure the comparability of different samples, four different dispersing methods, i.e. without dilution, diluted with purified water, diluted with drug powder saturated solution and diluted with drug powder saturated original dispersing medium, were investigated. The drug powder saturated solution/drug powder saturated original dispersing medium were prepared by adding overweighed quercetin bulk powder in purified water/original dispersing medium (including every materials in the formulation expect the drug) and magnetically stirring for 24 h in room temperature. Then cellulose acetate membrane (0.2 μm pore size, Sartorius Stedium Biotech) was used to filter the powder suspension to obtain saturated solution.

Final sample (after 20 cycles at 1500 bar high pressure homogenization) of quercetin nanocrystals were used as model sample.

Fig. 4 - 1 shows that different diluting ways led to variations, more or less, of the result of PCS diameter. The smallest particle size was obtained in non-diluting sample because the particles in the sample had no change after production till the measuring and the portion of ultrafine particles in the sample would remain. That was also the reason why the polydispersity index was the highest one. The sample diluted with purified water definitely held a disappearance of some ultrafine nanocrystals because of the dissolution. In the meantime, the size of large nanocrystals was decreased as well because of the same reason. When the sample was diluted with drug powder saturated solution, the ultrafine nanocrystals still dissolved till disappearance, while the large ones did not have the dissolution pressure as that in purified water because of the difference in concentration gradients.

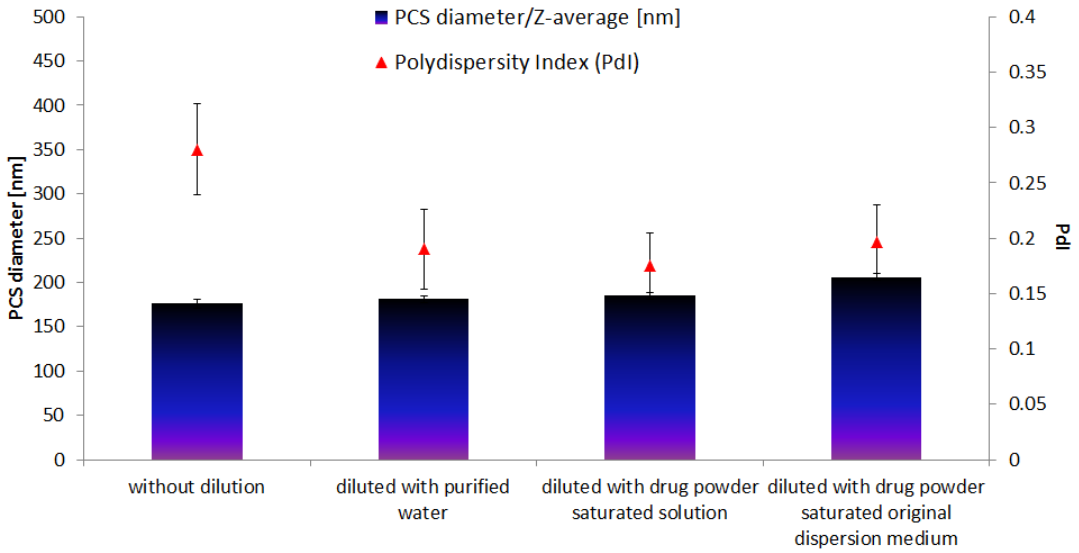

Figure 4 - 1 Results of PCS measurements of quercetin nanocrystals from different diluting methods

In drug powder saturated original dispersing medium, the results can be discussed in two directions. At first, the solubility of quercetin can be improved in original dis-

persing medium because of the solubilizing function of stabilizer, therefore the ultrafine nanocrystals dissolved faster and more. Secondly, due to the higher quercetin concentration in the drug powder saturated original dispersing medium, it was more difficult for large nanocrystals to dissolve. Therefore, with the small nanocrystals disappearing and large nanocrystals remaining, the average size detected was increased. Since the disappearance of small nanocrystals is the main reason of size changing, the PdIs were similar among the diluted samples but all lower than the undiluted. Based on the above understanding, if the dilution is unavoidable, the drug powder saturated solution should be used to dilute sample before PCS measurement because of its less influence on the measured value. The further study was proceeded in this way.

4.2.2. Size characterization

The size reduction (PCS diameter, polydispersity index) during HPH for all the flavonoids is shown in Fig. 4 - 2. All flavonoids showed a size reduction with increasing HPH cycle except rutin which had a size fluctuation and final size of 517 nm. That could be attributed to the formation of nanocrystals agglomerates during the energy inputting of HPH. Among the four flavonoids, quercetin had the most efficient particle diminution and finally achieved 197 nm after 20 HPH cycles. The apigenin nanocrystals had a steady decrease in size with increasing numbers of HPH cycle; the final size was 489 nm. The same was observed for the hesperetin nanocrystals which possessed a size of 416 nm at the end. All PdIs showed a general decline with increasing HPH cycle while there was one climb-up in apigenin nanocrystals at first cycle at 1500 bar. Only one cycle 1500 bar is perhaps not enough to let all large particles of apigenin into small. On the contrary, only a part of large particles become smaller could widen the size distribution.

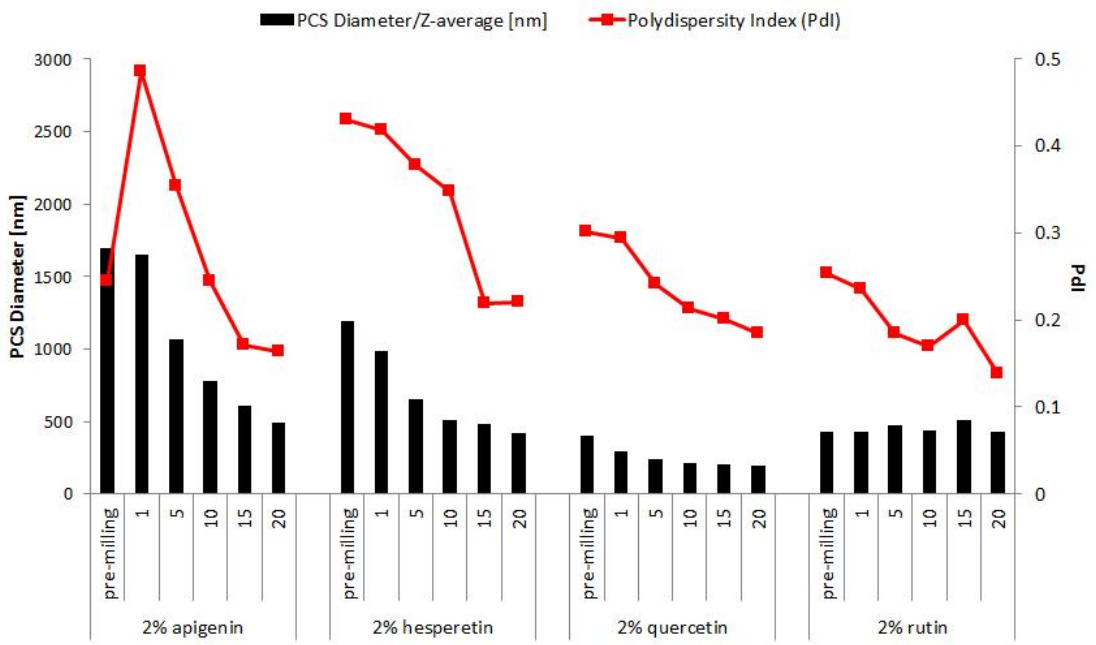

Figure 4 - 2 PCS diameters and PdIs of apigenin, hesperetin, quercetin and rutin nanocrystals as functions of pressure (250 bar to 1500 bar) and of number of high pressure homogenization cycles

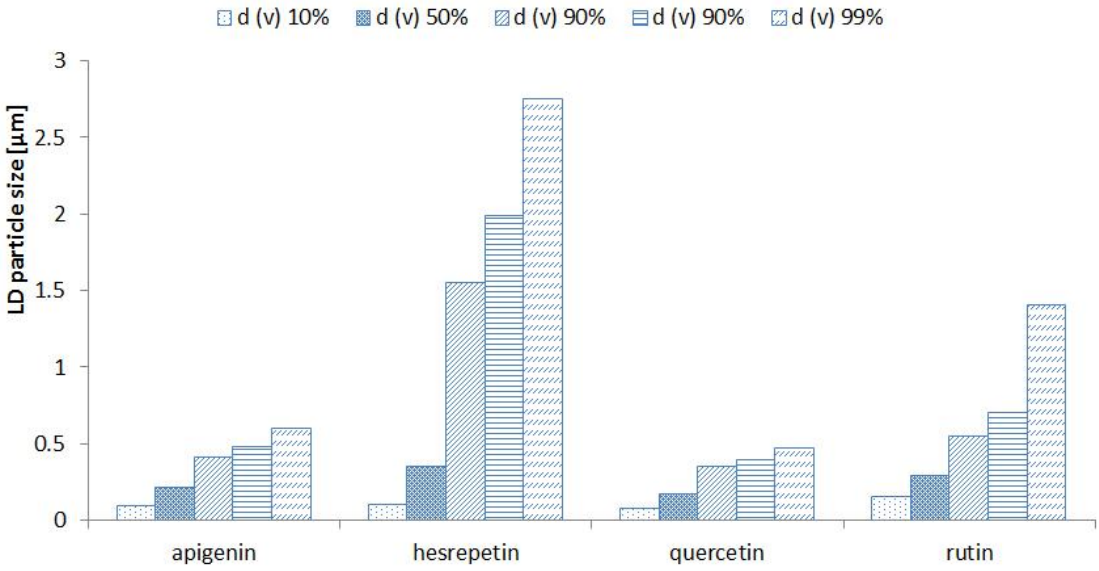

Figure 4 - 3 LD size of apigenin, hesperetin, quercetin and rutin nanocrystals after 20 cycles high pressure homogenization at 1500 bar (0.2% Poloxamer 188 as the surfactant)

The LD results of the final formulations are presented in Fig. 4 - 3. Only apigenin and quercetin were shown to contain no larger particles (> 1 µm). A few (< 1%) larger rutin particles were found, and hesperetin contained at least 10% of particles with a

size above 1.5 μm. Based on these results, quercetin and apigenin can be nanosized more efficiently by this method. From the results of size characterization, the ability to be nanosized of different flavonoids are different even they have very similar structure. This phenomenon would be attributed to the crystallinity and the hardness of the original powder. Higher crystallinity means less imperfection on the surface of the particles, thus make the particles difficult to be break. Proper hardness may indicate a good friability, which make the particles easy to be break.

4.2.3. Zeta potential

Normally, zeta potential of particles, which indicates the electrostatic repulsive interactions between the dispersed particles (Rosen 2004), can indicate partly the stability of nanosuspension.

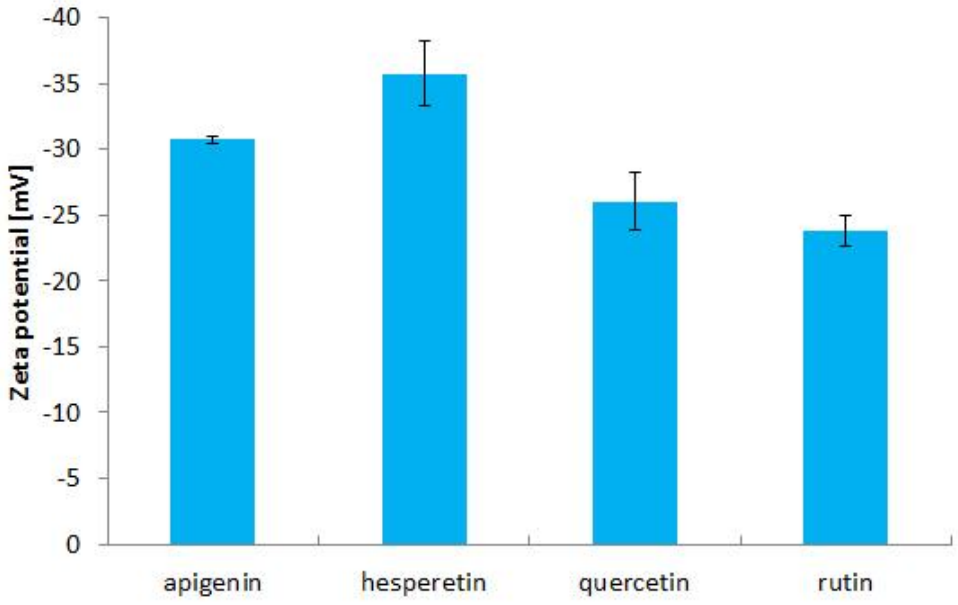

Figure 4 - 4 Zeta potential of respective final flavonoid nanosuspensions

Fig. 4 - 4 illustrates the different zeta potential values of nanosuspensions. Zeta potentials ranged from -24 mV (rutin) to -36 mV (hesperetin). For quercetin and apigenin the zeta potentials were -26 and -31 mV respectively. More -OH groups led to higher

zeta potentials. However, non-ionic polymer Poloxamer 188 was used as stabilizer, which implies that lower values of zeta potential means relatively higher stability because of the steric stabilizing effect (Keck 2006).

4.2.4. Short-term stability

Four-week short term stability test was evaluated based on the index of PCS particle size (Fig. 4 - 5).

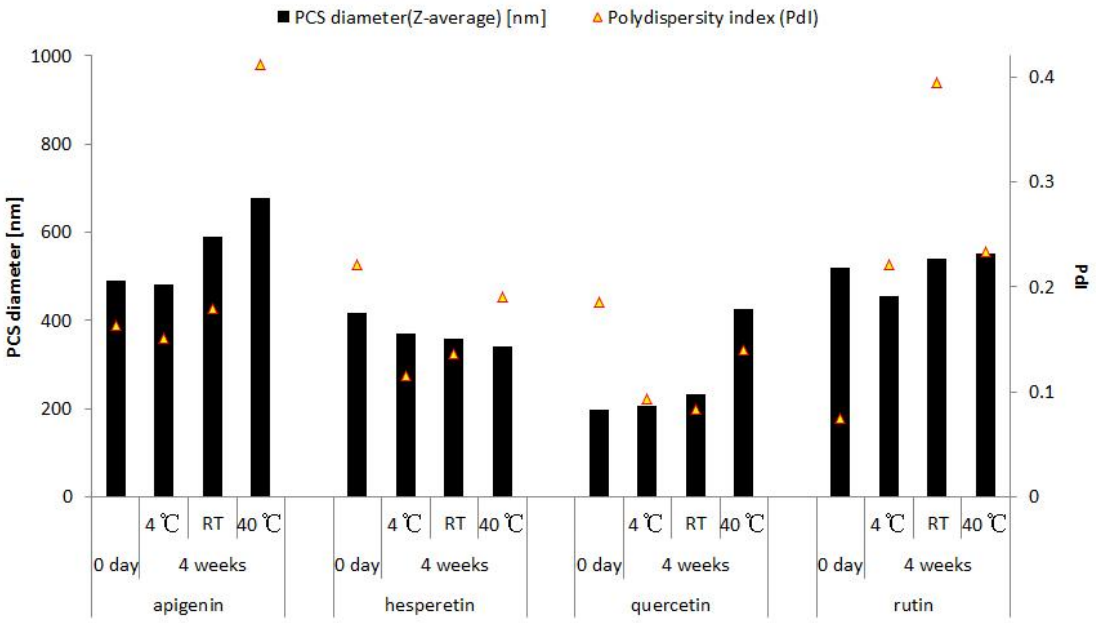

Figure 4 - 5 Short-term stability of nanosuspensions obtained after 20 cycles at 1500 bar under storage temperature of 4 ℃, room temperature (RT) and 40 ℃ after 4 weeks

The samples after 20 cycles HPH were stored at 4 ℃, room temperature and 40 ℃. All nanosuspensions stored at 4 ℃ remained unchanged over the period of observation. However, storage at room temperature led to an increase in size. The effect was even more pronounced when the suspensions were stored at elevated temperatures (i.e. 40 ℃). For hesperetin a decrease in size was observed. Nevertheless, this also indicates a pronounced increase in size, as larger particles escape from the measuring

range of the PCS instrument, leading to an over-all smaller size result. The results indicate that the flavonoid nanosuspensions need to be stored at low temperatures.

4.2.5. Correlation with physicochemical properties

The limitation of particle size of nanocrystals produced by the mentioned HPH method could be decided by inputted energy intensity, applied cycles of HPH, active concentration, stabilizer, and the physicochemical properties of actives. Since all the other factors were fixed, different suspensions could be compared and research the effect of physicochemical properties could be investigated. Different particles characteristics of the same formulation could be related to the inner properties of different actives.

Table 4 - 2 mw., mp., Log P and pKa of apigenin, hesperetin, quercetin, and rutin

Flavonoid	mw. [Da]	mp. [℃]	Log P	pKa	Final size [nm]
Apigenin (Rothwell, Day et al. 2005; Favaro, Clementi et al. 2007)	270.2	345-350	2.92	6.6; 9.3	489
Hesperetin (Chen 2009)	302.3	226-228	1.5	6.8; 10.4; 11.5	416
Quercetin (Rothwell, Day et al. 2005; Arshad, Janjua et al. 2009)	302.2	316	1.82	6.7	197
Rutin (Pedriali, Fernandes et al. 2008)	610.5	195	0.85	7.1	517

Tab. 4 - 2 presents some important physicochemical properties of these four flavonoids. The molecular weight (mw.) of these flavonoids varied from 270 (apigenin) to 610 Dalton (rutin), the melting points (mp.) from 195 ℃ (rutin) to 316 ℃ (querce-

tin), and the log P values from 0.85 (rutin) to 2.92 (apigenin). In conclusion, quercetin and apigenin possess lower mw., higher mp., and higher log P values than hesperetin and rutin and led to the most efficient size diminution. Therefore, in this study, lower mw., higher mp., and higher log P values led to smaller particle sizes.

Result from powder X-ray diffraction of apigenin, hesperetin, quercetin and rutin are displayed in Fig. 4 - 6, Fig. 4 - 7, Fig. 4 - 8 and Fig. 4 - 9, respectively.

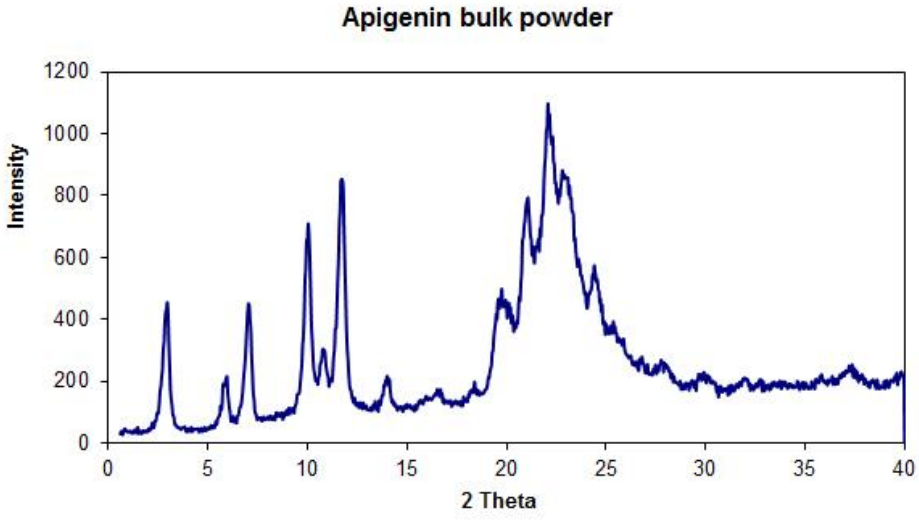

Figure 4 - 6 X-ray spectrum of apigenin bulk powder

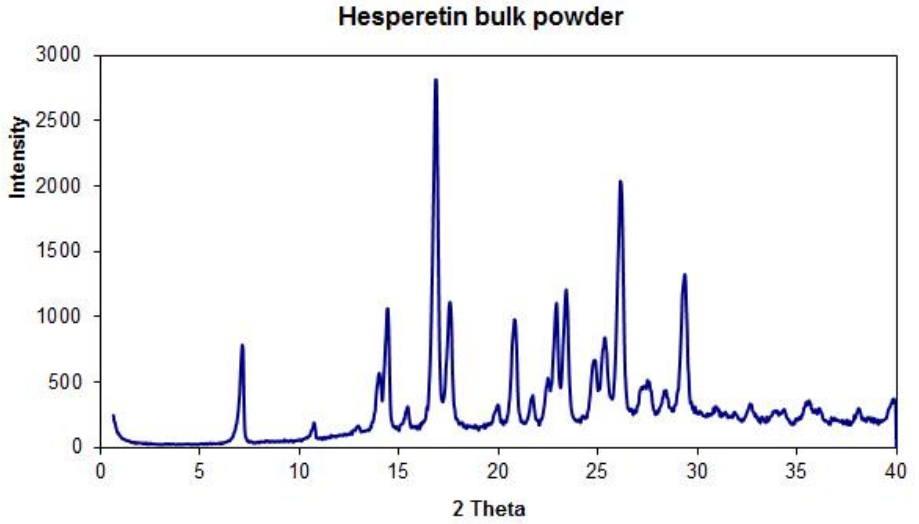

Figure 4 - 7 X-ray spectrum of hesperetin bulk powder

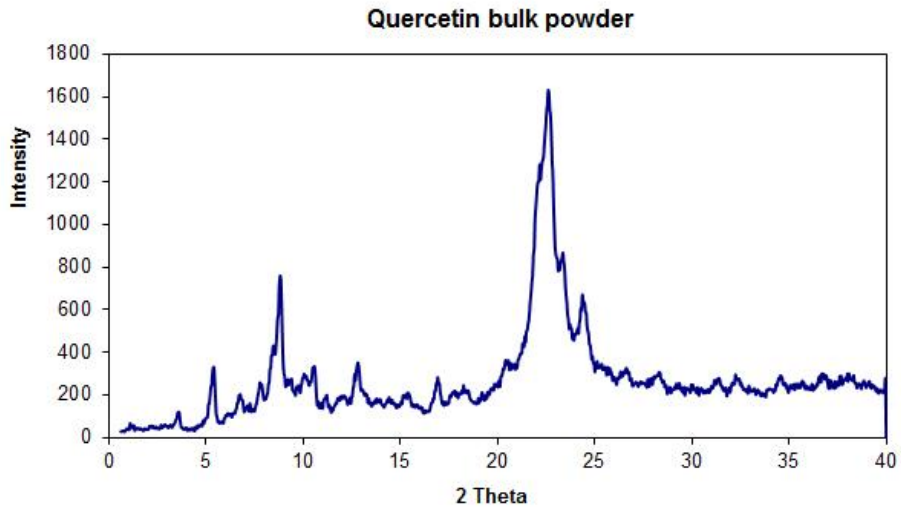

Figure 4 - 8 X-ray spectrum of quercetin bulk powder

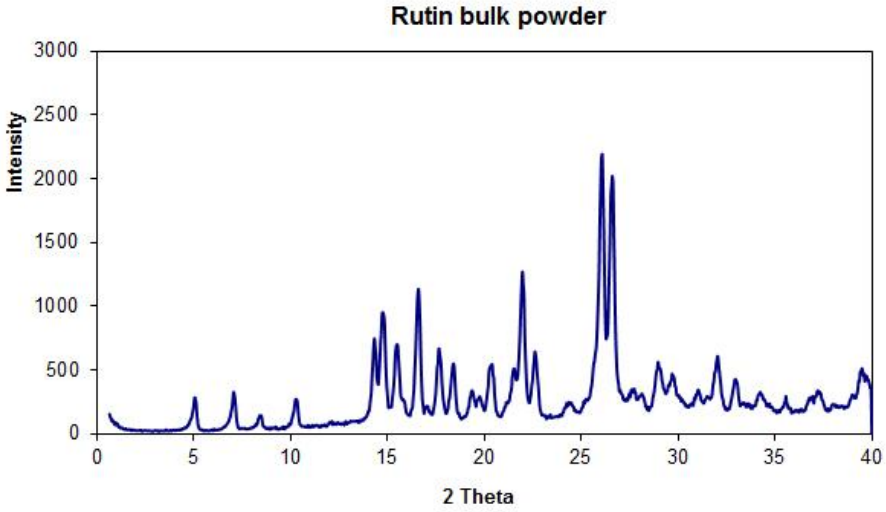

Figure 4 - 9 X-ray spectrum of rutin bulk powder

From the X-ray spectra, the peaks of apigenin, hesperetin and rutin are all sharper than that of quercetin. This means quercetin bulk powder has the least ordered lattice in the structure between its molecules among the four compounds. Because of the disordered area/imperfection on the surface of the quercetin powder, quercetin particles can be easier broken on the disordered sites by the force generated by HPH. The X-ray spectra results are in agreement with the size results that quercetin nanocrystals is the smallest below to 200 nm. The crystallinity of the initial material could play a very important role in the production of nanocrystals.

4.2.6. Influence of surfactant

In order to investigate the influence of surfactants on the efficiency of diminution of this method, formulations 4, 7, and 8 were utilized to produce rutin nanocrystals. The process was kept the same as 4.1.2 described with different surfactants, namely 0.2% Poloxamer 188, Plantacare® 2000 UP and Tween® 80, separately. The result showed in figure 4 - 10 indicated the significant influence of surfactant. Plantacare® 2000 UP proved to be the most efficient surfactant which facilitates the diminution process, only 2 cycles at 250 bar could reduce the PCS diameter below 500 nm. The small nanocrystals can be obtained easily by using Plantacare® 2000 UP as the surfactant. On the contrary, Tween® 80 showed a poor ability to maintain the rutin nanocrystals under 1 µm. This phenomenon was attributed to the loose particle aggregation caused by bridging effect. Therefore, different surfactants will lead to different sizes, thus special size can be obtained by choosing the suitable surfactant.

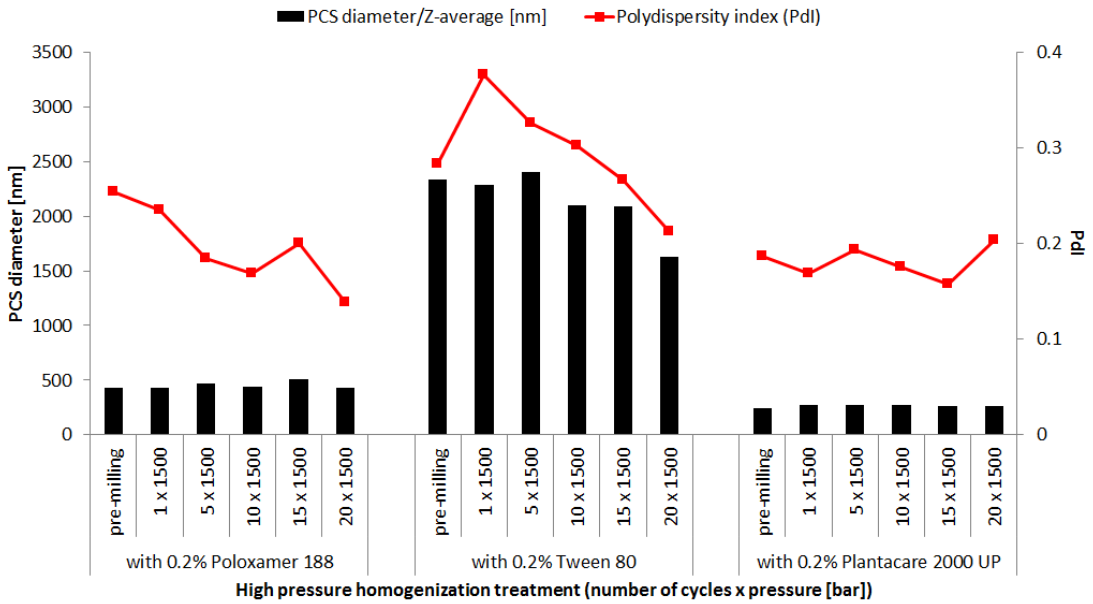

Figure 4 - 10 PCS diameters and PdIs of 2% rutin nanocrystals stabilized by Poloxamer 188, Tween® 80 and Plantacare® 2000 UP as functions of pressure (250 bar to 1500 bar) and of number of high pressure homogenization treatment

The results from zeta potential (Fig. 4 - 11) were in accordance with the size results. The rutin nanocrystals stabilized by Plantacare® 2000 UP possessed the highest absolution zeta potential value.

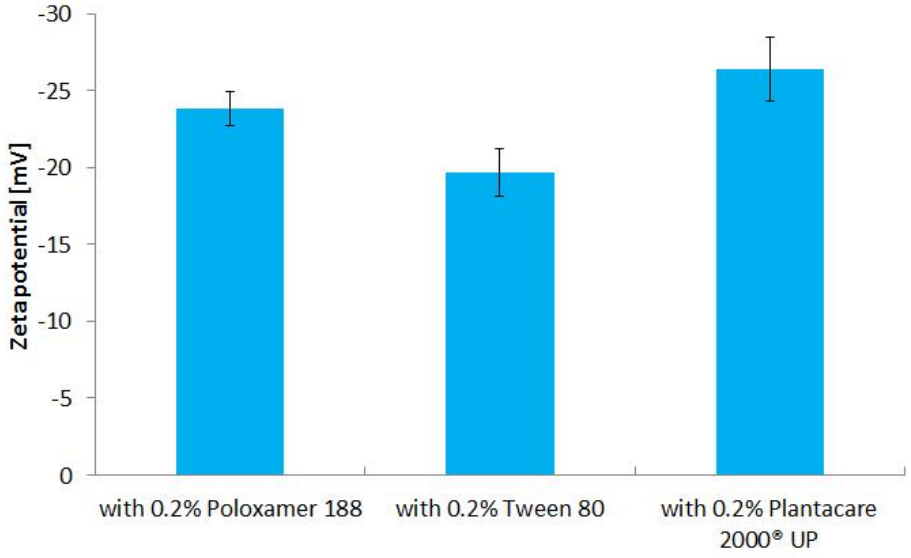

Figure 4 - 11 Zeta potential of 2% rutin nanocrystals stabilized by Poloxamer 188, Tween® 80 and Plantacare® 2000 UP after 20 cycles at 1500 bar high pressure homogenization

4.2.7. Influence of concentration

Besides the energy density and inputting time, physicochemical properties of active and stabilizer, the concentration of active in the nanosuspension system also plays an important role to the final size of nanoparticles. Rutin and quercetin nanocrystals with lower concentration were produced in the uniform way as described in 4.1.2.

In the case of rutin nanocrystals as described in Fig. 4 - 12, there was significant difference in particle size between 2% (about 550 nm) and 0.2% (about 300 nm) rutin nanocrystals suspensions while the PdIs were much close. The fact of that lower concentration resulted in a smaller size indicates that the particles in 0.2% rutin suspension is easier to be broken down by same power force, which means particle size is tunable by adjusting the concentration of rutin in this system. However, the increase

of energy density and inputting seems not very essential as the PCS diameter of nanocrystals nearly remained the same when higher pressure and more cycles were applied in a certain concentration. It could be the result of the re-aggregation after diminution. Applying other surfactants which can stabilize rutin nanocrystals faster may lead to a smaller final size. Consequently, regardless of surfactant, the concentration of rutin has more influence on the diminution in this system.

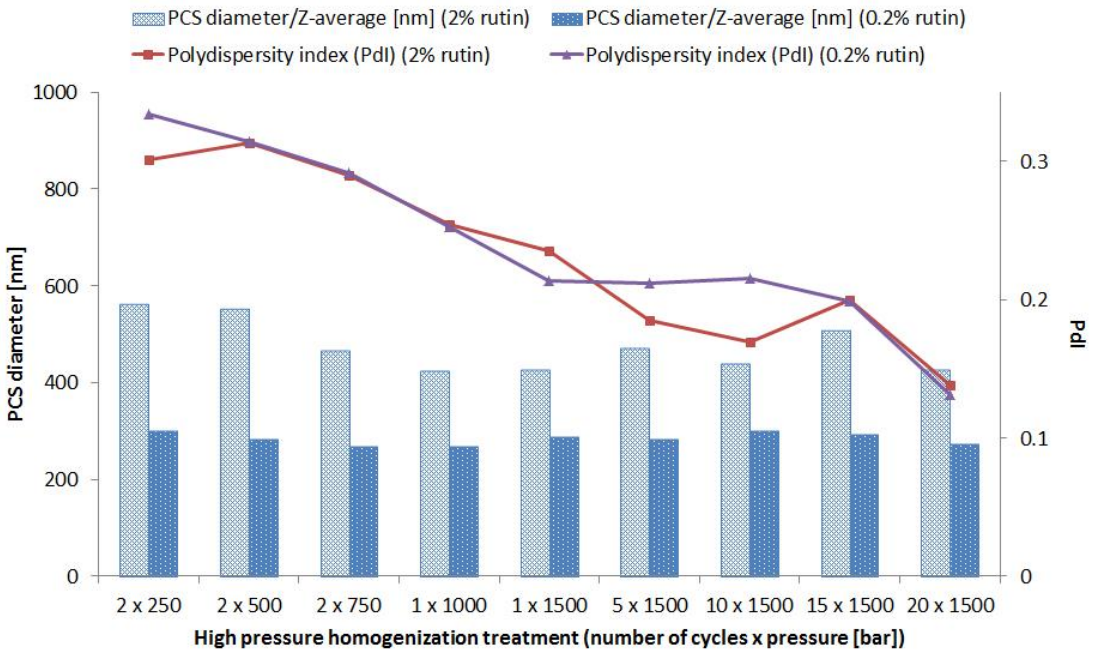

Figure 4 - 12 PCS diameters and PdIs of rutin nanocrystals with different concentration of active as functions of pressure (250 bar to 1500 bar) and of number of high pressure homogenization treatment

On the other side, the sizes of quercetin nanocrystals suspensions with 2% and 0.2% concentration did not have great difference. Very similar sizes and a simultaneous decrease were demonstrated in Fig. 4 - 13. Compared to rutin, quercetin needs more intense energy to attain smaller size. After 5 cycles at 1500 bar, when the size decreased to around 200 nm and PdI around 0.2, only little change happened in the further cycles. Thus, 5 cycles at 1500 bar was the limitation of energy's impact on diminution. Decreasing the concentration of quercetin was not helpful to get smaller size since the size of approximately 200 nm was also the limitation of concentration's impact. In

this case, if higher concentration of quercetin is involved in this system, the size could be also remain around 200 nm till the concentration go higher up than the critical point of concentration's impact.

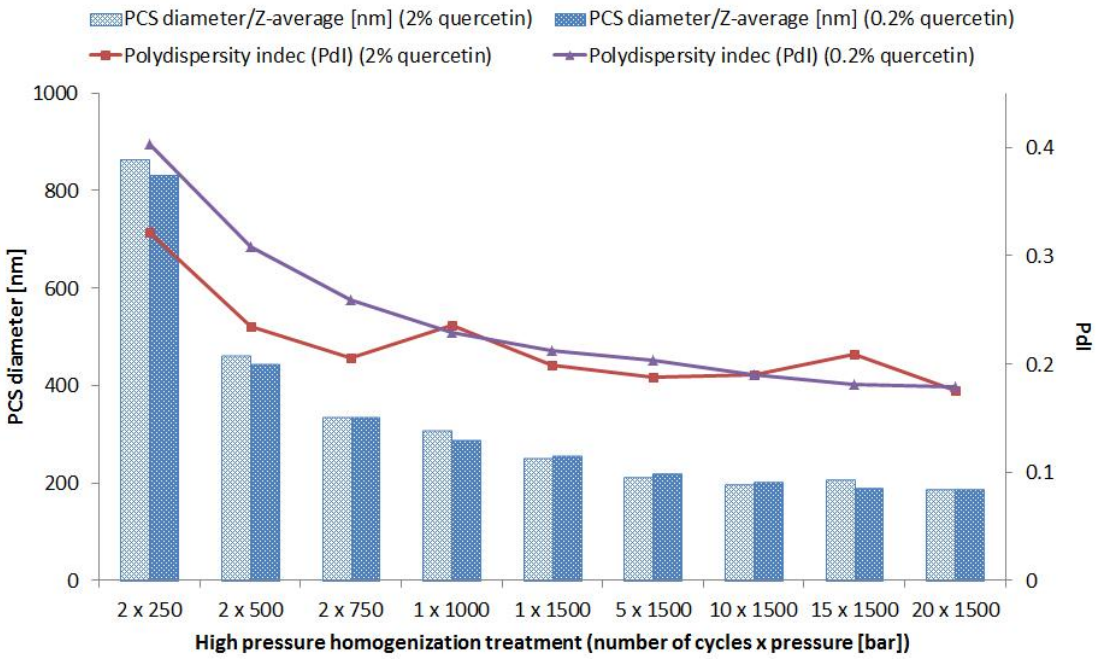

Figure 4 - 13 PCS diameters and PdIs of quercetin nanocrystals with different concentration of active as functions of pressure (250 bar to 15,00 bar) and of number of high pressure homogenization cycles

Many publications have already proven that, in the method of high pressure homogenization, energy (Keck and Müller 2006; Gao, Qian et al. 2010), selected surfactants (Zhang, Tan et al. 2007), physicochemical properties of active (Lindfors, Skantze et al. 2006) and concentration of active are the main factors determining the final size which can be obtained. It can be concluded firstly as a so-called "limitation theory" (Fig. 4 - 14).

For every factors mentioned above, they have limitations of the capability to make nanocrystals smaller. In different cases, the limitations of each factor are various. Changing one of them could lead to adjusted size or limited final size. When one has already met its limitation, further optimization makes no longer useful for decreasing

particle size. Instead of that, the optimization of the others factors that has not reached their limitation should be made.

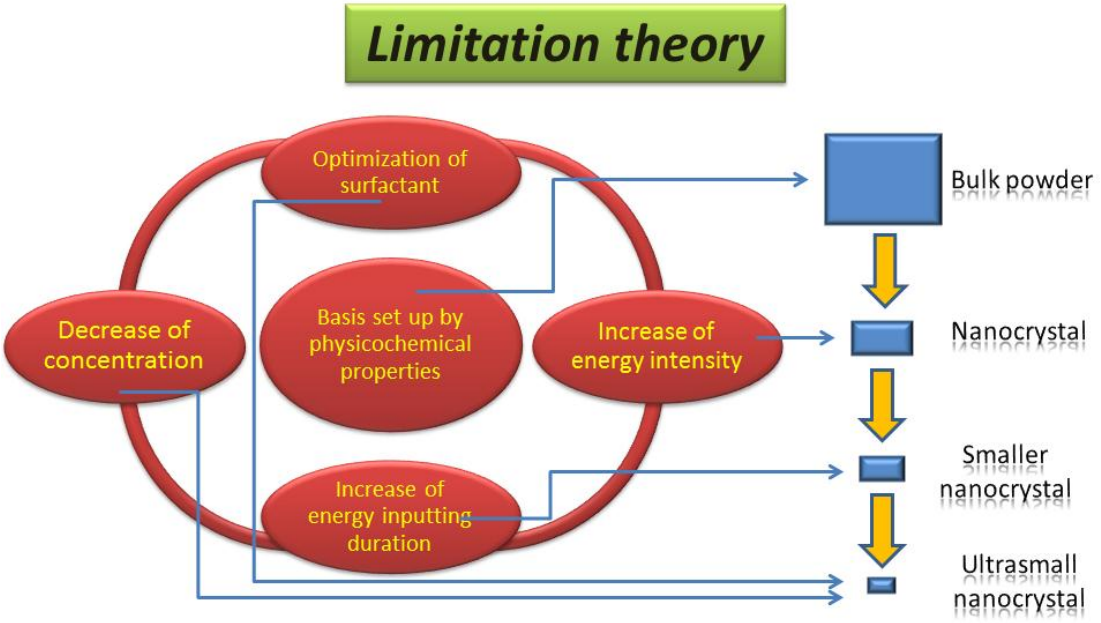

Figure 4 - 14 Diagram of "limitation theory" in production of nanocrystals with high pressure homogenization

The case was shown in Fig. 4 - 12, active and surfactant was unchangeable, energy had met their limitation, so decreasing concentration gave a decreased final size. On the other hand, in Fig. 4 - 13, decreasing concentration did not work, but more energy inputting yielded smaller size till the energy met its limitation as well. Different kinds of drug with different physicochemical properties set up the basic limitation, which is a reason why different final sizes were attained.

However, it is also possible to alter the basic limitation by changing the solid form, i.e. conversion from crystalline to amorphous. Technologies H42 (Möschwitzer and Müller 2006) and H96 (Möschwitzer and Lemke 2008) are in this case. Alteration of surfactants, including variety and concentration, has also been proven to have signifi-

cant influence to the result (Kobierski, Ofori-Kwakye et al. 2009) and the stability of product as well (Ghosh, Bose et al. 2011).

4.3. Summary

Different kinds of flavonoid nanosuspensions were produced by high pressure homogenization. After the investigation of the measured sizes of nanocrystals in different diluting medium, the drug powder saturated solution was chosen as the dilution method in PCS measurement. The influence of inputted energy intensity, applied cycles of HPH, surfactant, active concentration, and the physicochemical properties of actives on the resulted particle size were investigated. Each of them plays an essential role in the nanocrystals production.

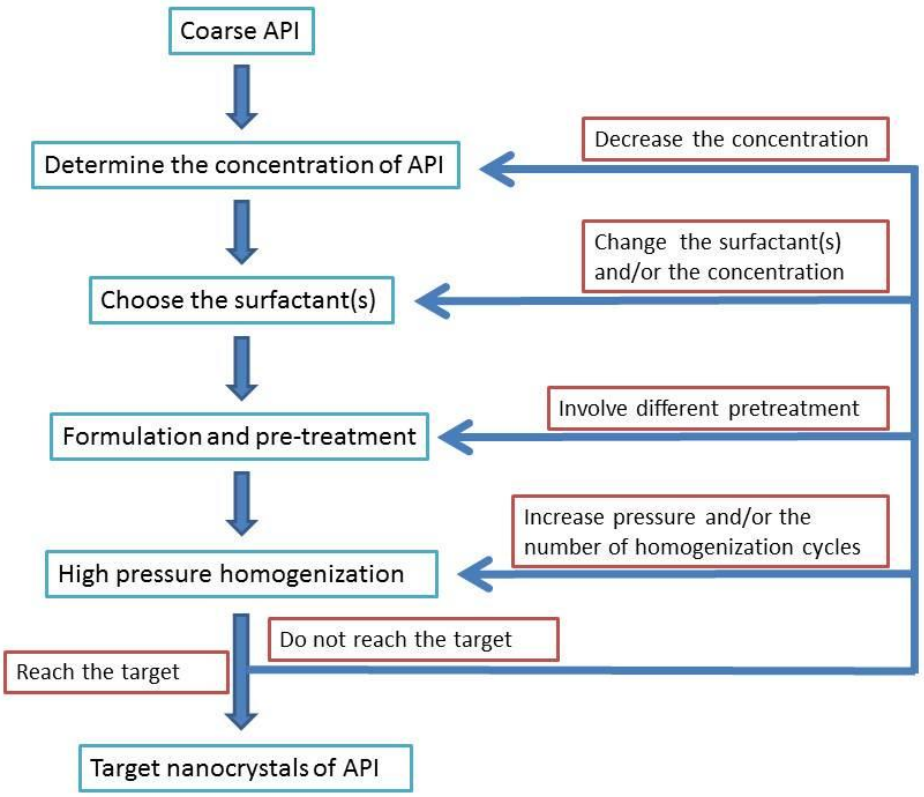

Figure 4 - 15 Pathways to the target nanocrystals in high pressure homogenization

Generally, higher HPH pressure, more HPH cycles, lower flavonoid concentration and active possessinging lower mw., higher mp., and higher log P values may lead to smaller particle sizes. Altering the surfactant can also introduce the change of particles size and the efficiency of diminution (Fig. 4 - 15). From the “limitation theory”, the influences mentioned in this study all have their limitations; particle size can only be further decreased by adjusting the influencing factors which have not met their limitations yet.

5. Tailor-made quercetin nanocrystals - size effect on in vitro efficacy

Except for the anti-inflammatory (Guardia, Rotelli et al. 2001), anti-cancer (Lamson and Brignall 2000) and anti-aging (Chondrogianni, Kapeta et al. 2010) effect which are presented with the anti-oxidative capacity, quercetin is mostly claimed being therapeutically beneficial to treat many oxidative stress-related neurodegenerative diseases, such as Parkinson's disease (PD) (Bournival, Quessy et al. 2009; Haleagrahara, Siew et al. 2011), Alzheimer's disease (AD) (Heo and Lee 2004; Ansari, Abdul et al. 2009; Suematsu, Hosoda et al. 2011) and Huntington's disease (HD) (Chen, Jeng et al. 2006) as well. Recently, more and more research has declared that quercetin and its reactive metabolites were potential toxic prooxidants as well (Decker 1997; Metodiewa, Jaiswal et al. 1999; Boots, Kubben et al. 2003; Utesch, Feige et al. 2008; Procházková, Boušová et al. 2011). Also due to the limited therapeutic dose-range (Ossola, Kääriäinen et al. 2009), it is difficult to control the administrative dose precisely to avoid the toxicity. Therefore, this powerful active can be used in cancer chemotherapy as well because of the cytotoxicity (Hirpara, Aggarwal et al. 2009; Xavier, Lima et al. 2011).

5.1. Preparation of quercetin nanosuspension for cell culture test

Quercetin nanosuspension comprises quercetin (2% or 0.2%), Poloxamer 188 (0.2%), glycerol (2.5%), and water add to 100%. All ratios used weight ratio. To begin with, Poloxamer 188 was dissolved in water to form surfactant solution. Adequate amounts of glycerol and surfactant solution were filtered through 0.2 μm cellulose acetate membrane (sterile, individual, Minisart®, Sartorius Stedim Biotech GmbH, Germany) for further use. Afterwards, quercetin bulk powder was added in the required amount of surfactant solution with gentle stirring. The obtained coarse suspension was subjected to high pressure homogenization using a Micron LAB 40 (APV Deutschland, Germany) with pre-milling and main-milling, sequentially. Pre-milling included two cycles at 250 bar, 500 bar, 750 bar, and 1000 bar which aimed to break large particles

gradually to avoid gap-blocking during the further main-milling. Main-milling comprised up to 20 cycles at 1500 bar. Nanocrystals with different size were obtained after different cycles of HPH (Tab. 5 - 1). Glycerol was added and mixed with the products after HPH to adjust osmotic pressure to attain final products for particles characterization and cell culture test.

Table 5 - 1 Different treatments of high pressure homogenization of obtained quercetin nanocrystals with different particles sizes

	Particle size [nm]	Treatment of high pressure homogenization
2% quercetin nanosuspension	602	2 cycles at 250 bar
	489	2 cycles at 250 bar; 1 cycle at 500 bar
	275	2 cycles at 250 bar; 2 cycles at 500 bar;2 cycles at 750 bar;2 cycles at 1000 bar
	217	2 cycles at 250 bar; 2 cycles at 500 bar; 2 cycles at 750 bar;2 cycles at 1000 bar; 5 cycles at 1500 bar
	172	2 cycles at 250 bar; 2 cycles at 500 bar; 2 cycles at 750 bar;2 cycles at 1000 bar; 20 cycles at 1500 bar
0.2% quercetin nanosuspension	426	2 cycles at 250 bar; 2 cycles at 500 bar
	286	2 cycles at 250 bar; 2 cycles at 750 bar
	183	2 cycles at 250 bar; 2 cycles at 500 bar; 2 cycles at 750 bar;2 cycles at 1000 bar; 20 cycles at 1500 bar

5.2. Measurement of cellular ATP content

Cellular ATP concentrations were assessed by the CellTiter-Glo cell viability assay, according to the manufacturer's instructions. Briefly, the assay is based on measurement of luminescence generated by the reaction of ATP and luciferin. Cells were plated on white 96-well microplates in 100 µl of DMEM containing 1% FBS. One

day after plating, quercetin nanocrystals in different particle sizes were added with various concentrations to the cells for 24 hours. Nanocrystals were added with the following volume: 1 µl, 20 µl, 50 µl, 100 µl. SAL (250 µM), 6-OHDA (50 µM), or 3-HK (300 µM) were given to the medium simultaneously with tested compounds for 24 h. The influence of original blank surfactant solution of quercetin nanosuspension on ATP concentration was also tested. The final media volume was 200 µl. Luminescence levels were measured using a Tecan microplate reader (Tecan, Austria). All experiments were done in triplicate. Luciferase activity of untreated cells was arbitrarily set to 100%. Data were expressed as % of control ATP. Each sample was cultivated and measured triply.

5.3. Preparation of quercetin nanosuspension kinetic saturation solubility test

The same method as described in 5.1. was applied to produce other batches of quercetin nanosuspension (2% quercetin) for investigating the kinetic saturation solubility. Due to the systematic variation, quercetin nanocrystals with the following sizes were obtained: 1061 nm, 501 nm, 361 nm, 288 nm and 197 nm.

5.4. Measurement of kinetic saturation solubility

For the determination of the kinetic saturation solubility an overweight of each sample was dispersed in water and 0.2% Poloxamer 188 solution, respectively, followed by incubation at 37 ℃ and 100 rpm shaking. Samples were drawn after 1 h, 6 h, 1 d, 2 d, and 3 d. After filtration (0.2 µm) and ultracentrifugation (16000 g, 1h), the supernatant was analyzed by HPLC.

5.5. Results and Discussion

5.5.1. Size characterization of quercetin nanocrystals

Via controlling production condition, tailor-made nanocrystals were successfully produced. PCS result in Fig. 5 - 1 showed that an increase in cycles of HPH could lead to a significant smaller size for quercetin. After five cycles high pressure homogenization at 1500 bar, the decrease of diameter was insignificant. Lower quercetin concentration had no obvious influence on size, although led to a relatively smaller final size. Polydispersity index in Fig. 5 - 1 shows a narrow size distribution for the lower concentration. Less particle number in under the same pressure in HPH may results in a more evenly distributed energy on each particle.

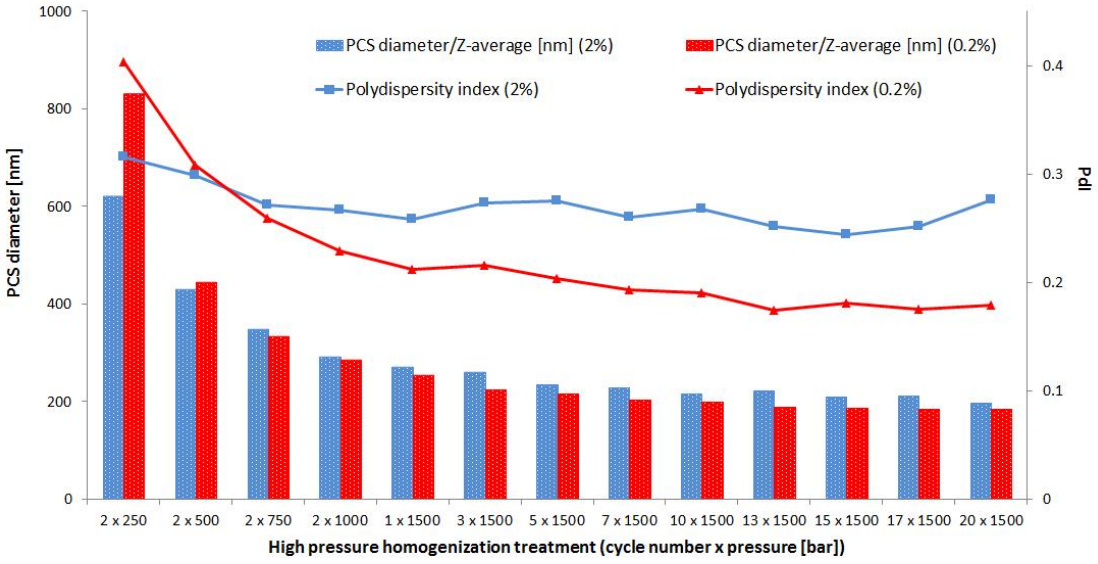

Figure 5 - 1 PCS diameters and polydispersity indices of quercetin nanocrystals (2% and 0.2%) as functions of pressure (250 bar to 1500 bar) and of number of high pressure homogenization cycles

LD size of 2% quercetin nanocrystals shown in Fig. 5 - 2 was in accordance with the PCS result. The main purpose of LD measurement is to detect large particles in the system. The d(v)10% and d(v)50% almost remained the same during the process,

however, significant decrease of d(v)90% and d(v)95% happened until after one cycle at 1500 bar and three cycles at 1500 bar, respectively. After seven cycles at 1500 bar high pressure homogenization, d(v)99% achieved was below 1 µm and remained stable, which means, after seven cycles at 1500 bar, further homogenization treatment had less influence on the size. It was different from the PCS result, therefore combining different analysis technologies to obtain a complete overview of the result is necessary.

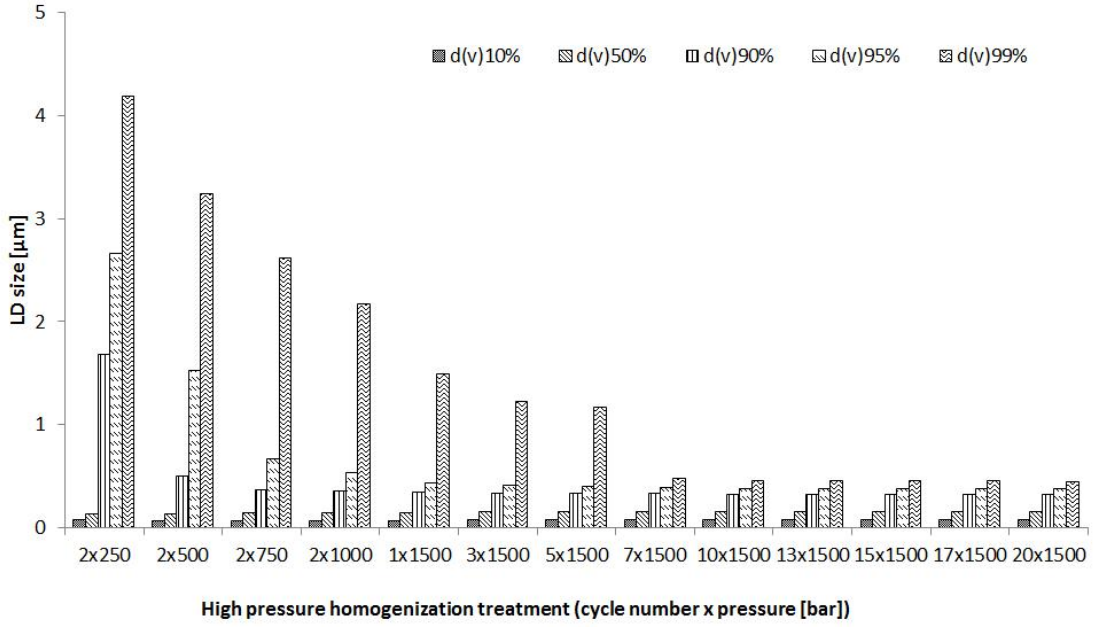

Figure 5 - 2 LD size of quercetin nanocrystals (2%) as function of pressure (250 bar to 1500 bar) and of number of high pressure homogenization cycles

The observation of size-time dependence of quercetin nanocrystals in cell culture medium was performed as well. The instant phenomenon of particle aggregation was detected when the nanocrystals were mixed with the medium. However, with gentle shake, the aggregation was proven to be very loose and the finest nanocrystal dissolved faster till no particle could be detected after 24 h incubation, while the larger ones had some aggregations which could be observed.

Based on the results of PCS and LD, specific condition for size differentiation was determined (Tab. 5 - 1). The nanocrystals could be divided into 5 groups with 2% quercetin content of different PCS sizes (602 nm, 489 nm, 275 nm, 217 nm, 172 nm) and three groups with 0.2% quercetin content of different PCS sizes (426 nm, 286 nm, 183 nm) to produce for further test.

5.5.2. Cellular ATP content with only toxins

Many evidences provided by researchers suggested that neurodegenerative disorders (PD, AD, HD, etc.) are related to the neuronal apoptosis (Sastry and Rao 2000; Yuan and Yankner 2000). Oxidative stress brought by reactive oxygen species (ROS) may be regarded as the main reason to generate apoptosis in nervous system (Kannan and Jain 2000; Martin 2001; Gazaryan and Ratan 2009). The studied three kinds of endogenous toxins, namely salsolinol (Wanpen, Govitrapong et al. 2004), 6-hydroxydopamine (Hwang and Jeong 2010) and 3-hydroxykynurenine (Okuda, Nishiyama et al. 1998) all generate oxidative stress, thus lead to an apoptosis.

Salsolinol may induce apoptosis, especially in dopamine neurons (Naoi, Maruyama et al. 2000) via activation of caspase 3 (Akao, Nakagawa et al. 1999), which plays as the last step in the activation process of apoptosis (Yuan and Yankner 2000). This mechanism was also revealed in 6-hydroxydopamine (Dodel, Du et al. 1999; Hanrott, Gudmunsen et al. 2006). 3-hydroxykynurenine was recently reported via kynurenine-NAD+ pathway to generate apoptosis (Bellac, Coimbra et al. 2010; Col ń-Gonz ález, Maldonado et al. 2013). Fig. 5 - 3 shows the cell viability when the toxins were administrated in cell culture medium after 24 h. Without any addition of quercetin, 250 μM SAL, 50 μM 6-OHDA and 6-HK resulted in 55%, 42% and 50% cell viability, respectively. They showed evident ability to induce cell death in accordance to what the literature reported.

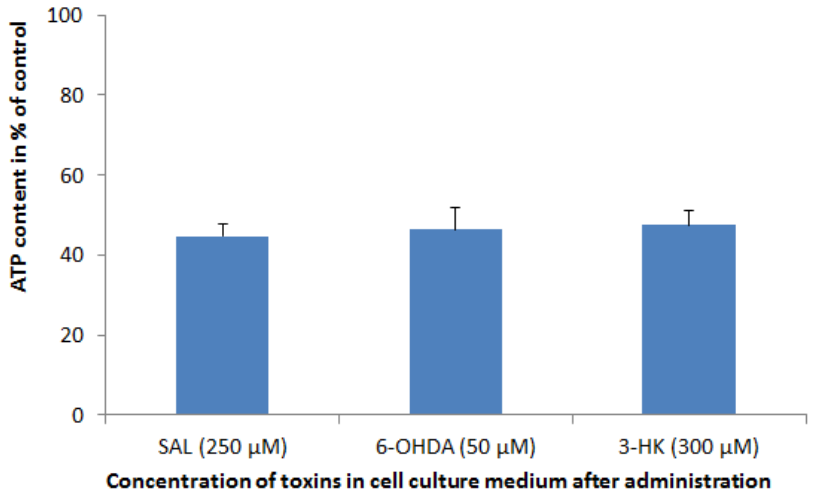

Figure 5 - 3 Cell viability after 24 h incubation in presence of only toxins: salsolinol (250 µM), 3-HK (300 µM), or 6-OHDA (50 µM)

5.5.3. Cellular ATP content with only quercetin nanocrystals

Quercetin has been accepted as an efficient antioxidant. However, some research also argued that it also possesses the prooxidative effect based on the structural variation during the metabolism (Spencer, Kuhnle et al. 2003; Zhang, Swarts et al. 2011). To determine whether the blank solution used to suspend the quercetin nanocrystals could influence the ATP level in neuroblastoma cells, SH-SY5Y cells were treated with the blank solution (1 µl, 20 µl, 50 µl, 100 µl) for 24 h. Interestingly, the exposure of SH-SY5Y cells to 100 µl solution for 24 hours decreased slightly ATP concentration by 10%. Moreover, the treatment with nanocrystals of quercetin with particle size 602 nm; 489 nm; 275 nm; 217 nm and 172 nm revealed a reduction in cellular ATP level compared with control, as shown in Fig. 5 - 4. Compared to the other sizes, quercetin nanocrystals with the smallest size of 172 nm nanocrystals of particularly showed very high toxicity in the concentration of 30 mM. An inclination of toxicity could be observed with declination of the size.

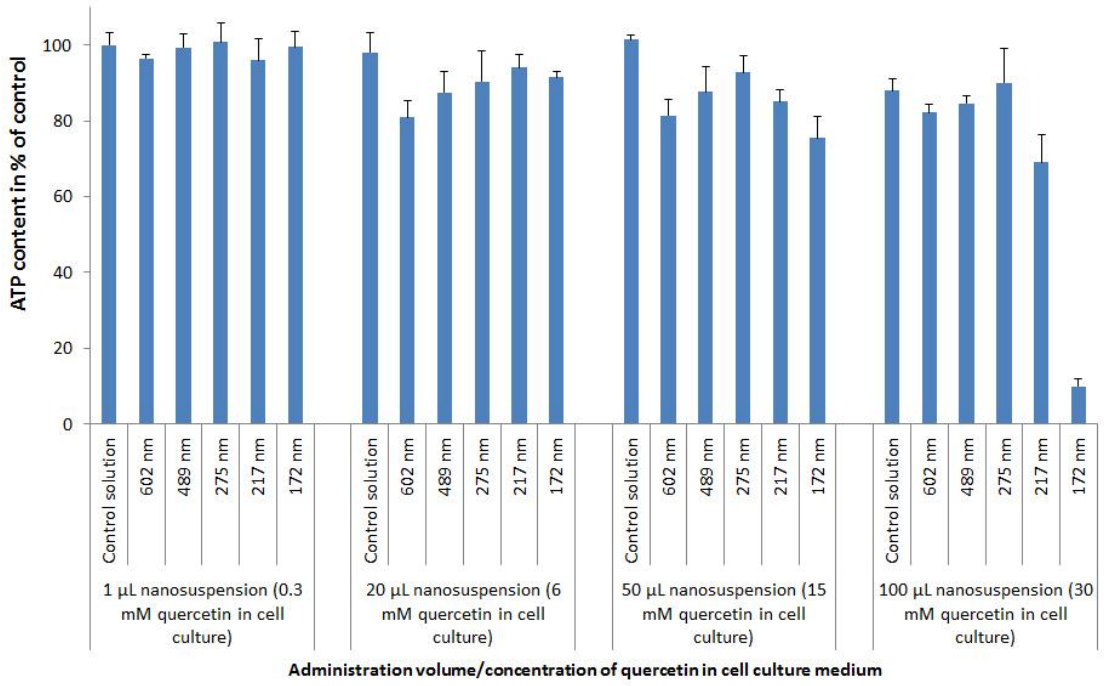

Figure 5 - 4 Cell viability after 24 h incubation in presence of blank control solution, and quercetin nanocrystals with different concentration (original concentration of nanosuspension was **2%**) and sizes (control solution means solution including all the materials except quercetin)

In addition, quercetin nanocrystals with lower concentrations were tested. After 24 h exposure of diluted quercetin nanocrystals (0.2%) to SH-SY5Y cells no statistical significance variation in ATP level was found when comparing to the intact cells (Fig. 5 - 5). Smaller size represents higher solubility, more contact points with cell membrane and more chances for the nanocrystals to be taken up by cells. During the dissolution process of nanocrystals, the size is decreasing. When it achieves below for example 50 nm, the endocytosis can easily happen. Therefore, higher concentration and smaller size make quercetin more potent, including toxic.

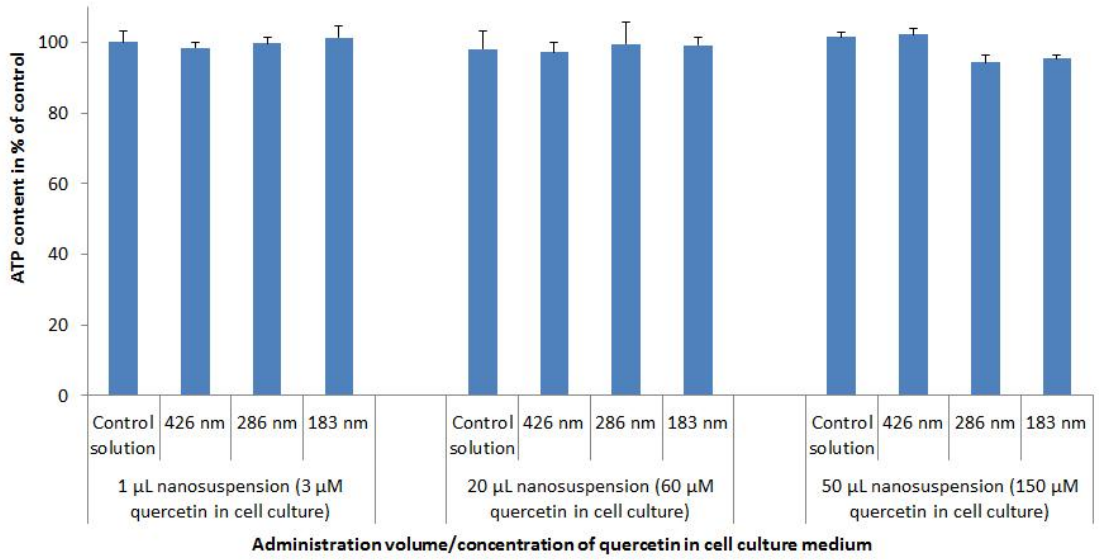

Figure 5 - 5 Cell viability after 24 h incubation in presence of blank control solution, and quercetin nanocrystals with different concentration (original concentration of nanosuspension was **0.2%**) and sizes (control solution means solution including all the materials except quercetin)

5.5.4. Cellular ATP content with toxins and quercetin

The possible neuroprotective effects of nanocrystals of quercetin against SAL-, 3-HK- and 6-OHDA-induced decrease of ATP concentration was evaluated in SH-SY5Y cells. The ATP level in cells was measured after nanocrystals of quercetin or neurotoxins treatment for 24 h as described in 5.2.

To explore whether quercetin DMSO solution and quercetin nanocrystals protect against SAL-, 3-HK- and 6-OHDA-induced ATP depletion in SH-SY5Y cells, neuroblastoma cells were treated with DMSO solution and nanocrystals. The cells were stressed with neurotoxins for 24 h before ATP concentration was measured.

Results from quercetin DMSO solution (Fig. 5 - 6) shows cell viability decreased with the increase of quercetin concentration. 50 µM quercetin administrated via DMSO solution resulted in 63% cell viability, while 60 µM quercetin administrated via nanocrystals (Fig. 5 - 5) all resulted in cell viability above 95%.

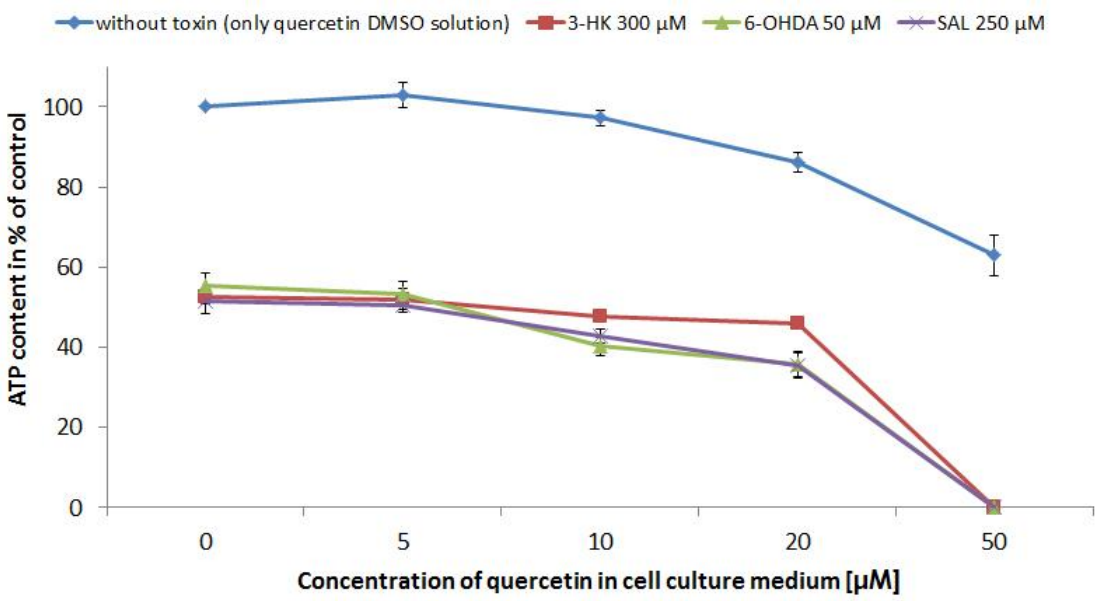

Figure 5 - 6 Cell viability after 24 h incubation with quercetin DMSO solution in presence of toxins (data generated by N. Wszelaki and M. F. Melzig, FU Berlin, Pharm. Biology)

With oxidative stress from the toxins, quercetin DMSO solution presented no positive effect on cell viability. In contrast, application of the solution with concentration of 50 µM even exacerbated the death down to zero cell viability, which is corresponding to the result without toxins. It is obvious that the toxicity mainly came from the solvent DMSO. Although DMSO is used as the vehicle of many poorly soluble actives because of the excellent dissolving ability, the cytotoxicity and the potential to damage cell (Da Violante, Zerrouk et al. 2002; Qi, Ding et al. 2008) have to be concerned. This is another important reason to develop nanocrystals for poorly soluble actives.

Fig. 5 - 7, Fig. 5 - 8 and Fig. 5-9 display that none of the tested 2% quercetin nanosuspensions at any of the concentrations and particle sizes were able to reverse SAL-, 6-OHDA, and 3-HK-induced ATP loss in cultured neuroblastoma SH-SY5Y cells, except for the 172 nm nanocrystals with concentration of 0.3 mM in presence of 6-OHDA. Moreover, it was found that quercetin nanocrystals with small particle sizes with concentrations above 300 µM potentiated the cell death mediated by these neurotoxins.

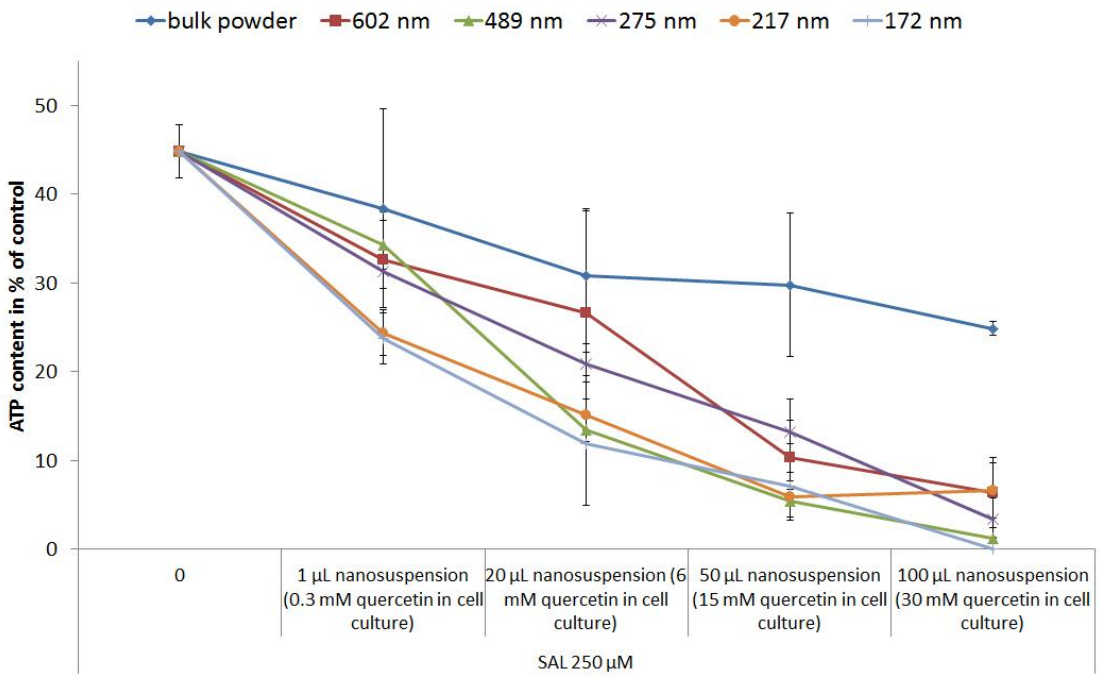

Figure 5 - 7 Cell viability after application of quercetin nanocrystals with different concentrations (original concentration of nanosuspension was 2%) and sizes in presence of SAL 250 µM (data generated by N. Wszelaki and M. F. Melzig, FU Berlin, Pharm. Biology)

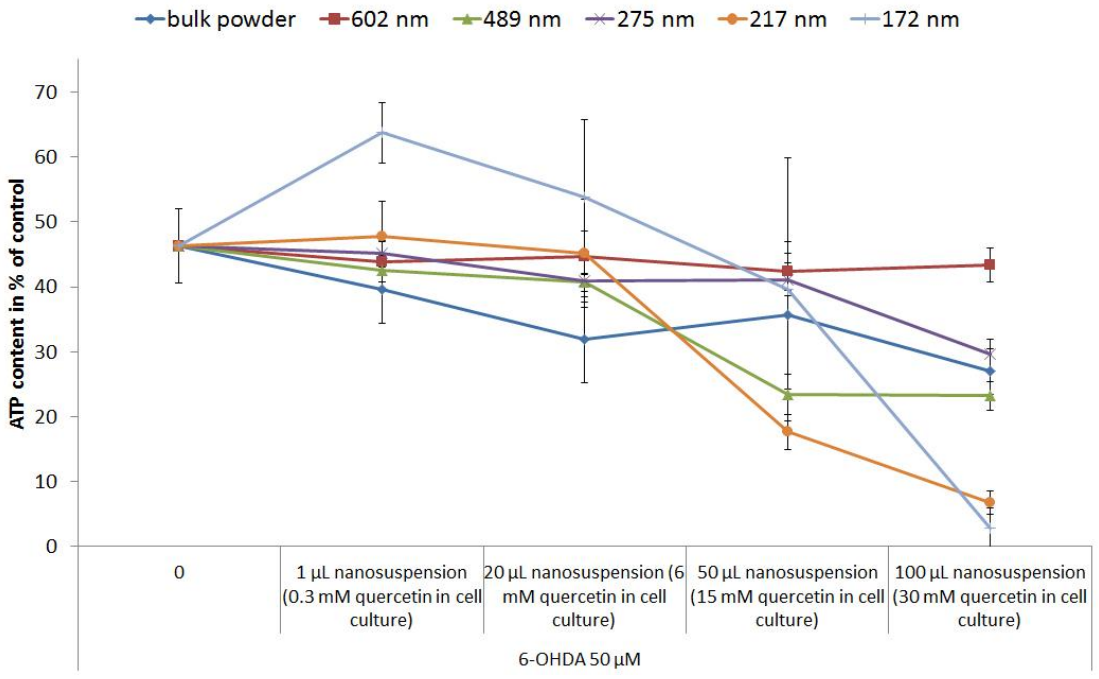

Figure 5 - 8 Cell viability after application of quercetin nanocrystals with different concentrations (original concentration of nanosuspension was 2%) and sizes in presence of 6-OHDA 50 µM (data generated by N. Wszelaki and M. F. Melzig, FU Berlin, Pharm. Biology)

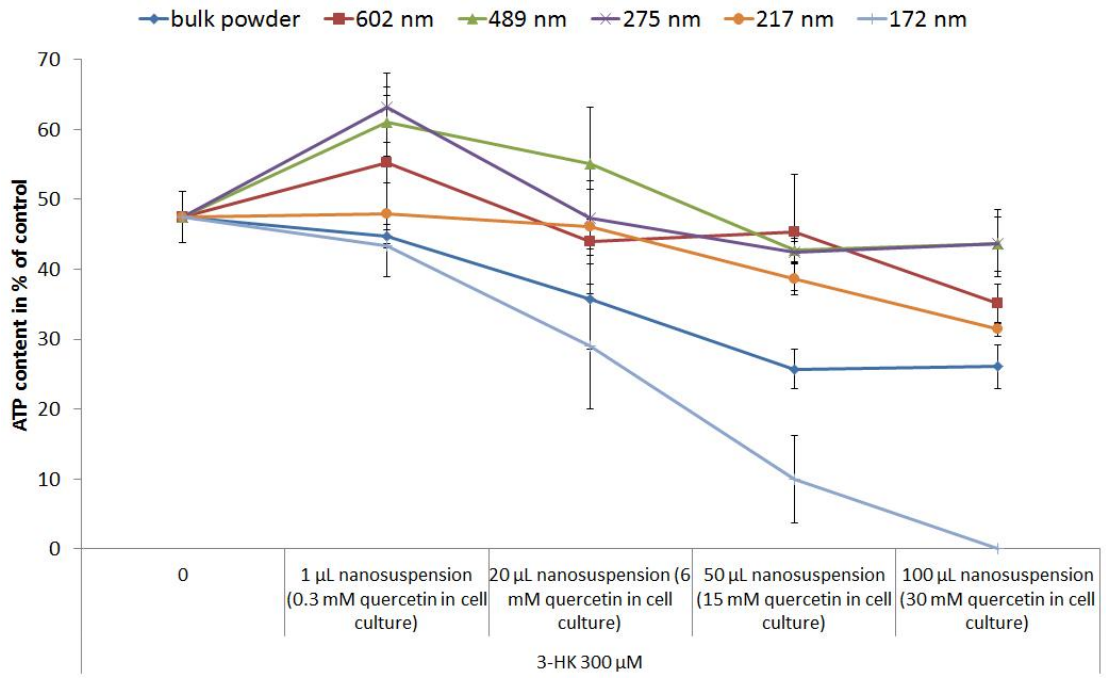

Figure 5 - 9 Cell viability after application of quercetin nanocrystals with different concentrations (original concentration of nanosuspension was 2%) and sizes in presence of 3-HK 300 µM (data generated by N. Wszelaki and M. F. Melzig, FU Berlin, Pharm. Biology)

Contrary to expectations, nanocrystals of quercetin at none of the tested concentrations or particle size were able to increase the reduced level of intracellular ATP induced by SAL, 6-OHDA and 3-HK. Additionally, nanocrystals of quercetin were found toxic to SH-SY5Y neuroblastoma cells. Addition of higher concentrations of nanocrystals of quercetin elevated cytotoxicity caused by neurotoxins in SH-SY5Y. A possible explanation for these results might be that quercetin at higher concentrations induce cell death in many neuronal cell lines due to prooxidative effect (Decker 1997; Metodiewa, Jaiswal et al. 1999; Procházková, Boušová et al. 2011).

Results from these investigations show that quercetin under certain circumstances display prooxidative and cytotoxic (Spencer, Kuhnle et al. 2003) effects. These results further support the idea that the neurotoxicity of nanocrystals of quercetin is due prooxidative effects of quercetin. Furthermore, solution used to suspend the nano-

crystals of flavonoids was found slightly toxic (Fig. 5 - 4, 100 µL nanosuspension). Notably, it demonstrated a correlation between the toxicity of nanocrystals and the particle size. Hence, it could be conceivably hypothesized that the nanocrystals were able to penetrate cell membranes, but rather than the neuroprotective effect, the cytotoxic effect was exerted combined with the neurotoxins of SAL, 3-HK and 6-OHDA to impair, not protect, SH-SY5Y cells. Future studies on the current topic are therefore recommended.

Fig. 5 - 10, Fig. 5 - 11 and Fig. 5 - 12 show that the tested 0.2% quercetin nanosuspensions at lower concentrations in cell culture was less toxic, and the fluctuation with size was also not very significant. This may indicate that only in higher concentration can the influence of size on the in vitro performance be more obvious.

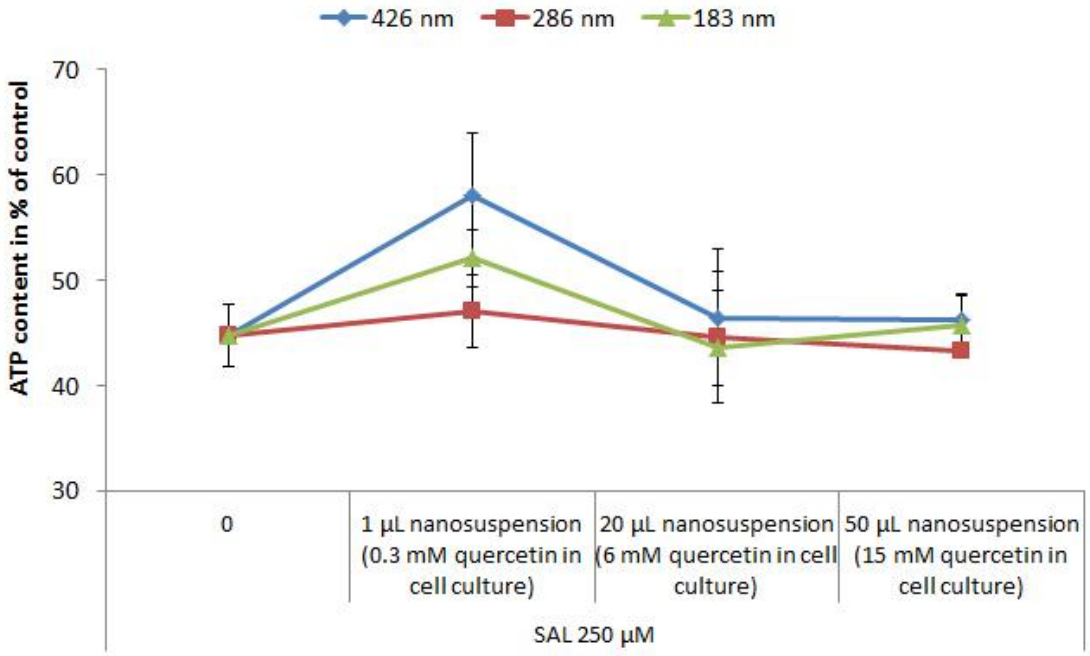

Figure 5 - 10 Cell viability after application of quercetin nanocrystals with different concentrations (original concentration of nanosuspension was 0.2%) and sizes in presence of SAL 250µM (data generated by N. Wszelaki and M. F. Melzig, FU Berlin, Pharm. Biology)

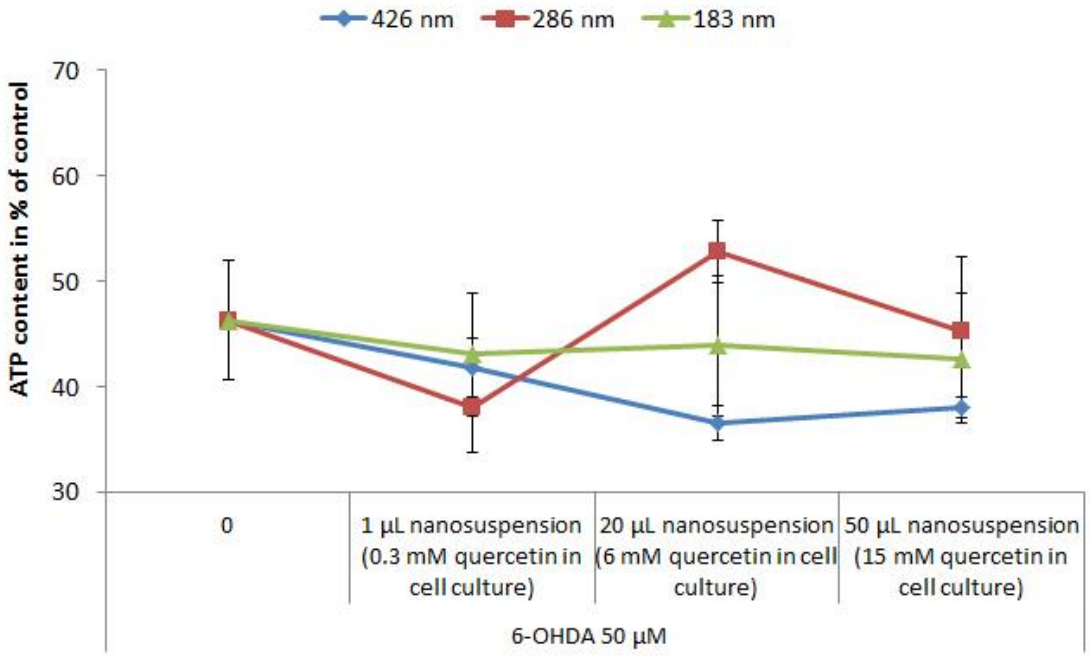

Figure 5 - 11 Cell viability after application of quercetin nanocrystals with different concentrations (original concentration of nanosuspension was 0.2%) and sizes in presence of 6-OHDA 50 µM (data generated by N. Wszelaki and M. F. Melzig, FU Berlin, Pharm. Biology)

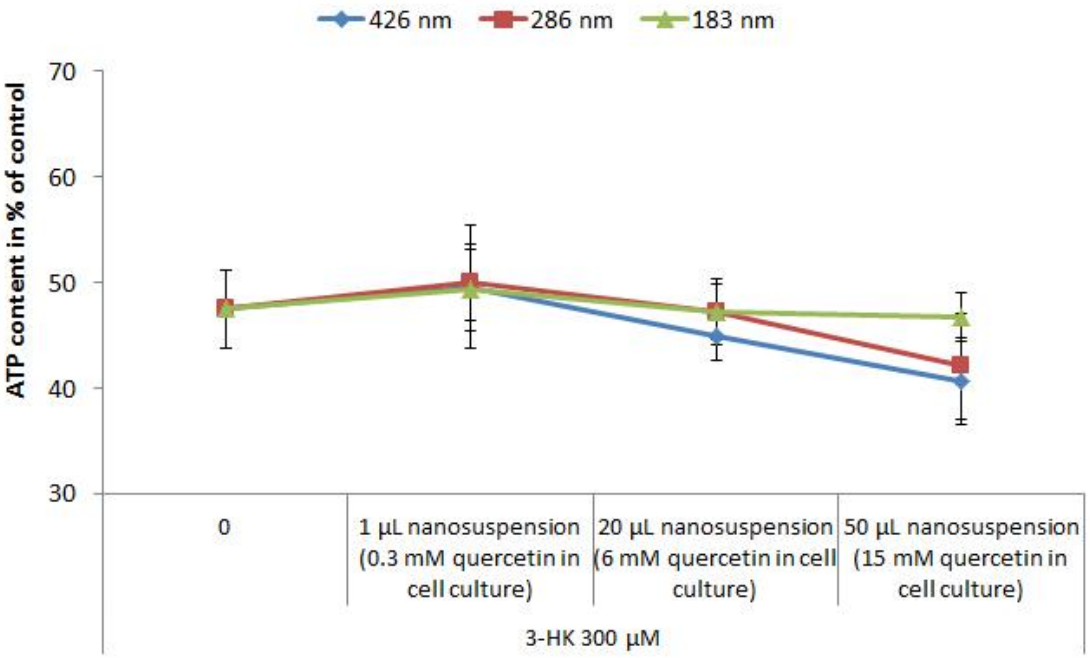

Figure 5 - 12 Cell viability after application of quercetin nanocrystals with different concentrations (original concentration of nanosuspension was 0.2%) and sizes in presence of 3-HK 300 µM (data generated by N. Wszelaki and M. F. Melzig, FU Berlin, Pharm. Biology)

5.5.5. Kinetic saturation solubility of quercetin powder and nanocrystals

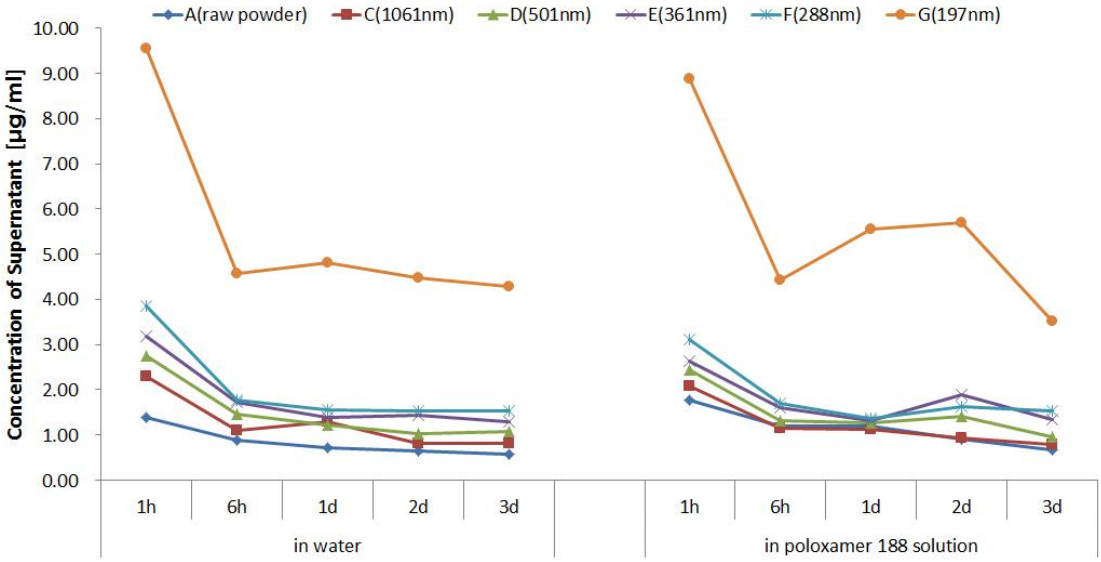

Figure 5 - 13 Kinetic solubility of obtained quercetin nanocrystals in water and in 0.2% Poloxamer 188 solution at 37 °C

Fig. 5 - 13 shows the results of the kinetic solubility of the nanocrystals. With the decreased particle size, the kinetic solubility was increased. The increase was exponential, e.g. nanocrystals of a size of about 500 nm increased the solubility only 2-fold, nanocrystals of a size of about 300 nm increased the solubility 3-fold, whereas nanocrystals of a size of about 200 nm increased the solubility nearly 10-fold. There was no significant difference in the solubility between water and Poloxamer 188 solution (original medium), which means enhanced solubility was also achieved without surfactants. Highest solubility was found after 1 h. After 6 hours, the solubility decreased and remained unchanged over 3 days. The observed changes in solubility over time are well in agreement with further studies. Due to smaller size, the particle surface of nanocrystals possesses a greater curvature, thus a higher dissolution pressure (Müller and Akkar 2004). This leads to a faster and increased dissolution. However, dissolved molecules create a supersaturated environment for large crystals, which leads to recrystallization over time.

This result is corresponding with the in vitro result that the higher solubility brought by the smaller particle size

5.6. Summary

Nanocrystals of different sizes were successfully prepared by high pressure ho-moge-nization. The sizes can be tailor-made from 172 nm to 602 nm via controlling produc-tion parameters. Compared to the quercetin DMSO solution, quercetin nano-crystals in cell culture showed less toxicity because of the exclusion of DMSO. Moreover, size of the nanocrystals was shown to strongly affect the bioactivity of the compound. Smaller crystals lead to a more efficient activity, e.g. uptake by the cells. However, hormesis effect which may be due to the prooxidative effect was shown and related to the concentration as well as the size. Smaller nanocrystals can be absorbed better. Therefore, the identification of the proper concentration and size is important for an efficient neuroprotection of cells. The results also imply that the concern of toxicity should be always noticed, because the variation of properties brought by the decrease of size could be exaggerated in bio-performance. Otherwise, to make active in nano-dimension could be a double-edged sword.

6. ARTcrystals - a new method for the production of nanocrystals on industrial scale

6.1. Preparation of rutin nanocrystals

6.1.1. Pre-treatment of rutin suspension

1 kg batch formulated with 18% (w/w) rutin bulk powder, 2% (w/w) Tween® 80 and 80% (w/w) water was processed by a Miccra D-27 rotor/stator dispersion system (ART Prozess- & Labortechnik GmbH & Co. KG, Germany) with temperature control which kept the temperature under 30℃ during the treatment. Briefly, surfactant solution was attained by dissolving 20 g Tween® 80 in 800 g water, afterwards 180 g rutin was added in to obtain rutin coarse powder suspension. Miccra D-27 system with rotating speed of 24,000 rpm was applied for 4 min continuously to obtain the pre-treated suspension (Fig. 6 - 1). Sample was collected at the end of the dispersing process.

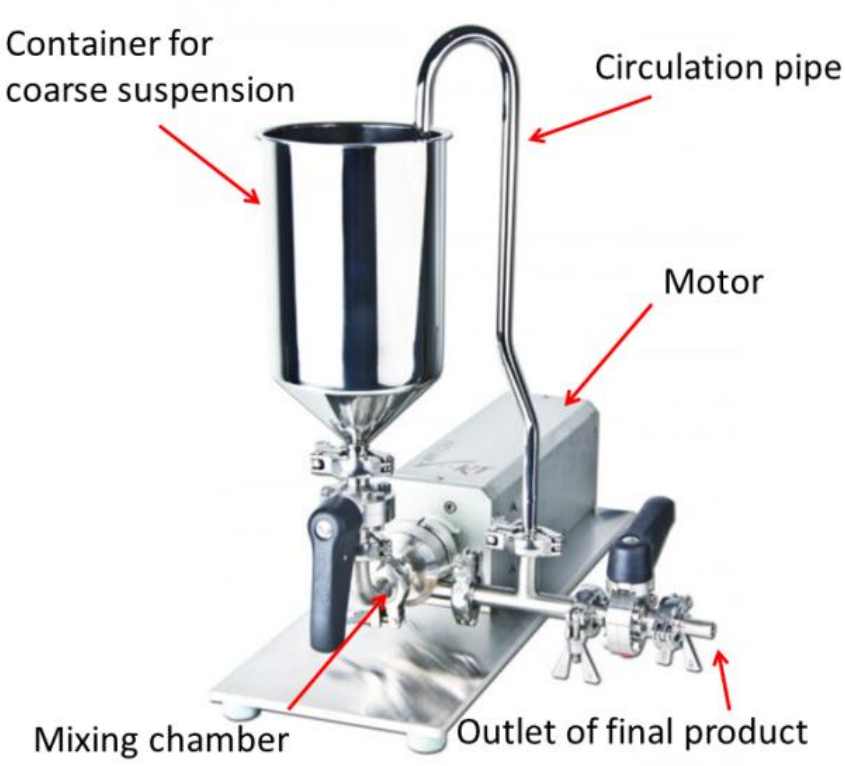

Figure 6 - 1 Miccra D-27 dispersion system (modified after http://www.miccra.com) B: LAB 40 high pressure homogenizer)

6.1.2. Preparation of rutin nanosuspension with low energy/high energy HPH

The pre-treated suspension was diluted with various surfactants solutions to form a series of new formulations (Tab. 6 - 1) with 5% (w/w) rutin concentration. The followed HPH step was conducted by homogenizer LAB 40 (APV Deutschland GmbH, Germany) (Fig. 6 - 2) with a batch size of 40 g. All formulations were treated by an Ultra Turrax T25 (Janke and Kunkel GmbH, Germany) for 1 min at 8000 rpm to re-disperse the samples, followed by two homogenization cycles at 300 bar and 10 cycles at 500 bar, which was called low energy HPH. After 1 and 2 cycles at 300 bar, 1, 5 and 10 cycles at 500 bar, samples were collected to perform further characterization.

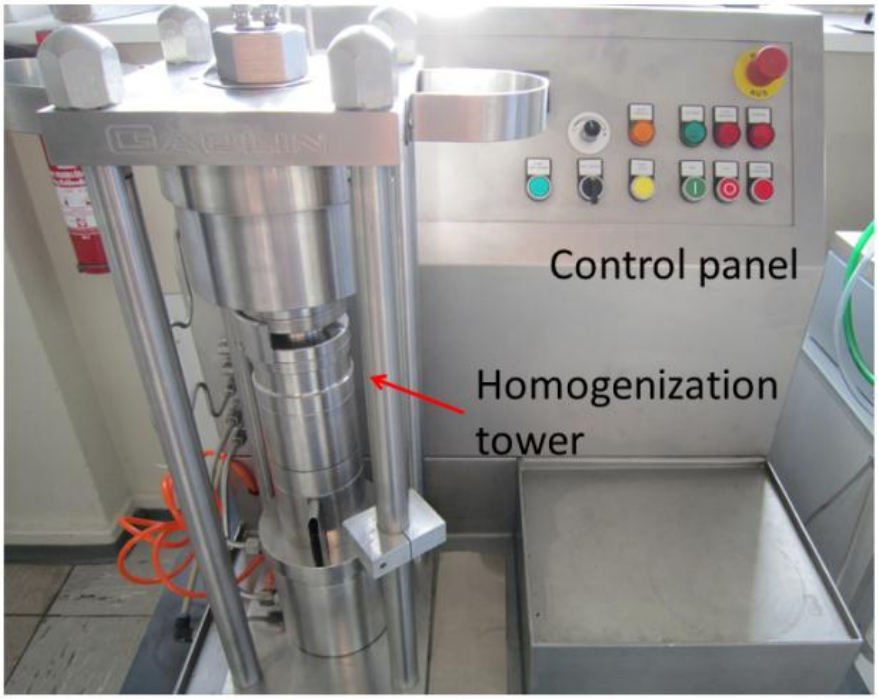

Figure 6 - 2 APV Micron LAB 40 high pressure homogenizer

To compare the efficiency of production, formulation A was also performed by high energy HPH, which included two cycles at 250 bar, 500 bar, 750 bar and 1000 bar

respectively as pre-milling followed by 20 cycles at 1500 bar, after re-dispersion. Samples were collected after pre-milling, 1, 5, 10, 15, and 20 and homogenization cycles at 1500 bar. Production parameters for the formulations in all related figures in this study are listed in Table 6-2.

Table 6 - 1 Formulations of rutin suspension after dilution with different surfactant solutions

Formulation	Formulation composition (% w/w)					
	Rutin	Tween® 80	Poloxamer 188	Plantacare® 2000 UP	SDS	water
A	5%	2%	-	-	-	93%
B	5%	0.56%	1%	-	-	93.44%
C	5%	0.56%	-	1%	-	93.44%
D	5%	0.56%	-	-	0.2%	94.24%

Table 6 - 2 Production parameters in related figures

		Pre-treatment with MICRRA D27	Pretreatment with Ultra Turrax T25	Pre-milling (cycle number*pressure [bar])	Main-milling (cycle number*pressure [bar])
Figure 6 - 3	Without HPH	4 min	No	No	No
Figure 6 - 4	High energy HPH	4 min	1 min	2*250, 2*500, 2*750, 2*1000	20*1500
Figure 6 - 5	Low energy HPH	4 min	1 min	No	2*300, 10*500
Figure 6 - 6	Low energy HPH	4 min	1 min	No	2*300, 10*500
Figure 6 - 7	Low energy HPH	4 min	1 min	No	2*300, 10*500
Figure 6 - 8	Low energy HPH	4 min	1 min	No	2*300, 10*500

6.2. Result and discussion

6.2.1. Pre-treatment

The pretreatment step by using the Miccra D27 decreased the size of the bulk material. The median size of the bulk material was 22 µm (d(v)50%). About 10% of the particles possessed a size larger than 99 µm (d(v)90%). 1% of the particles possessed a size larger than 644 µm (d(v)99%). After processing the median particle size was reduced to 5 µm (d(v)50%). 90% of the volume of the particles were smaller than 55 µm (d(v)90%) and 99% of the particles were smaller than 92 µm (d(v)99%). Light microscopy revealed the presence of some agglomerates (Fig. 6 - 2).

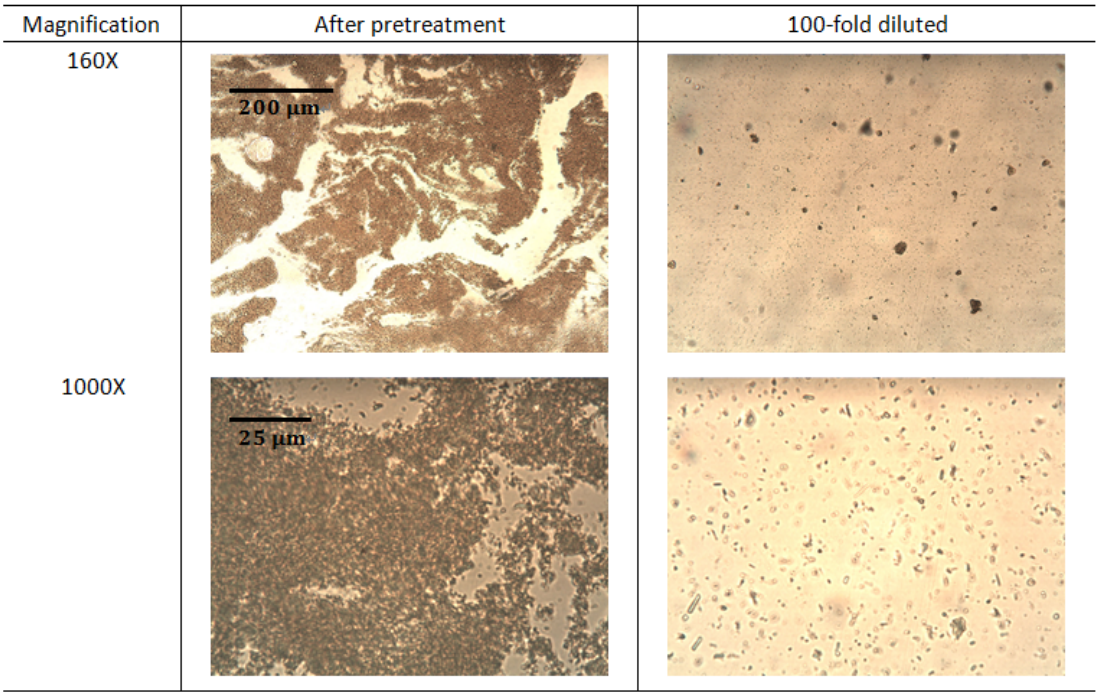

Figure 6 - 3 Light microscopy pictures of pretreated rutin suspension by Miccra D-27

6.2.2. Production of nanocrystals by conventional HPH

The pre-suspension obtained was then subjected to the conventional homogenization process, being typically applied to produce nanocrystals by high pressure homogeni-

zation. This procedure involves three steps (Grau, Kayser et al. 2000; Krause and Müller 2001; Keck and Müller 2006; Kobierski, Ofori-Kwakye et al. 2009):

1. the dispersion of the material with a rotor/stator system to destroy agglomerates and larger particles,

2. pre-milling with the homogenizer to diminish large particles,

3. high pressure homogenization.

The pre-milling step is the homogenization at lower pressures, i.e. below 1000 bar. In this step the energy input into the suspension is low. Homogenization at lower pressures only reduces the size of large particles, whereas smaller sized particles remain unchanged in size. Consequently, the pre-milling step does not necessarily lead to a decrease in the mean size, but to a narrower size distribution.

Subsequent homogenization at high pressures, i.e. by applying multiple cycles at 1500 bar reduces the particle size, leading to drug nanocrystals. The size of the nanocrystals obtained depends on the physicochemical properties of the material, e.g. hardness, crystalline state and number of imperfections within the crystalline lattice of the raw material.

The final size of nanocrystals also depends on the size of the raw material. Typically it is observed, that a smaller the size of the starting material leads to a smaller size of the nanocrystals. The same applies for the size distribution of the particles, the narrower the size distribution of the starting material is, the narrower the distribution of the nanocrystals after HPH will be.

A narrow size distribution is a pre-requisite for a long-term physically stable nanosuspension, because homogenously sized particles possess least Ostwald-Ripening. In that sense the pre-milling step is an essential treatment for the pre-suspension, be-

cause it reduces the size distribution. The pre-milling step is a low energy step, i.e. mild conditions are applied to the homogenized material.

The subsequent homogenization of the material at high pressure is a high energy step, i.e. the material is forced through a very small gap with high energy. This leads to a high energy input into the system and due to dissipation of most of the energy, to a strong increase in temperature. Hence, there is a harsh condition for both the suspension and the homogenization equipment. Consequently, the production of nanocrystals by using this method should minimize the number of homogenization cycles at higher pressures and ensure an efficient pre-milling step.

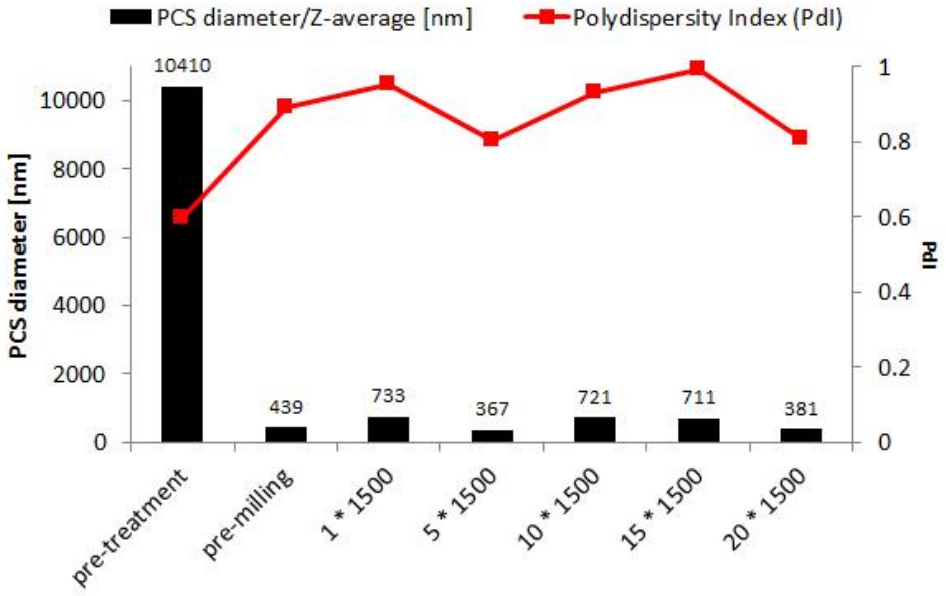

Figure 6 - 4 PCS diameters and PdIs of ruin nanocrystals produced in high energy HPH (formulation A)

In this study step 1 (dispersion with rotor/stator) was performed for 1 min. The pre-milling step was performed by applying 2 cycles at 250 bar, 500 bar, 750 bar and 1000 bar, respectively. HPH was performed by applying 20 cycles at 1500 bar. The particle size was analyzed after step 1 and 2 and after 1, 5, 10, 15 and 20 cycles of HPH within step 3. As starting material the suspension pre-treated with the Miccra D27 was used (cf. 6.1.1). The results obtained are shown in Fig. 6 - 4 and Fig. 6 - 5.

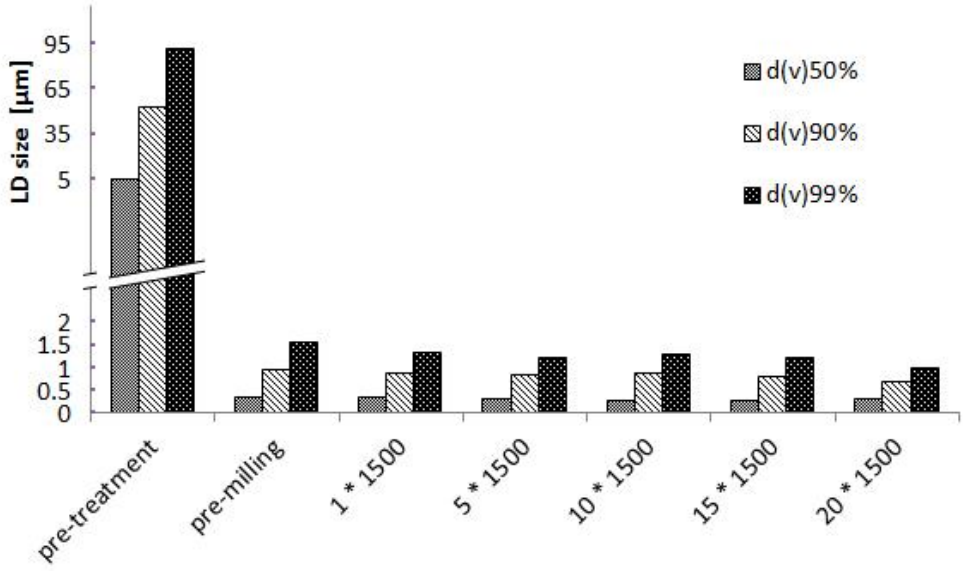

Figure 6 - 5 LD sizes of ruin nanocrystals produced in high energy HPH (formulation A)

After pre-treatment, PCS diameter came to about 6 µm with PdI of 0.6. The particle sizes decreased obviously to less than 500 nm only after pre-milling, then fluctuated when the cycles at 1500 bar were applied. Interestingly, the PdIs were extremely high when the samples were subjected to HPH. It may be due to the existence of a large number of aggregates during PCS measurement. Because of the high energy input, particles could be diminished and de-aggregated more efficiently whereas the large particles still existed even after 20 cycles at 1500 bar homogenization, which contributed to the high PdI.

The LD size of rutin nanosuspensions in Fig. 6 - 5 also shows a reasonable accordance with PCS results. After the pre-milling step, the size of most particles (>99%) was decreased to below 1.6 µm. From the 1st to the 20th cycle at 1500 bar homogenization, the size distributions have a general but very slight decline. In theory, more ordered crystals lattice leads to better stability and hardness, imperfection or disorder in between the crystals lattice will make that part unstable and easy to be broken (Kobierski, Ofori-Kwakye et al. 2009). In the process of particle diminution, the imperfection part of rutin crystals is becoming less. Meanwhile, the disordered lattice

could be also structurally rearranged into the ordered because of the energy input during the homogenization process. The fluctuation of PCS diameter and high PdI may imply that prolonged homogenization time are not necessary for decreasing the size of particles further but could bring reversible aggregate formation due to the heat generated by the excessive energy.

6.2.3. Production of nanocrystals by low energy HPH

Based on the observation, the size reduction of the particles after the pre-treatment step was only small, while a production with a modified pre-milling step was performed. The aim of this study was to analyze the efficacy of the pre-milling step and to investigate if pre-milling alone can be used for the production of nanocrystals after a pre-treatment with the Miccra system. For this the suspension pre-treated with the Miccra D27 was only subjected to step 1, followed by 2 cycles at 300 bar and 10 cycles at 500 bar. Step 3, i.e. HPH at 1500 bar was not performed. The results obtained from this low energy production method are shown in Fig. 6 - 6.

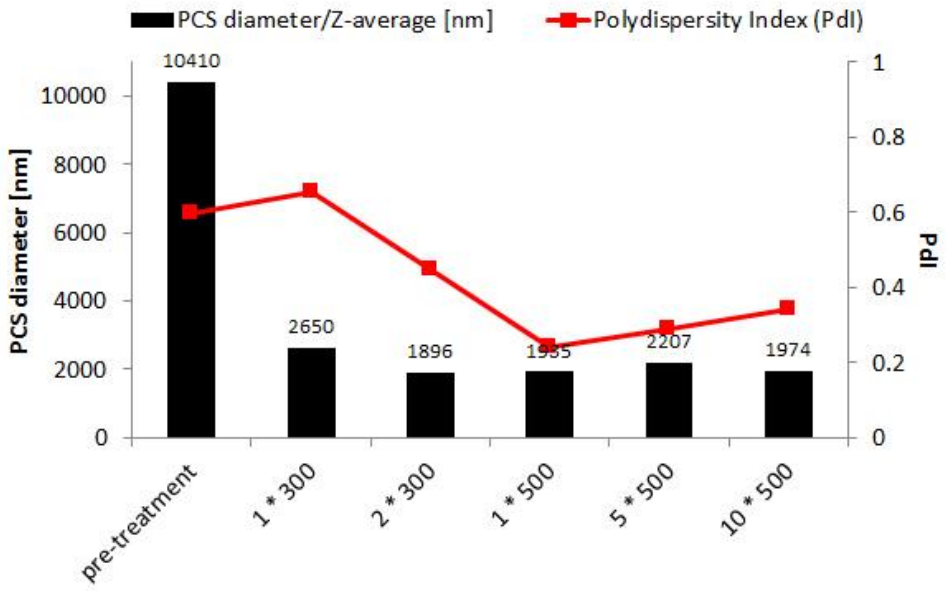

Figure 6 - 6 PCS diameters and PdIs of ruin nanocrystals produced in low energy HPH (formulation A)

PCS diameter came to about 10 μm with PdI of 0.5 after pre-treatment with the Miccra system. The particles size of each sample slightly fluctuated except a sharp decline in the first cycle at 300 bar homogenization. However all of them were above 1500 nm, while the PdI had a general decrease in the first three cycles. This phenomena indicates an aggregation of particles on account of less of energy input in the system, also implies the narrowing of size distribution range with the increase of homogenization cycles.

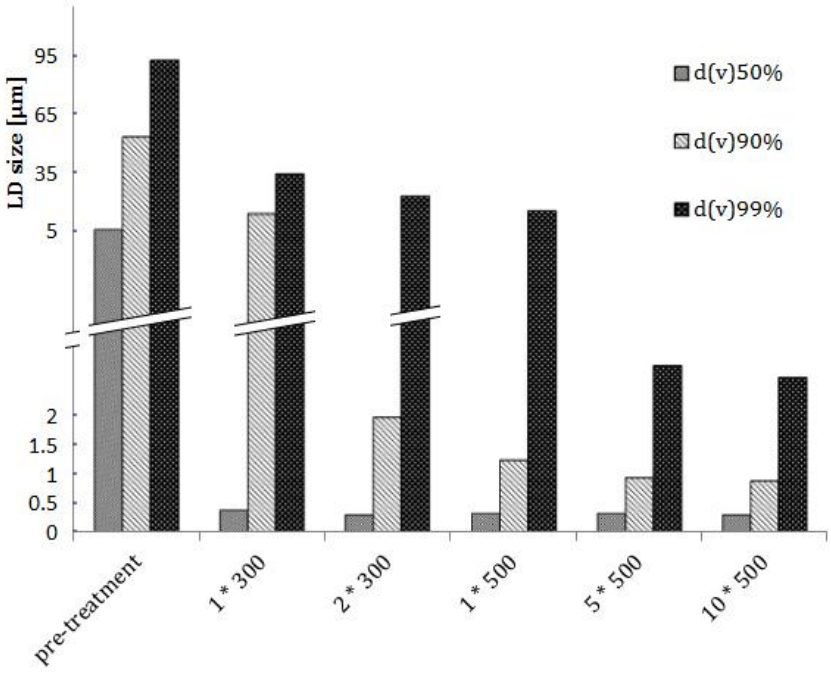

Figure 6 - 7 LD size of ruin nanocrystals produced in low energy HPH (formulation A)

The LD size of rutin nanosuspensions under low energy HPH was shown in Fig. 6 - 7. After pre-treatment, d(v)50% was about 5 μm, however d(v)99% was around 92 μm which indicated there were large rutin particles and wide distribution range. Pronounced decreases were found in all the three parameters after only one cycles at 300 bar homogenization, especially the d(v)50% was quickly reduced to 380 nm, which means that the most fragile part of the particles can be easily broken into very smaller nanocrystals by a low energy HPH. Then in the second cycle at 300 bar, d(v)90% was

reduced to less than 2 µm. Less than 3 µm of d(v)99% was observed in the fifth cycles at 500 bar and the size stayed steady in the further cycles.

6.2.4. Production of nanocrystals with different surfactants by low energy HPH

The results obtained led to the conclusion, that the efficacy of Tween® 80 to stabilize the particles is only limited. This may be due to the poor stabilizing ability of Tween® 80 (Mishra, Al Shaal et al. 2009). Surfactant can occupy the surface of particles to prevent the aggregation and maintain the dispersion status. The covering speed of surfactant and the repulsion between surfaces determine the final size of nanocrystals and the stability, which are influenced by the physicochemical properties of active and surfactant.

What needs to be concerned as well is "bridging effect" (Otsubo 1994) which could happen when particle is small enough to be trapped by the polymer chain of non-ionic surfactant, thus forming an irreversible increase of particle size. Monolayer of Tween® 80 on the surface of the particles could be also sufficient. Combining different surfactants could improve this situation via stabilizing the nanosuspension in different mechanisms and methods. Therefore, the low energy production was repeated by using different stabilizers, i.e. Poloxamer 188, Plantacare® 2000 UP and SDS. Similar to Tween® 80, these surfactants are generally recognized as safe for human use and were previously shown to be suitable for the stabilization of various nanocrystals (Teeranachaideekul, Junyaprasert et al. 2008; Kobierski, Ofori-Kwakye et al. 2009; Lai, Pini et al. 2011). The pre-formulations were prepared by diluting the pre-suspension with the different surfactant solutions. The composition of the formulations is shown in table 6 - 1. Fig. 6 - 8 gives the result of PCS, Fig. 6 - 9 displays the LD size, and Fig. 6 - 10 presents the light microscopic images of the four formulations after 10 cycles at 500 bar.

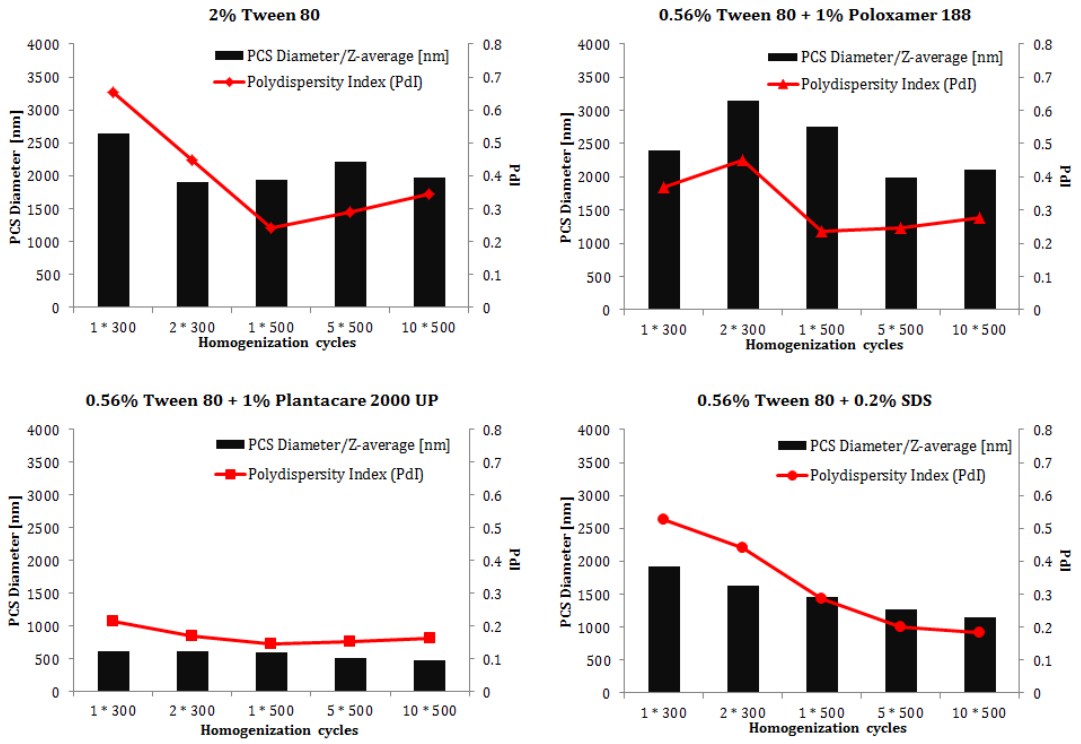

Figure 6 - 8 PCS diameters and PdIs of rutin nanocrystals as a function of homogenization cycles in low energy HPH using different surfactants combinations

Fig. 6 - 8 presents the results of PCS diameter and PdI of the four formulations as function of homogenization cycles. The smallest particle size was obtained by formulation including Tween® 80 and Plantacare® 2000 UP (formulation C) as the stabilizers. After the first cycle at 300 bar, the size of C had already achieved 600 nm whereas the other three were all above 1500 nm. After the preliminary step that only 4 min dispersing process without separation by Miccra D-27 and one cycle at 300 bar low energy HPH, nanocrystals with size around 600 nm can be obtained. In formulation with only Tween® 80 (formulation A) and with Tween® 80 plus Poloxamer 188 (formulation B), particle size fluctuated around 2000 nm with an overall decline in PdI. Formulation with Tween® 80 and SDS (formulation D) had a steady down-sizing but all the sizes were all above 1000 nm. Therefore, only Tween® 80, or Tween® 80 plus Poloxamer 188, or Tween® 80 plus SDS are all insufficient to stabilize rutin nanocrystals well. During the 500 bar homogenization, the size of formulation C de-

creased from 587 nm after the first cycle to 479 nm with PdI about 0.15 which implied a narrow size distribution. The addition of Plantacare® 2000 UP may effectively de-aggregate the sample from pre-treatment and during the homogenization.

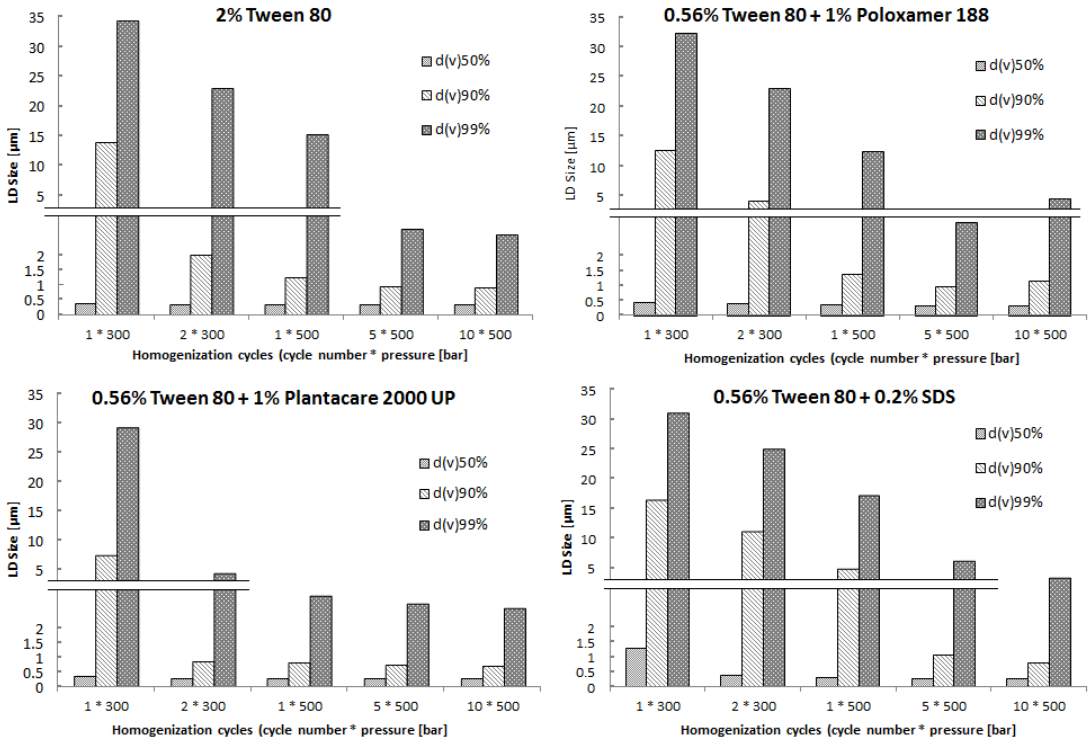

Figure 6 - 9 LD size of rutin nanocrystals as a function of homogenization cycles in low energy HPH using different surfactants combinations

The LD size results from Fig. 6 - 9 are in accordance with PCS results. Unsuited surfactants in formulation A, B, and D made the production of rutin nanocrystals difficult and time-consuming. However, the involvement of Plantacare® 2000 UP, which can be considered as a suitable surfactant in this comparison, made the process easy and fast, only after two cycles at 300 bar, d(v)99% was less than 4 µm.

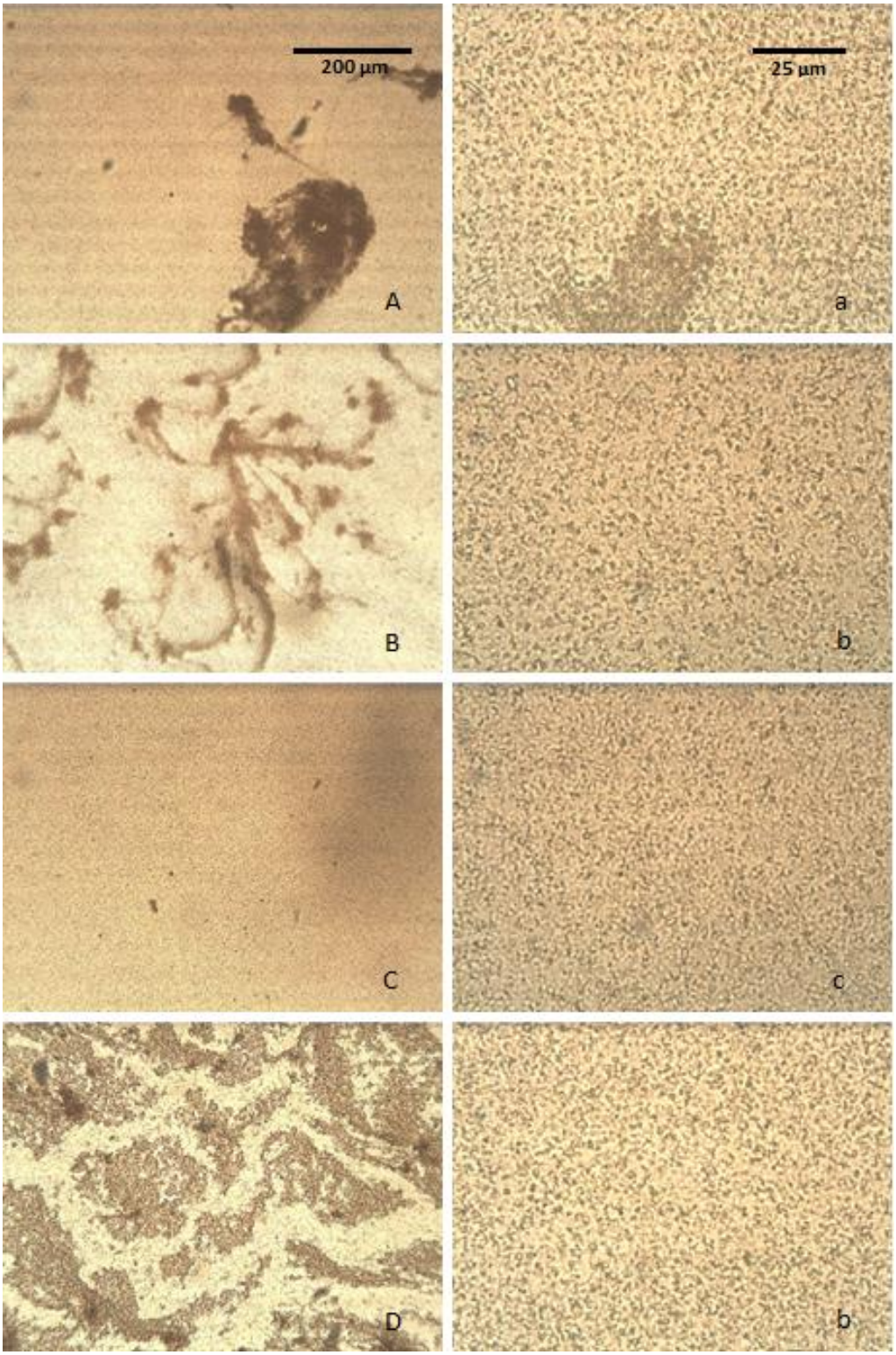

Figure 6 - 10 Light microscopic pictures of rutin nanosuspensions produced in low energy HPH after 10 cycles at 500 bar in 160 fold magnification (capital letter) and 1000 fold magnification (small letter) (A and a represent “formulation A”, and so forth)

Light microscopy is normally applied to detect the aggregate of nanocrystals and the large crystals existing in the system which are larger than 1μm. In smaller magnification, it can confirm the results from PCS and LD. In higher magnification, it can estimate the surfactant efficiency by observing the movement of particles under the microscope. Fig. 6 - 10 shows the pictures of the four formulations after 10 cycles at 500 bar in the low energy HPH. In 160 fold magnification, A, B, and D all show obvious aggregations, only nanocrystals in C dispersed evenly. The size difference which is indicated in the pictures of 1000 fold magnification is not as obvious as that the PCS results showed, while formulation C indeed presents the smallest nanocrystals. This phenomenon was caused by that in formulation A, B, and D, the PCS results were mainly influenced by the aggregations rather the true size of nanocrystals. Either for the efficiency of nano-sizing or for de-aggregating, the advantage of Tween® 80 combined with Plantacare® 2000 UP has been both proven by direct observation.

In addition the zeta potential of the suspensions was analyzed. The results are shown in Fig. 6 - 11.

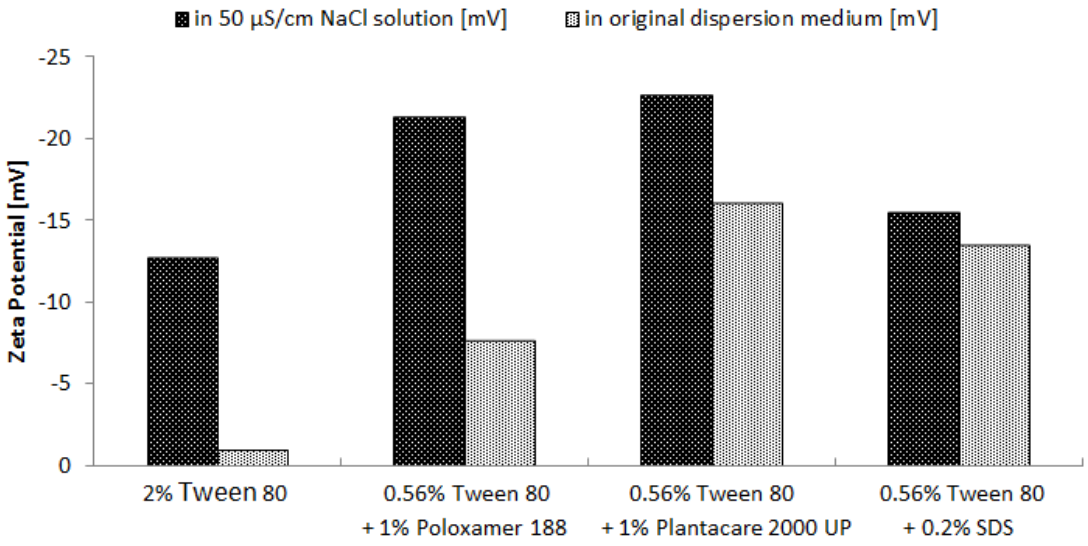

Figure 6 - 11 Zeta potential of rutin nanosuspensions produced in low energy HPH after 10 cycles at 500 bar in original dispersing medium and in purified water (conductivity adjusted to 50 µS/cm using 0.9% NaCl solution)

The measured zeta potential fully confirms the size results and the results obtained by light microscopy. The nanocrystals stabilized by 2% Tween® 80 had the lowest ZP value because of the long spacer of Tween® 80 around the surface of the particle. Normally, long loop of the polymer could exclude particles each other in a long distance, thus ZP is low based on the DLVO theory. However, in this case, the long loop might lead to the bridging effect causing the aggregation. On the other hand, in NaCl solution the Tween® 80 was diluted. The particles could be closer, hence higher ZP value. In contrast, the nanocrystals stabilized by 0.56% Tween® 80 and 1% Plantacare® 2000 UP had the lowest ZP value in NaCl solution and original medium as well. Therefore, compared to the others, this formulation made the diffusion layer closer to the Stern layer and brought higher electrostatic repulsive force between particles. In NaCl solution this repulsive force was enhanced by more ions.

6.2.5. Comparison to conventional production methods

The size results from this study were compared to the conventional, most commonly applied production techniques, i.e. high pressure homogenization, bead milling, bead milling and subsequent homogenization (CT process) (Keck 2007). Results from the new method led to almost similar results as BM and BM+HPH, furthermore resulted in smaller particles when compared to HPH. However, the time needed for the production of equal amounts of nanosuspensions was much less. Due to an efficient pre-treatment by Miccra D-27 system, the size of bulk powder is significantly decreased in two ways:

1. The particle itself is broken into several pieces;

2. The aggregate of the particles is disintegrated.

Furthermore, the smaller crystals may be damaged on the surface to generate defect which can be exaggerated during the further HPH. The structure of more aggregates

which have been not yet disintegrated may become much looser, which can facilitate the diminution in further HPH as well.

6.2.6. Long-term stability

Physical stability of produced nanosuspensions can be affected by the production method. Reasons for this are differences in homogeneity of particle size and supersaturation effects which can cause crystal growth or crystal bridging. For the smartCrystal CT process of combining bead milling with subsequent HPH it was reported that the long-term stability was higher compared to bead milling alone (Al Shaal, Müller et al. 2010). The obtained nanosuspensions were stored at room temperature and size analyzed by PCS and LD. The produced nanosuspension was stable at room temperature for 6 months, no relevant size increase occurred (Fig. 6 - 10).

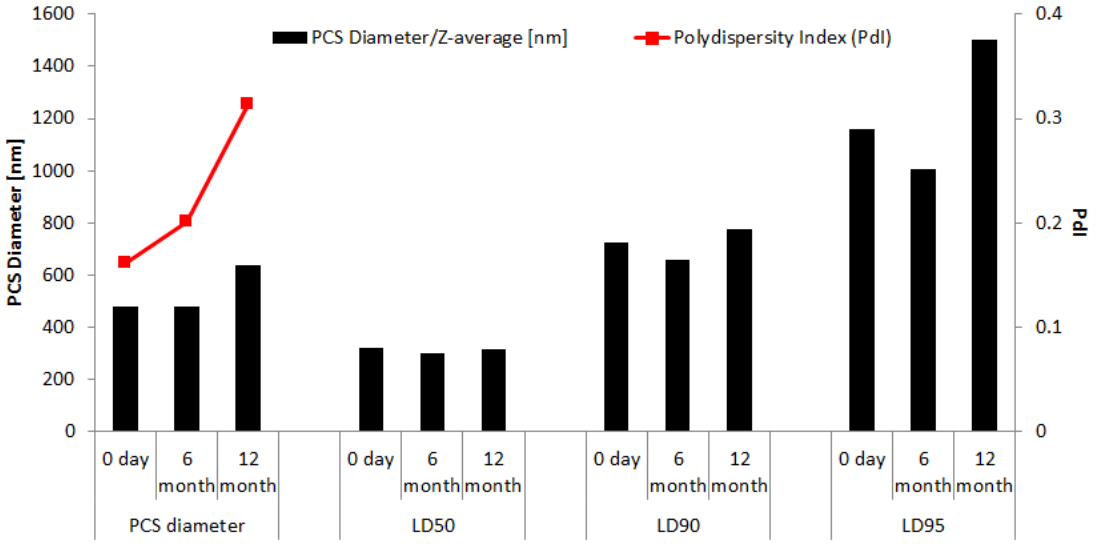

Figure 6 - 12 Stability of rutin nanosuspension stabilized with 0.56% Tween® 80 and 1% Plantacare® 2000 UP (optimized formulation) as function of time (PCS diameter and polydispersity index (PdI), LD diameters 50%, 90% and 95%, stored at room temperature)

However, after 1 year, the increase in size was significant which indicates that the existence of aggregates lead to an overall size increase in a long run because of the

Ostwald ripening. Therefore, the further work should focus on how to diminish the remained small portion of large particles.

6.3. Summary

The combination of rotor/stator dispersion using the ART D27 Miccra system followed by HPH at a low pressure is a suitable method for the production of nanocrystals. The size of the obtained particles is similar to the conventional methods, e.g. high pressure homogenization, bead milling or the combination of bead milling and HPH at low pressures (CT-process). The advantage of the new method is the efficacy. The time required for production is less than the requirement of the conventional methods. Furthermore, the method is simple and less energy-consuming, meanwhile it avoids harsh production conditions. Therefore, the new method is a promising alternative for the production of drug nanocrystals.

7. smartCrystals - large scale production and reproducibility of hesperidin nanocrystals

7.1. Production procedure

Wet bead milling and high pressure homogenization are both regarded as the main efficient method to production drug nanocrystals (Keck and Müller 2006; Merisko-Liversidge and Liversidge 2011). Each of them can individually produce drug nanocrystals. However, wet bead milling has a very long processing time and has high risk of introducing microbial contamination. High pressure homogenization is a high energy process and is normally not as efficient as the wet bead milling can do to diminish the particles.

The smartCrystal technology (Keck, Kobierski et al. 2008; Al Shaal, Müller et al. 2010; Al Shaal, Shegokar et al. 2011) combines the wet bead milling and high pressure homogenization together to produce nanocrystals, which can generate smaller size, save energy and involve the anti-bacteria process in the final step. The production in this study can be divided into the following steps: (Tab. 7 - 1)

1. Drug bulk powder was dispersed in surfactant solution with preservative in high concentration, i.e. 18%, in 18 kg batch.
2. The powder suspension was passed through bead mill PML-2 (Bühler, Switzerland) with 1050 ml milling chamber and 75% volume of Yttria stabilized zirkonia milling beads of size 0.4–0.6 mm (Hosokawa Alpine, Germany) as milling media. After several passages in continuous mode with 2000 rpm of rotator speed and 10% of pump capacity, the concentrate was obtained. During the production, the milling chamber was kept at 5 ℃.
3. The milled nanosuspension was diluted to 5% drug content (18 kg batch) dilution, followed by once or twice high pressure homogenization using a homogenizer Avestin EmulsiFlex-C50 in low pressure to obtain the final product. During the production, the product from inlet of the HPH was kept at 5 ℃. Totally, three batches were performed identically.

Table 7 - 1 Formulation and production conditions of hesperidin nanosuspension in different steps

Condition of hesperidin nanosuspension production		
Formulation of concentrate	Content of drug	18%
	Surfactant	1% Kolliphor® P 188
	Preservative	1% Euxyl® PE9010
	Injectable water	80%
WBM	Number of pass through WBM	5
	Pump efficiency	10%
	Size of beads	0.4–0.6 mm
	Milling speed	2000 rpm
Formulation of dilution	Content of drug	5%
	Surfactant	1% Kolliphor® P 188
	Preservative	1% Euxyl® PE9010
	Content of glycerin 87%	5%
	Injectable water	88%
HPH	Pressure of HPH	500 bar
	Number of cycle	1

The whole process can be graphically displayed as Fig. 7 - 1.

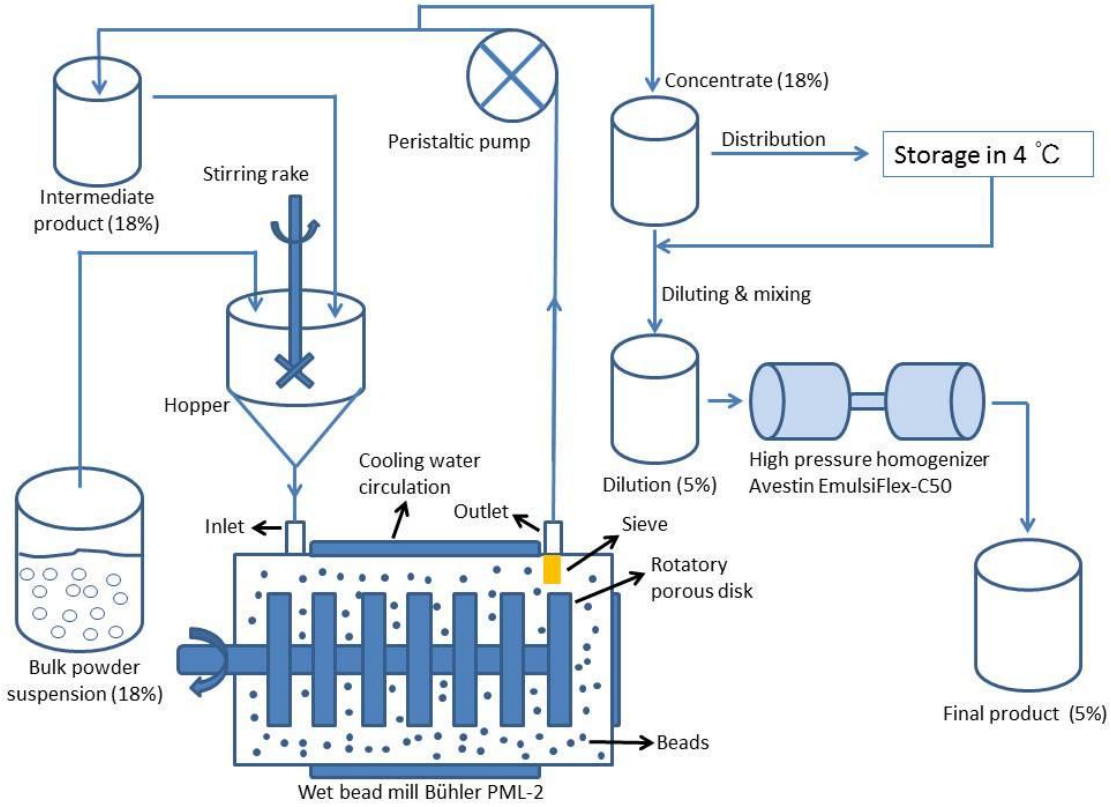

Figure 7 - 1 Schematic diagram of the production process (% means concentration of drug)

7.2. Wet bead milling step

The principles of diminution in wet bead milling is: (Fig. 7 - 2)

a. The collision between the particle and beads.

b. The attrition between the beads.

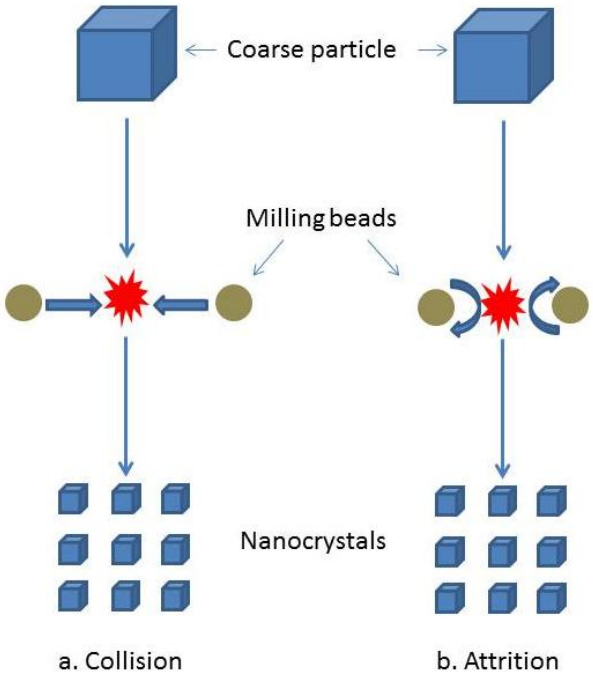

Figure 7 - 2 Principles of diminution in wet bead milling: a. collision; b. attrition

When the rotatory porous disk is moving, the beads inside the milling chamber will also move fast to collide each other to generate force to break the particles. The attrition also happens intensively when the beads move form bottom to up. Because the beads are harder than the drug particles, the beads can break the drug particles with integrity of themselves. The density of the beads (3.8 kg/L) is higher than the drug, therefore to prevent the drug particles from dropping to the bottom. An efficient mixing, collision and attrition can be ensured. Theoretically, the beads with smaller size will also gain smaller product because the contact surface and collision intensity and attrition will be also lifted (Peltonen and Hirvonen 2010).

Generally, the size should be decreased with increasing of the milling time. The process of particles' diminution during the wet bead milling was monitored. Fig. 7 - 3 shows the results of PCS and LD after each passage of the milling for hesperidin. The steady decrease of size can be observed in both of them. Only after one passage, the PCS diameter was decreased to 539 nm. However, the existence of large particles was declared by LD since the d(v)50% was 1.748 µm. From the second passage on, the d(v)10% was stayed below 0.15 µm, which means the smallest mean size of the

nanocrystals was achieved only after two passage. On the other hand, further milling is still essential due to the large particles in the suspension would broaden the size distribution thus cause the instability of the nanosuspension system according to the Ostwald Ripening. After the 5th passage, the PCS diameter achieved around 290 nm with PdI of 0.237. The decrease of average size was not very significant, but d(v)90% became lower than 1.5 µm, which indicated that only a little part of large particles existed.

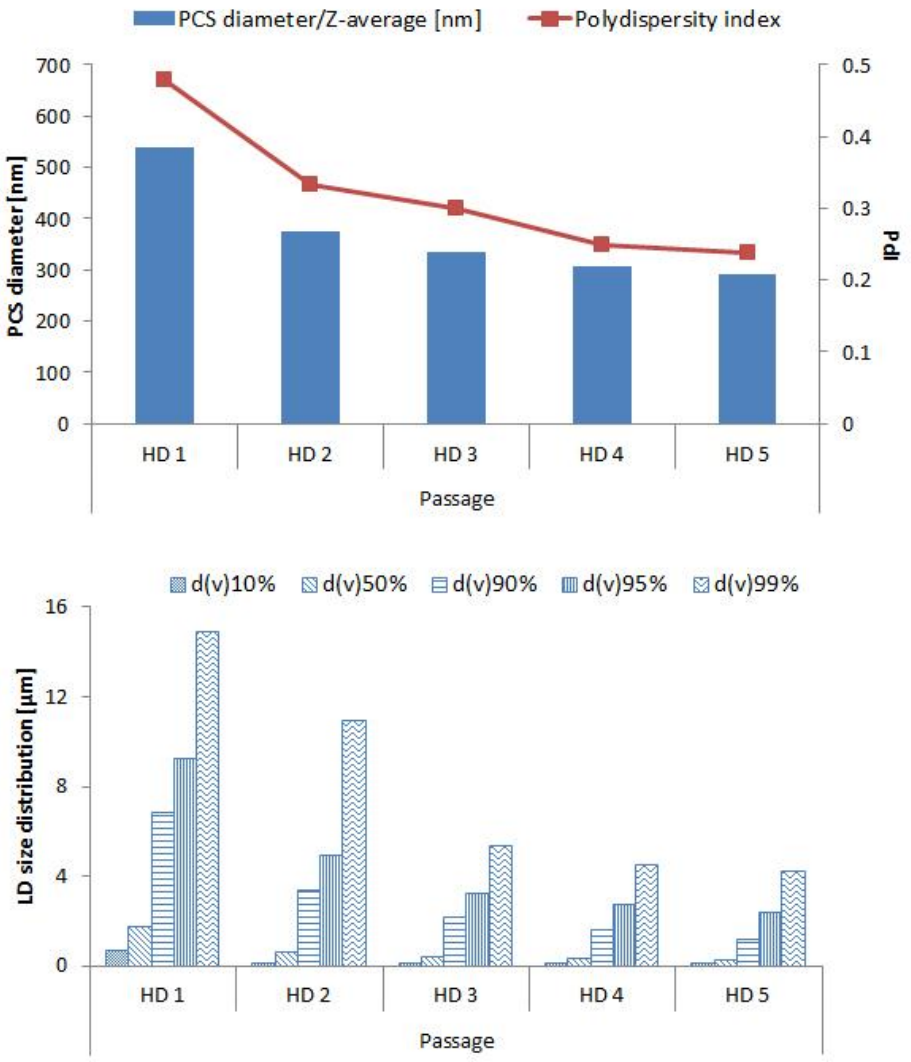

Figure 7 - 3 Size changing of hesperidin nanocrystals during the milling process: PCS (upper) and LD (lower). (HD1 means after 1st passage of milling)

This wet bead milling step was the main particle diminution step in this study. However, the capability of the surfactant is also essential to the stability of the nanosus-

pension system. Good surfactants can enhance the diminution, maintain the obtained size and gain a long stability. On contrary, poor surfactants are insufficient to stabilize the obtained nanocrystals and lead to a fast aggregation, even worse no nanoparticles can be observed during the process. The utilized surfactant, Kolliphor® P 188, also known as Poloxamer 188, is a non-ionic surfactant with potent steric stabilizing effect. It was proven that it can stabilize the diminished drug nanocrystals to prevent them from aggregation. Its hydrophobic end attaches tightly on the surface of the nanocrystals, while the long hydrophilic chain of the polymer stretch into the media (water) and prevent the nanocrystals from coming closer to each other.

To monitor the large scale production and to avoid the content variation, the concentrations of hesperidin and Euxyl® PE 9010 were both determined by HPLC after each passage. The results showed in Fig. 7 - 4 implied that the concentration of hesperidin during the production was a little varied in the range from 17.20% to 18.30%, while the concentration of Euxyl® PE 9010 was almost steady, ranging from 0.99% to 1.01%. To make the concentration of hesperidin more uniform, more efficient dispersion before the inlet may be introduced. However, regarding to the large scale production and the next dilution and HPH step, this little variation is reasonable and controllable.

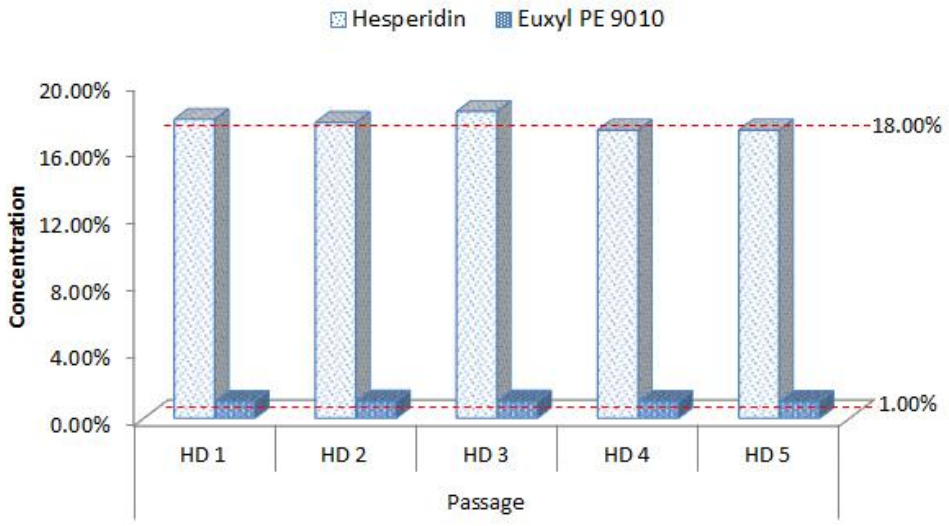

Figure 7 - 4 Content variation of hesperidin and Euxyl® PE 9010 during the WBM

7.3. High pressure homogenization step

The instrument used was an Avestin EmulsiFlex-C50, which is a piston-gap high pressure homogenizer. Via changing the section area of the flow in a closed system, the speed of flow in different areas is varied. From a wide area to a narrow area (gap), the flow speed will be massively lifted, therefore the dynamic pressure will also significantly increased, which leads to an extreme decrease in static pressure to below the vapor pressure at the local temperature in the gap (Fig. 7 - 5). As a result, the water starts boiling and many bubbles are generated, which immediately implode after the flow leaves the narrow area due to the return of the normal static pressure and boiling point, thus form intensive shockwaves to break particles (Keck and Müller 2006). The prerequisite for using piston-gap high pressure homogenization is the particles size of bulk suspension have to be smaller than the size of the gap, otherwise the blockage could happen. In this study the main treatment of wet bead milling definitely acquired this requirement.

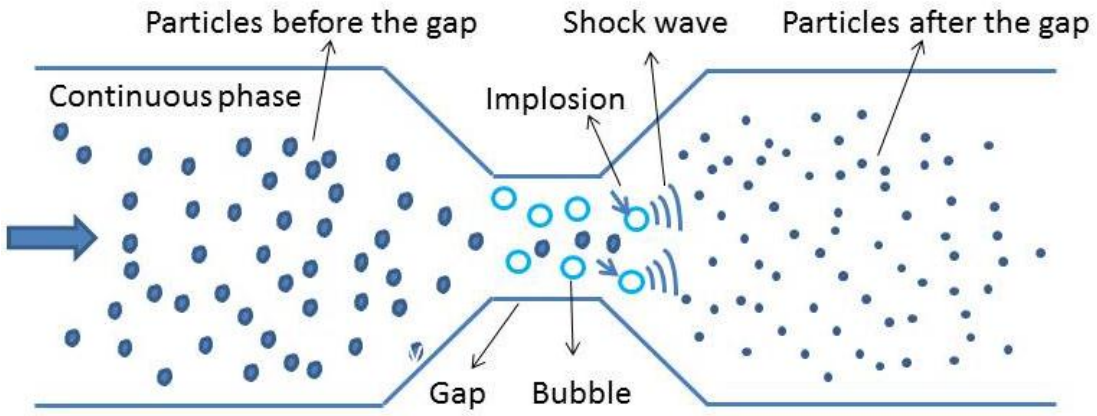

Figure 7 - 5 Disintegration process of particles passing through the gap in high pressure homogenization

When the concentrate of hesperidin nanosuspension was obtained, it was divided into three parts and stored at 4℃ separately. Each of the parts was diluted (cf. 7.1. Tab. 7 - 1) and high pressure homogenized after different storage time. Storage in the form of concentrate aims to save the time of production and reduce the cost, and the fol-

lowed step of HPH aims to re-disperse and sterilize the product thus provide fresh final product. Fig. 7 - 6 displays the size variation of all three batches after HPH. All of them had little size decrease compared to the original concentrate to around 265 nm, PdI remained stable between 0.20 and 0.25. LD result was corresponding to the PCS result, only showed a little decrease in large particles. The evident stability in sizes among the three batches implied a good reproducibility.

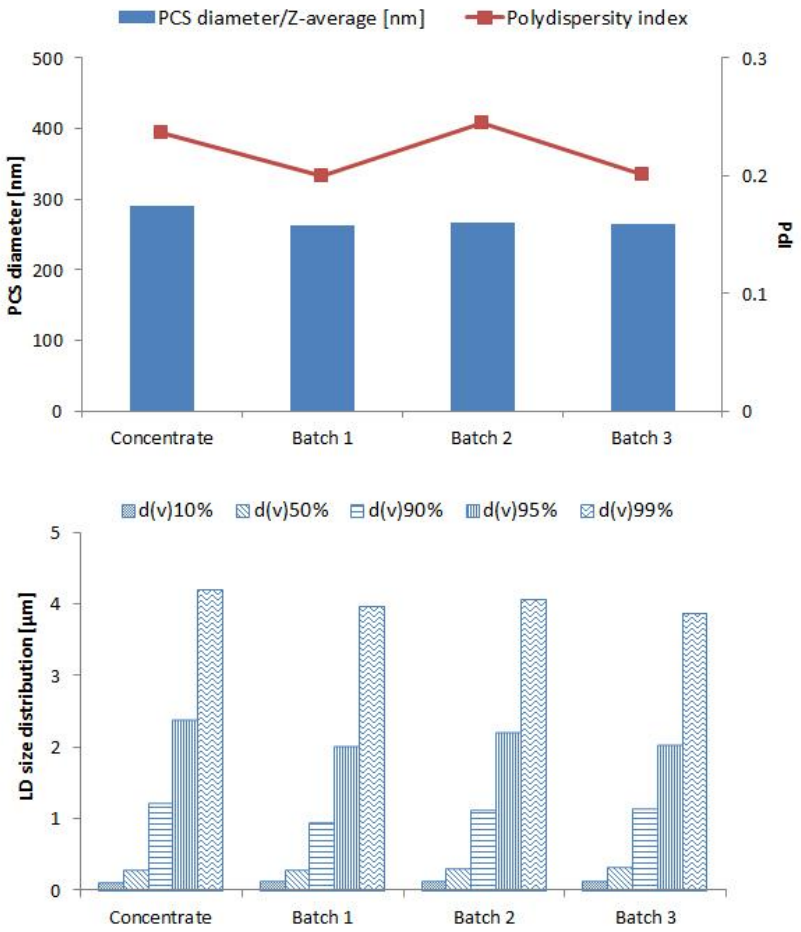

Figure 7 - 6 Size variation of hesperidin nanocrystals in three batches (1 to 3) of dilution and subsequent high pressure homogenization: PCS (upper) and LD (lower)

The reproducibility is not only verified by the steadiness of the size, but also need the support of the uniform content of the ingredients of each batch. This support is displayed in Fig. 7 - 7. The three batches all had the content of hesperidin very close to 5% and Euxyl® PE 9010 to 1%, which ensured the uniformity of products produced in different time.

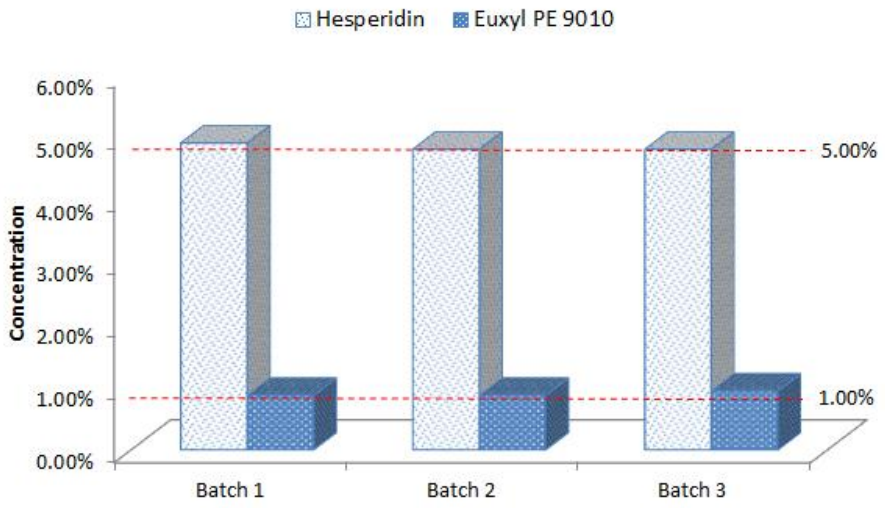

Figure 7 - 7 Content variation of hesperidin and Euxyl® PE 9010 in different batches

7.4. Determination of dry residue test and pH value

Stable dry residue and pH value are also important items concerning the quality assurance. Therefore, the variation of the dry residue and pH value among the batches were investigated, too.

Fig. 7 - 8 shows the dry residue and pH change among the batches. The dry residue stayed around 10% and pH around 6. No significant variation was observed, which was in accordance with the results from particles size characterization. The reproducibility is qualified.

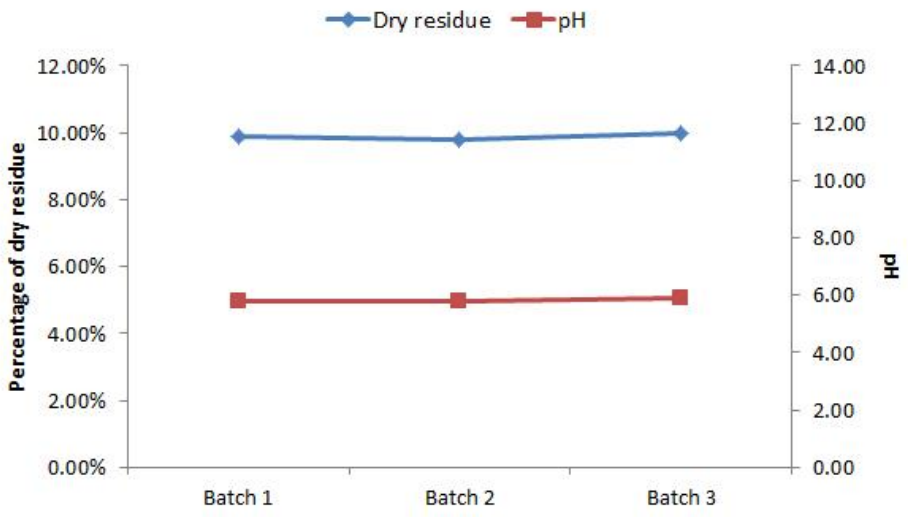

Figure 7 - 8 Dry residue and pH of different batches

7.5. Summary

Drug nanocrystals, as a proven solution for the dissolution and absorption for poorly soluble actives, have been applied in pharmaceutical industry for more than decades. It also can be used in cosmetic field due to the enhanced permeability and penetrability. All the nanocrystals products on the market are manufactured by "top-down" method, including wet bead milling and high pressure homogenization. This smartCrystals technology involved the combination of the two different "top-down" methods and produced hesperidin, which is poorly soluble and widely used as the active ingredients in cosmetic products, nanocrystals in large scale. It was firstly producing the concentrate (18% active) via bead milling followed by a dilution and disinfection operation via high pressure homogenization to obtain the final product including 5% active. Three batches of each product were processed to investigate the reproducibility. The results strongly prove that this smartCrystals technology could successfully produce those nanocrystals (c.a. 260 nm hesperidin nanocrystals) in large scale and show the feasibility in industry. The results from three batches displayed little variation which could ensure the reproducibility. The properties of the attained nanocrystals also showed sound stability. Therefore, this combinational method is efficient and fit for cosmetic industry.

8. Antioxidative capacity - KRL Test in hesperidin, rutin and quercetin nanocrystals

The improved antioxidative performance is the main reason to use nanocrystals in cosmetic products. Therefore, the obtained nanocrystals products in above chapters were compared to the respective bulk powder suspensions to investigate the antioxidative capacity. Based on Kelvin equation and Noyes-Whitney equation, the smaller particles have higher dissolution pressure, thus higher saturation solubility, smaller dissolution distance, larger surface area and higher dissolution rate (Fig. 8 - 1).

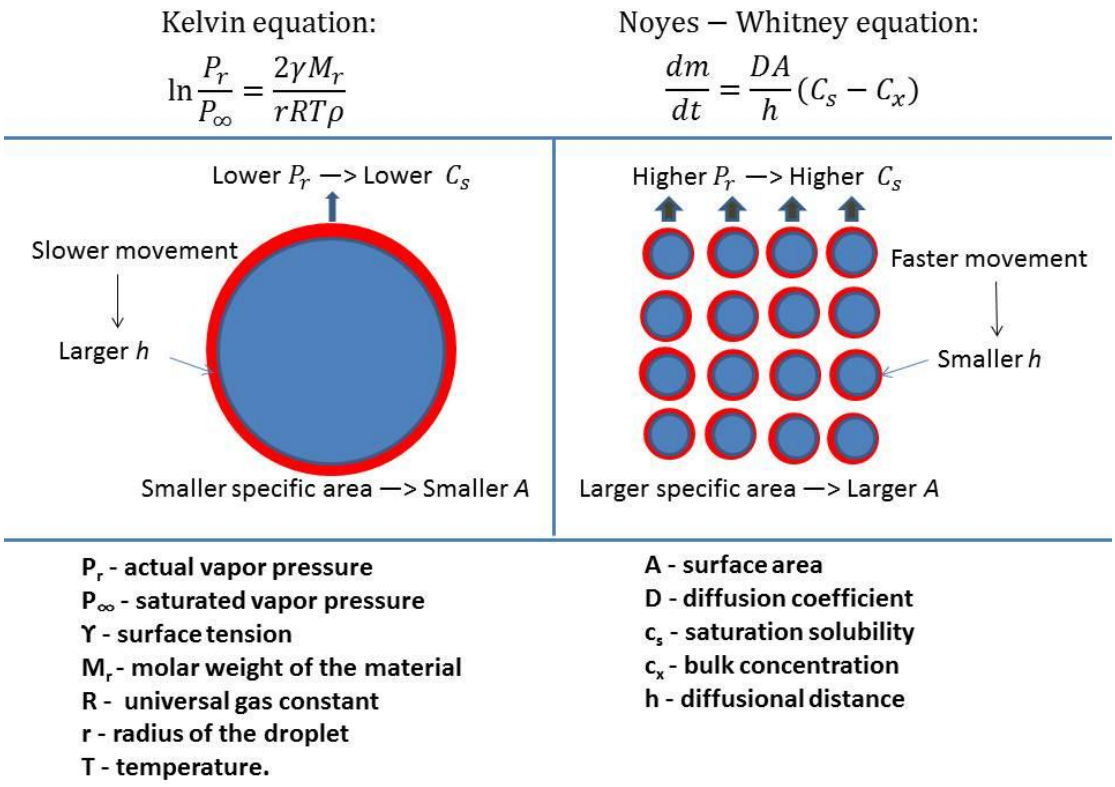

Figure 8 - 1 Kelvin equation and Noyes-Whitney equation applied on large crystals and nanocrystals

Therefore, the nanocrystals should have higher antioxidative capacity when compared to the respective bulk powders due to the higher concentration in the medium. The KRL Test gives results about antioxidant efficiency which relates to the antiradical performance in cell culture by testing the half-hemolysis time.

8.1. Hesperidin nanocrystals

Fig. 8 - 2 gives the results of the obtained hesperidin nanocrystals and the bulk powder. Both of them had increased AOC with increased concentration. What's more, the hesperidin nanocrystals presented a higher increase of half-hemolysis time than bulk powder suspension, thus the antioxidative capacity.

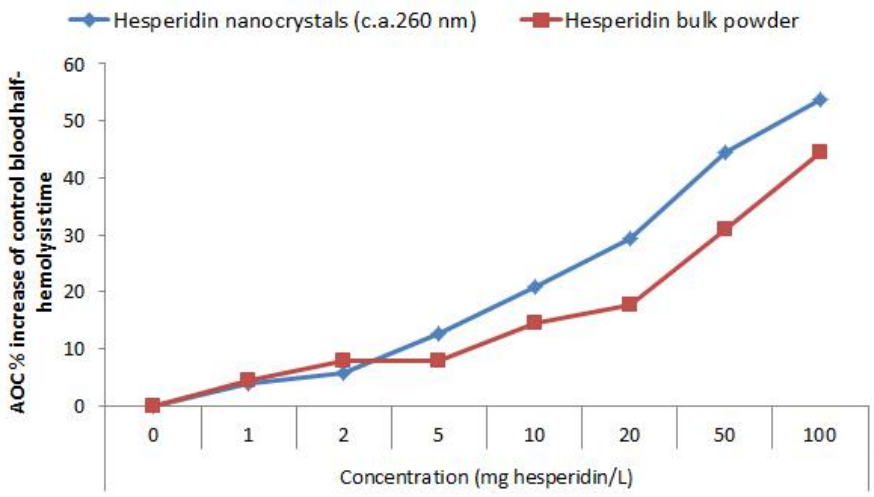

Figure 8 - 2 KRL Test AOC results of the hesperidin nanocrystals and hesperidin bulk powder (data generated by M. Prost, Kirial International, Couternon, France)

8.2. Quercetin nanocrystals

To investigate the antioxidant capacity of quercetin nanocrystals and the capacity variation with size, quercetin nanocrystals with sequential sizes were produced by altering production parameter (cf. 5.1.). The obtained samples were also investigated by KRL Test. The results of size of tested samples are shown in Fig. 8 - 3. The correspondents AOC results are displayed in Fig. 8 - 4.

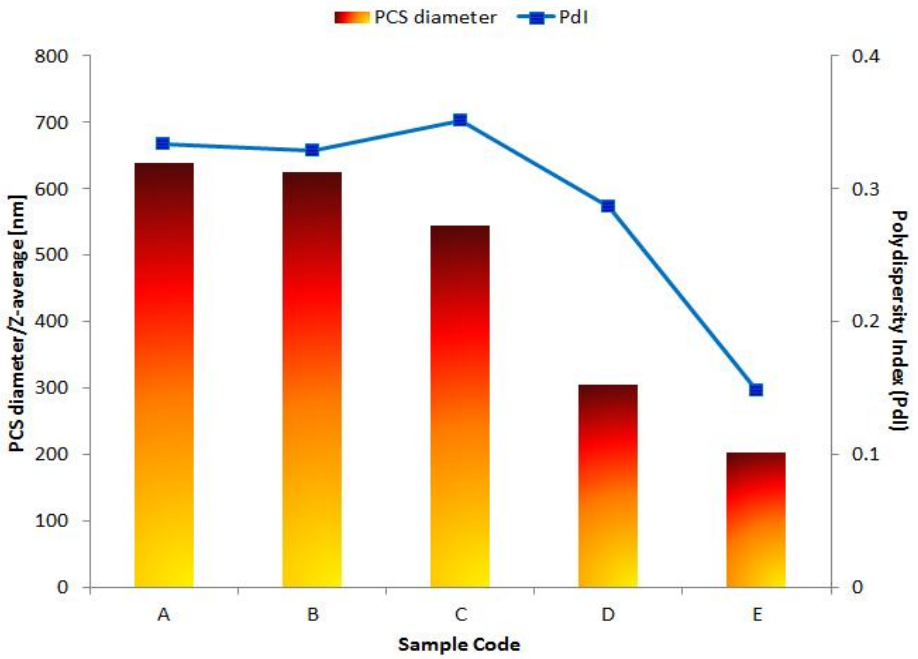

Figure 8 - 3 PCS diameters and PdIs of tested quercetin nanocrystals listed with descending size (Chen, Prost et al. 2013)

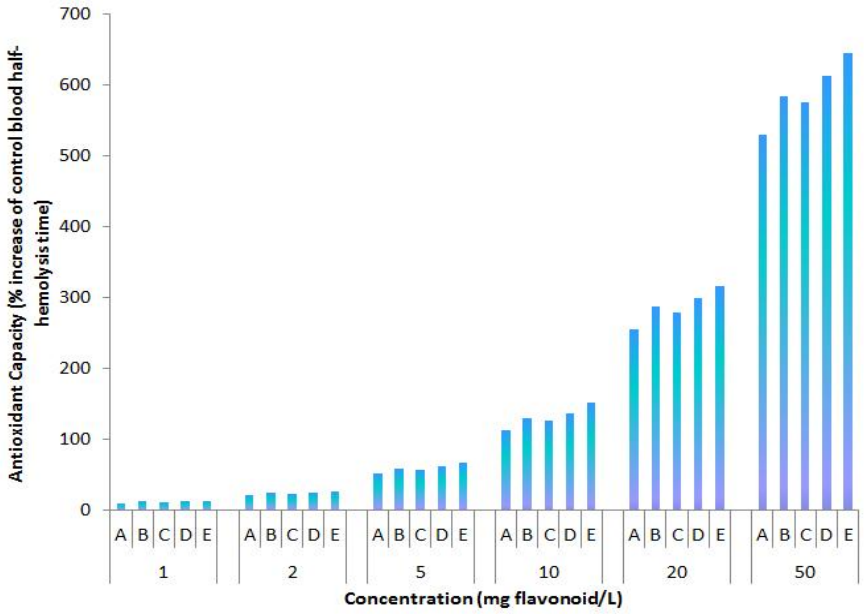

Figure 8 - 4 KRL Test results of the samples in different testing concentrations listed with descending size (Chen, Prost et al. 2013)

The KRL Test gives results about antioxidant efficiency which relates to the antiradical performance in cell culture by testing the half-hemolysis time. Fig. 8 - 4 gives the results of the five samples in different concentrations. Clearly, higher concentration in

each sample all presented an increase of half-hemolysis time, thus the antioxidative capacity. Owing to the enhanced kinetic solution of nanocrystals, all samples showed an active performance. More interestingly, there was an obvious increase in AOC with the decrease of size of quercetin nanocrystals, especially in higher concentration. Smaller nanocrystals had an exponentially enlarged curvature on the surface, thereby enhanced dissolution pressure which brought higher content in medium to protect cell from the radicals.

8.3. Rutin nanocrystals

Three formulations of rutin nanocrystals were investigated:

- Formulation A: Rutin 2%, Poloxamer 188 0.2%, Glycerol 2.5%, water 95.3%
- Formulation B: Rutin 2%, Plantacare® 2000 UP 0.2%, Glycerol 2.5%, water 95.3%
- Formulation C: Rutin 5%, Tween® 80 2%, Glycerol 5%, Euxyl® PE 9010 1%, water 87%

Formulation A & B were produced as described in 4.1. Formulation C was the sample from large scale production which was similarly as described in 7.1. These nanocrystals were compared with each other and with the corresponding bulk powder suspensions as well.

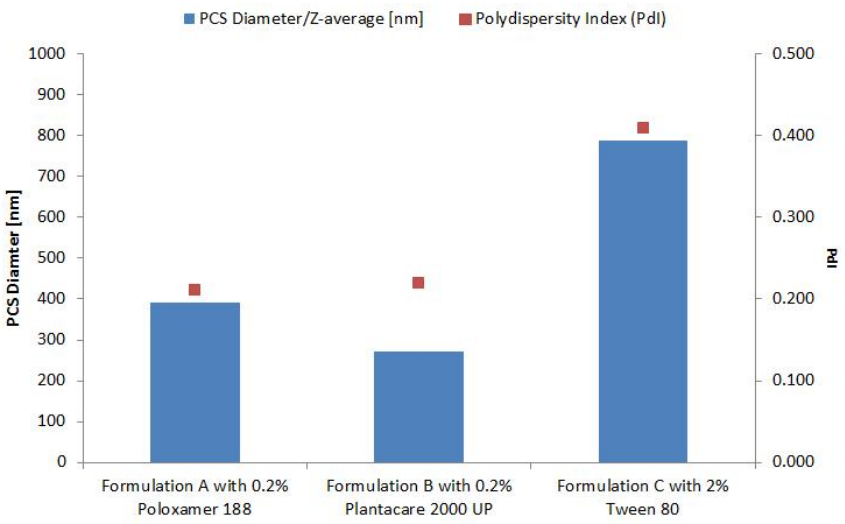

Figure 8 - 5 PCS diameters and PdIs of tested rutin nanocrystals with different formulations

The rutin nanocrystals with different formulations (concentrations from 2% to 5%) and sizes were successfully obtained, which had size range from 271 nm to 789 nm. Results from the KRL Test (Fig. 8 - 6) implied a significant increase (up to 250%) of antioxidative capacity on rutin nanocrystals compared to the respective bulk powder suspension. Nanosizing could increase the kinetic solubility and possibility of endocytosis, thus enhance the absorption. The intensified antioxidant capacity was reflected by the increased half-hemolysis time.

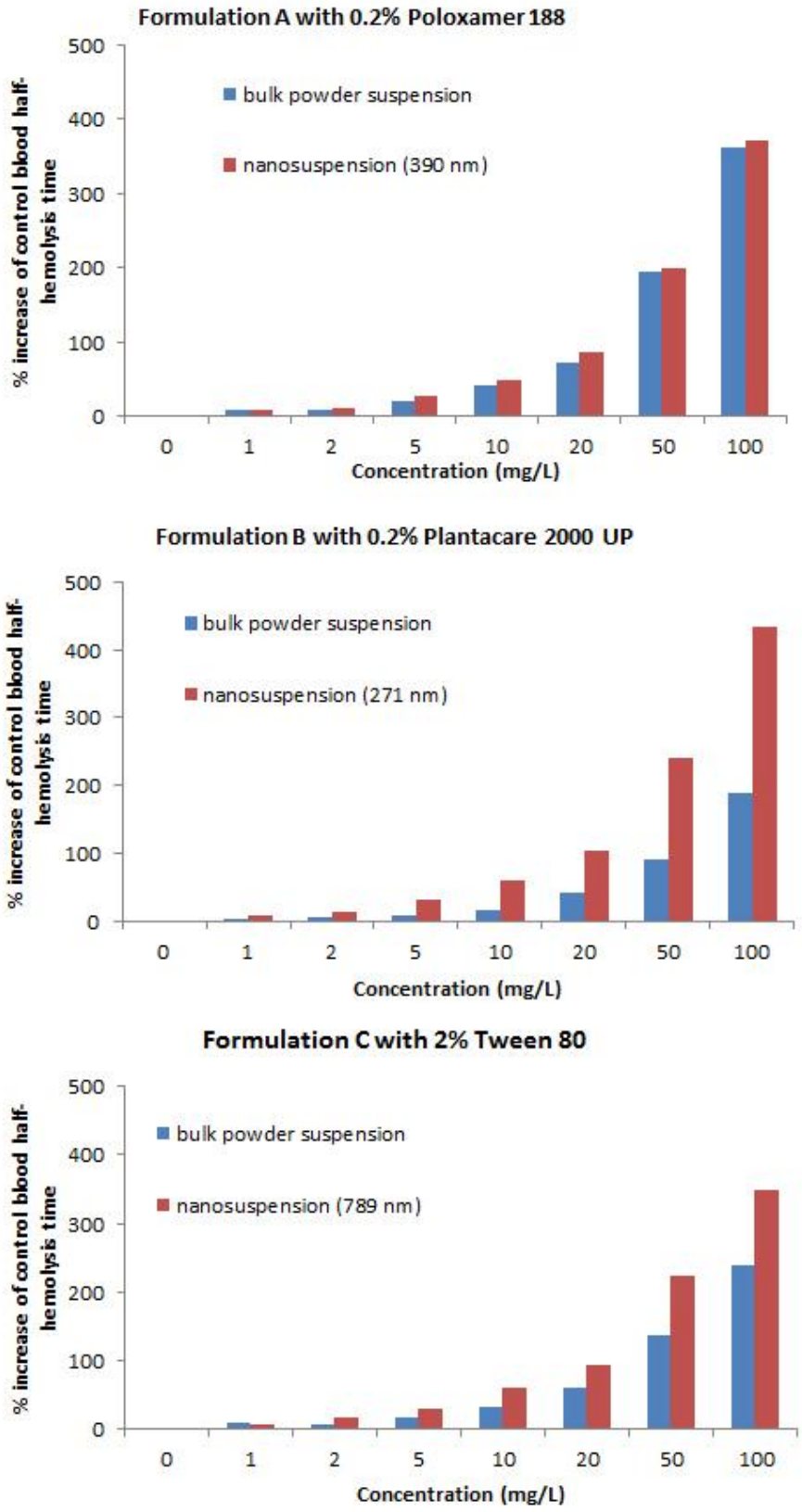

Figure 8 - 6 AOC enhancement of nanocrystals compared to respective bulk powder suspensions (data generated by M. Prost, Kirial International, Couternon, France)

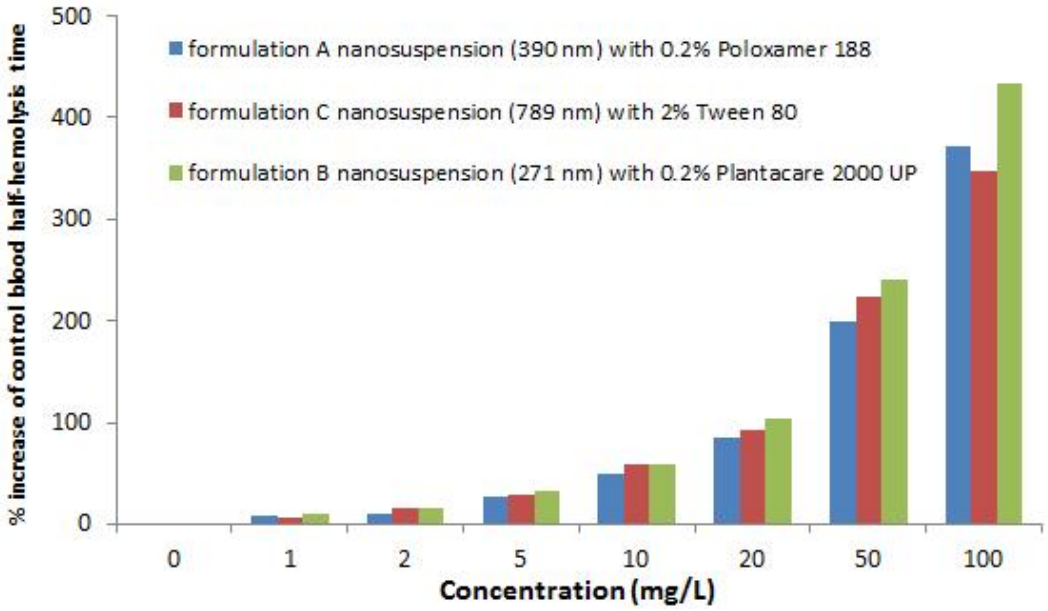

Figure 8 - 7 Comparison of AOC enhancement between nanocrystals with different sizes and formulations (data generated by M. Prost, Kirial International, Couternon, France)

Results shown in Fig. 8 - 7 give a clear depiction about the size effect. Smaller size had higher AOC in this study. Formulation B with 271 nm had the highest AOC.

When the reactive oxygen species (ROSs) attack the blood cells, the antioxidants dissolved in the medium can protect them firstly by scavenging the ROSs outside the cells. In addition, if the ROSs have already entered the cells, the absorbed antioxidants can function in the cells. The absorption of antioxidants requires the dissolution of them or the nanocrystals of the antioxidants are smaller enough so that can be taken up by the cells. In other words, smaller the nanocrystals, better the protective effect.

8.4. Summary

From the above, the size effect in AOC was proven by the new AOC measurement – the KRL Test. The AOC is directly related to the integrity and viability of blood cells, which is more similar as the real therapeutic condition compared to the traditional 2,2-diphenyl-1-picrylhydrazyl (DPPH) assay (Sharma and Bhat 2009). For the same API, smaller size would have a higher AOC. Therefore, enclosing nanocrystals in the final formulation should present better performance in antioxidative activity.

9. Conclusion

Flavonoid nanosuspensions were produced via high pressure homogenization. After the investigation of the intensity of inputted energy, homogenization cycles, kind of surfactants, concentration of active and the physicochemical properties of actives, their influences on the size of obtained nanocrystals were discussed. The results indicated that higher HPH pressure, more HPH cycles, lower concentration of active can contribute to the diminution of the particles. The active's properties, i.e. mw., mp., log P values and pKa can impact the final sizes. Poorer crystallinity may help the decreasing of particle size. The kind of surfactant can also influence the final particles size and the efficiency of diminution. The "limitation theory" was concluded that all the influencing factors mentioned in the study have their own limitations. The size of nanocrystals may only be decreased by varying the ones which have not reached their own limitations.

The different sizes of quercetin nanocrystals were successfully tailor-made from 172 nm to 602 nm via controlling production parameters of HPH. In cell culture test, quercetin nanocrystals showed less toxicity than the quercetin DMSO solution. Furthermore, size of the nanocrystals strongly influence on bioactivity of the compound. Smaller nanocrystals possess a more efficient activity due to higher solubility and uptake by the cells. Nevertheless, adverse effect was also shown which might be due to the prooxidative effect. The unexpected effect was related to the concentration as well as the size. Smaller nanocrystals can be absorbed better, thus higher bioavailability can be achieved. Therefore, a proper concentration and size is vital for an efficient neuroprotection of cells when applied nanocrystals. The toxicity should be always concerned when nanocrystals are formulated and applied in view of the more sensible bio-performance.

The ARTcrystals technology is a feasible method for the production of nanocrystals on large scale. The size of the obtained nanocrystals is close to the conventional methods but with higher production efficacy. Compared to the conventional methods, less time and energy are required for production. Furthermore, the method is so sim-

ple that it can avoid harsh production conditions. Therefore, ARTcrystals technology can be regarded as a useful method for the production of drug nanocrystals.

Hesperidin nanocrystals can be produced on large scale with the smartCrystals technology. High concentrate of hesperidin nanocrystals can be produced with bead milling followed by high pressure homogenization as the dilution and sterilizing step. Three batches of final nanosuspensions with 5% hesperidin nanocrystals were of convincing reproducibility, including the particle sizes, contents of active and preservative and the dry residues. The intermediate concentrate can be stored at 4 ℃ with a good quality. The technology shows a great feasibility in industry production on account of its tunable batch size and flexible production time. It can easily be applied in other BCS II drugs after a proper formulation as well.

A new AOC test – the KRL Test was utilized to measure the obtained hesperidin, quercetin and rutin nanocrystals. All nanocrystals products showed a better performance in the test compared to the respective bulk powder. Furthermore, research on quercetin and rutin gave a clear description that smaller size could bring higher AOC. It proves that making nanocrystals can improve the capability of the APIs for antioxidating. Size does matter. Smaller size can make the result different due to the increasing concentration of APIs in the medium or the endocytosis.

To sum up, this thesis realized the targets of innovation and improvement of production process, tailor-made nanocrystals and providing the evidence of the superiority of nanocrystals in cell absorption and in vitro AOC.

10. Summary

High pressure homogenization was applied to produce apigenin, hesperetin, quercetin and rutin nanocrystals. The factors influencing the final particle size were investigated in order to find an efficient method to control the particle size. The final sizes ranged from 197 nm to 517 nm. It was implied that the physicochemical properties of actives could influence the size. Higher intensity of inputted energy, more cycles of high pressure homogenization, lower active concentration could facilitate the formation of smaller nanocrystals. The summarized "Limitation theory" indicates that every factor has its limitation in devoting to the diminution. For efficiently decreasing particle size, factors that do not meet their limitations should be modified.

Quercetin nanocrystals with various sizes were produced and the size influence on the neuroprotective effect on human neuroblastoma cells SH-SY5Y in presence of endogenous neurotoxins salolinol, 6-hydroxydopamine and 3-hydroxykynurenine was investigated. Via controlling the production conditions, different sizes were achieved. Compared with the quercetin DMSO solution, quercetin nanocrystals showed less toxicity. Interestingly, quercetin nanocrystals showed toxicity in the researched concentration. Furthermore, smaller size presented higher toxicity. The main reason might be the prooxidative effect of quercetin. However, it was also proven that to make active into nanocrystals could enhance the absorption due to the increased solubility and the potential endocytosis. Not only the concentration affects the performance of quercetin, but the size of the quercetin particle also affects.

Rutin nanocrystals were prepared by a simple combinational method involving an ultra-high speed rotor/stator dispersion system and the high pressure homogenization. This method with ultra-high speed R/S dispersion followed by low energy HPH can be successfully applied to the production of rutin nanocrystals. Nanocrystals produced in high energy HPH achieved a size of 381 nm after twenty cycles at 1500 bar. However, with optimized formulation in low energy HPH, only 4 min pre-treatment with ultra-high speed rotor/stator dispersion system and one cycle at 300 bar, 606 nm rutin nanocrystals were yielded. Further 10 cycles HPH at 500 bar produced nanocrystals

with 479 nm. The surfactants combination of Tween® 80 and Plantacare 2000® UP was proven more reliable to stabilize the researched system. The product from optimized formulation held a considerable long-term stability. Compared with the traditional high pressure homogenization, bead milling, or the combinational technology of bead milling and high pressure homogenization, this method presents as a simpler and more convenient production method and can be easily adopted in industrial scale.

Hesperidin nanocrystals was produced by smartCrystals technology on large scale (18 kg scale 18% concentrate by WBM then 18 kg scale 5% dilution by HPH). With more passages proceeded by wet bead milling, the size of hesperidin nanocrystals became smaller down to 290 nm. After dilution one cycle at 500 bar, the size achieved 260 nm. High reproducibility was observed by the PCS diameters within ± 10 nm and LD size with less fluctuation. The content of hesperidin and preservative were both stable in three dilution batches as well. The established process is reliable in produce hesperidin nanocrystals and suitable for industrial production. Now it is used for production of the cosmetic nanocrystal concentrate smartCrystal-lemon extract.

AOCs of hesperidin, quercetin and rutin nanocrystals were measured using the KRL Test, which is unlike traditional chemical method but applied cells' viability as the indicator of the AOC. The comparisons between nanocrystals of each API, each API and the corresponding bulk powder as well as the comparison between the nanocrystals with different sizes were performed. Rutin has the highest AOC compared to the others. The nanocrystals of each API have higher AOC than the bulk powder. The smaller size presents higher AOC, which certifies the advantages of the nanocrystals in antioxidative effect.

11. Zusammenfassung

Apigenin, Hesperetin, Quercetin und Rutin Nanokristalle wurden mittels Hochdruckhomogenisation hergestellt. Um eine effiziente Methode zur Steuerung der Partikelgröße zu ermitteln, wurden Faktoren untersucht, welche die endgültige Partikelgröße beeinflussen. Die finalen Größen reichen von 197 nm bis 517 nm. Es wurde impliziert, dass die physikochemischen Eigenschaften der Wirkstoffe die Größe beeinflussen können. Höhere Intensitäten der eingesetzten Energie, mehrere Hochdruckhomogenisationszyklen, sowie geringere Wirkstoffkonzentration können die Bildung kleinerer Nanokristalle erleichtern. Die zusammengefasste „Grenztheorie“ besagt, dass jeder Faktor seine eigene Limitierung im Hinblick auf die Partikelreduzierung besitzt. Für eine effiziente Verringerung sollten nur Faktoren, welche ihre Grenze nicht erreicht haben, modifiziert werden.

Im Anschluss wurden Quercetin Nanokristalle verschiedener Größen produziert und der Einfluss der Partikelgröße auf den neuroprotektiven Effekt menschlicher Neuroblastom-Zellen SH-SY5Y in Gegenwart von endogenen Neurotoxinen wie Salolinol, 6-Hydroxydopamin und 3-Hydroxykynurenin untersucht. Mittels Kontrolle der Produktionsbedingungen konnten verschiedene Größen erzielt werden. Verglichen mit der Quercetin-DMSO-Lösung, wiesen die Quercetin Nanokristalle eine geringere Toxizität auf. Allerdings zeigten sich toxische Effekte der Quercetin Nanokristalle in der untersuchten Konzentration. Weiterhin verwiesen kleinere Partikelgrößen auf eine höhere Toxizität. Der Hauptgrund könnte der prooxidative Effekt von Quercetin sein. Jedoch hat sich ebenfalls bewährt, dass die Zugabe von Wirkstoffkomponenten in Nanokristalle die Absorption durch gesteigerte Löslichkeit und gesteigerter Endozytose verbessern können. Nicht nur die Konzentration wirkte sich somit auf die Leistung von Quercetin aus, sondern auch ihre Partikelgrößen.

Rutin Nanokristalle wurden durch eine einfache Kombinationsmethode hergestellt, welche ein Ultra-Hochgeschwindigkeits-Rotor/Stator-Dispersionssystem und Hochdruckhomogenisation (HDH) umfassten. Diese Methode mit Ultra-Hochgeschwindigkeits-R/S-Dispersion gefolgt von HDH mit geringer Energie,

konnte sehr erfolgreich in der Produktion von Rutin Nanokristallen angewendet werden. Nanokristalle, welche mit hoher Energie in HDH produziert wurden, erreichten nach 20 Zyklen und 1500 bar eine Größe von 381 nm. Allerdings ergaben sich aus der optimierten Formulierung aus HDH mit niedriger Energie und nur 4 Minuten Vorbehandlung mittels Ultra-Hochgeschwindigkeits-Rotor/Stator-Dispersion System sowie einem Zyklus bei 300 bar, 606 nm große Rutin Nanokristalle. Weitere 10 Zyklen HDH bei 500 bar produzierten Nanokristalle mit 479 nm. Es wurde nachgewiesen, dass die Tensidkombination aus Tween® 80 und Plantacare® 2000 UP das untersuchte System zuverlässig stabilisierten. Das Produkt der optimierten Formulierung besaß eine erhebliche Langzeitstabilität. Verglichen mit der traditionellen Hochdruckhomogenisation, Perlmahlung oder der Kombinationstechnologie aus beiden Verfahren, repräsentiert diese Methode die einfachste und bequemste Produktion und kann folglich leicht in den industriellen Maßstab übernommen werden.

Hesperidin Nanokristalle wurden mittels „smartCrystals“ Technologie im großen Maßstab produziert (18 kg Charge mit 18% Konzentrat mittels Nass-Perlmahlung mit anschließender Verdünnung von 18 kg Charge auf 5% mittels HDH). Nach mehreren Durchgängen der Nass-Perlmahlung, nimmt die Größe der Hesperidin Nanokristalle weiter bis auf 290 nm ab. Nach Verdünnung und Durchführung eines Zyklus bei 500 bar, erreichte die Partikelgröße 260 nm. Hohe Reproduzierbarkeit konnte anhand des PCS Durchmesser mit einer Schwankung um ±10 nm und einer geringen Abweichung der LD Größe festgestellt werden. Die Gehalte von Hesperidin und dem Konservierungsmittel waren in allen 3 produzierten Chargen stabil. Der etablierte Prozess ist zuverlässig im Produzieren von Hesperidin Nanokristallen und geeignet für die industrielle Produktion. Derzeit wird es für die Herstellung von kosmetischem Nanokristall-Konzentrat in smartCrystal-Zitonenextrakt genutzt.

Antioxidative Kapazitäten (AOK) von Hesperidin, Quercetin und Rutin Nanokristallen wurden mittels KRL-Test gemessen, welche im Gegensatz zur

herkömmlichen chemischen Methode, die Zelllebensfähigkeit als Indikator für die AOK verwendet. Vergleiche zwischen Nanokristallen jedes einzelnen Wirkstoffes und des dazugehörigen Grobpulvers sowie die Gegenüberstellung von Nanokristallen verschiedener Größen wurden durchgeführt. Rutin besaß die höchste AOK im Vergleich zu allen anderen Wirkstoffen. Die Nanokristalle von jedem Wirkstoff hatten höhere AOKs als das dazugehörige Grobpulver. Kleinere Partikelgrößen wiesen höhere AOKs auf, welche die Vorteile von Nanokristallen im Hinblick auf antioxidative Effekte bescheinigen.

References

Abbasi, E., M. Nassiri-Asl, et al. (2012). "Neuroprotective effects of vitexin, a flavonoid, on pentylenetetrazole-induced seizure in rats." Chemical Biology & Drug Design **80**(2): 274-278.

Akao, Y., Y. Nakagawa, et al. (1999). "Apoptosis induced by an endogenous neurotoxin, N-methyl(R)salsolinol, is mediated by activation of caspase 3." Neuroscience Letters **267**(3): 153-156.

Al Shaal, L., R. H. Müller, et al. (2010). "smartCrystal combination technology--scale up from lab to pilot scale and long term stability." Pharmazie **65**(12): 877-884.

Al Shaal, L., R. Shegokar, et al. (2011). "Production and characterization of antioxidant apigenin nanocrystals as a novel UV skin protective formulation." International Journal of Pharmaceutics **420**(1): 133-140.

Ansari, M. A., H. M. Abdul, et al. (2009). "Protective effect of quercetin in primary neurons against Abeta(1-42): relevance to Alzheimer's disease." The Journal of Nutritional Biochemistry **20**(4): 269-275.

Arshad, N., N. K. Janjua, et al. (2009). "Electrochemical investigations of antioxidant interactions with radical anion and dianion of 1,3-dinitrobenzene." Electrochimica Acta **54**(26): 6184-6189.

Ayoub, M., N. Ahmed, et al. (2011). "Study of the effect of formulation parameters/variables to control the nanoencapsulation of hydrophilic drug via double emulsion technique." Journal of Biomedical Nanotechnology **7**(2): 255-262.

Bei, W., L. Zang, et al. (2009). "Neuroprotective effects of a standardized flavonoid extract from Diospyros kaki leaves." Journal of Ethnopharmacology **126**(1): 134-142.

Bellac, C. L., R. S. Coimbra, et al. (2010). "Inhibition of the Kynurenine-NAD+ Pathway Leads to Energy Failure and Exacerbates Apoptosis in Pneumococcal

Meningitis." Journal of Neuropathology & Experimental Neurology **69**(11): 1096-1104 1010.1097/NEN.1090b1013e3181f1097e1097e1099.

Belsito, M., R. A. Hill, et al. (2011). "Decyl Glucoside and Other Alkyl Glucosides as Used in Cosmetics."

Boots, A. W., G. R. M. M. Haenen, et al. (2008). "Health effects of quercetin: From antioxidant to nutraceutical." European Journal of Pharmacology **585**(2–3): 325-337.

Boots, A. W., N. Kubben, et al. (2003). "Oxidized quercetin reacts with thiols rather than with ascorbate: implication for quercetin supplementation." Biochemical and Biophysical Research Communications **308**(3): 560-565.

Bors, W. and M. Saran (1987). "Radical scavenging by flavonoid antioxidants." Free radical research communications **2**(4-6): 289-294.

Bournival, J., P. Quessy, et al. (2009). "Protective Effects of Resveratrol and Quercetin Against MPP+ -Induced Oxidative Stress Act by Modulating Markers of Apoptotic Death in Dopaminergic Neurons." Cellular and Molecular Neurobiology **29**(8): 1169-1180.

Cevc, G. (1996). "Transfersomes, liposomes and other lipid suspensions on the skin: permeation enhancement, vesicle penetration, and transdermal drug delivery." Critical Reviews™ in Therapeutic Drug Carrier Systems **13**(3-4): 257-388.

Chen, J. L. (2009). "Comparision of succinate- and phthalate-functionalized etched silica hydride phases for open-tubular capillary electrochromatography." Journal of Chromatography A **1216**(34): 6236-6244.

Chen, R., M. Prost, et al. (2013). Antioxidant Capacity of Tailor-made Quercetin Nanocrystals with KRL Test. 40th CRS Annual Meeting & Exposition, Honolulu.

Chen, T.-J., J.-Y. Jeng, et al. (2006). "Quercetin inhibition of ROS-dependent and -independent apoptosis in rat glioma C6 cells." Toxicology **223**(1–2): 113-126.

Chondrogianni, N., S. Kapeta, et al. (2010). "Anti-ageing and rejuvenating effects of quercetin." Experimental Gerontology **45**(10): 763-771.

Chowdhury, A. R., S. Sharma, et al. (2002). "Luteolin, an emerging anti-cancer flavonoid, poisons eukaryotic DNA topoisomerase I." Biochemical Journal **366**(Pt 2): 653-661.

Colín-González, A. L., P. D. Maldonado, et al. (2013). "3-Hydroxykynurenine: An intriguing molecule exerting dual actions in the Central Nervous System." Neurotoxicology **34**(0): 189-204.

Cragg, G. M. and D. J. Newman (2005). "Plants as a source of anti-cancer agents." Journal of Ethnopharmacology **100**(1-2): 72-79.

Da Violante, G., N. Zerrouk, et al. (2002). "Evaluation of the cytotoxicity effect of dimethyl sulfoxide (DMSO) on Caco2/TC7 colon tumor cell cultures." Biological and Pharmaceutical Bulletin **25**(12): 1600-1603.

Dajas, F., A. C. Andres, et al. (2013). "Neuroprotective actions of flavones and flavonols: mechanisms and relationship to flavonoid structural features." Central Nervous System Agents in Medicinal Chemistry **13**(1): 30-35.

Davis, W. (1947). "Determination of flavanones in citrus fruits." Analytical Chemistry **19**(7): 476-478.

Decker, A. (1997). "Phenolics: Prooxidants or Antioxidants?" Nutrition Reviews **55**(11): 396-398.

Dodel, R. C., Y. Du, et al. (1999). "Caspase-3-like proteases and 6-hydroxydopamine induced neuronal cell death." Molecular Brain Research **64**(1): 141-148.

European Union (2011). "COMMISSION RECOMMENDATION of 18 October 2011 on the definition of nanomaterial." Official Journal of the European Union **L 275/38**.

Favaro, G., C. Clementi, et al. (2007). "Acidichromism and ionochromism of luteolin and apigenin, the main components of the naturally occurring yellow weld: a spectrophotometric and fluorimetric study." Journal of Fluorescence **17**(6): 707-714.

Gao, R. C., T. Y. Ren, et al. (2013). "Improvement in the efficacy of dexketoprofen by its prodrug in lipid emulsion." European Journal of Lipid Science and Technology **115**(2): 153-160.

Gao, Y., S. Qian, et al. (2010). "Physicochemical and pharmacokinetic characterization of a spray-dried cefpodoxime proxetil nanosuspension." Chemical & Pharmaceutical Bulletin (Tokyo) **58**(7): 912-917.

Garcia-Lafuente, A., E. Guillamon, et al. (2009). "Flavonoids as anti-inflammatory agents: implications in cancer and cardiovascular disease." Inflammation Research **58**(9): 537-552.

Gazaryan, I. G. and R. R. Ratan (2009). Oxidative Damage in Neurodegeneration and Injury. Encyclopedia of Neuroscience. R. S. Editor-in-Chief: Larry. Oxford, Academic Press**:** 327-336.

Ghosh, I., S. Bose, et al. (2011). "Nanosuspension for improving the bioavailability of a poorly soluble drug and screening of stabilizing agents to inhibit crystal growth." International Journal of Pharmaceutics.

Gopinath, K., D. Prakash, et al. (2011). "Neuroprotective effect of naringin, a dietary flavonoid against 3-nitropropionic acid-induced neuronal apoptosis." Neurochem Int **59**(7): 1066-1073.

Grau, M. J., O. Kayser, et al. (2000). "Nanosuspensions of poorly soluble drugs--reproducibility of small scale production." International Journal of Pharmaceutics **196**(2): 155-159.

Guardia, T., A. E. Rotelli, et al. (2001). "Anti-inflammatory properties of plant flavonoids. Effects of rutin, quercetin and hesperidin on adjuvant arthritis in rat." Il Farmaco **56**(9): 683-687.

Haag, R., A. Sunder, et al. (2000). "An approach to glycerol dendrimers and pseudo-dendritic polyglycerols." Journal of the American Chemical Society **122**(12): 2954-2955.

Haleagrahara, N., C. J. Siew, et al. (2011). "Neuroprotective effect of bioflavonoid quercetin in 6-hydroxydopamine-induced oxidative stress biomarkers in the rat striatum." Neurosci Lett **500**(2): 139-143.

Hanrott, K., L. Gudmunsen, et al. (2006). "6-Hydroxydopamine-induced Apoptosis Is Mediated via Extracellular Auto-oxidation and Caspase 3-dependent Activation of Protein Kinase Cδ." Journal of Biological Chemistry **281**(9): 5373-5382.

He, C., Y. Hu, et al. (2010). "Effects of particle size and surface charge on cellular uptake and biodistribution of polymeric nanoparticles." Biomaterials **31**(13): 3657-3666.

Heim, K. E., A. R. Tagliaferro, et al. (2002). "Flavonoid antioxidants: chemistry, metabolism and structure-activity relationships." The Journal of Nutritional Biochemistry **13**(10): 572-584.

Heo, H. J. and C. Y. Lee (2004). "Protective Effects of Quercetin and Vitamin C against Oxidative Stress-Induced Neurodegeneration." Journal of Agricultural and Food Chemistry **52**(25): 7514-7517.

Hirpara, K. V., P. Aggarwal, et al. (2009). "Quercetin and Its Derivatives: Synthesis, Pharmacological Uses with Special Emphasis on Anti-Tumor Properties and Prodrug with Enhanced Bio-Availability." Anti-Cancer Agents in Medicinal Chemistry (Formerly Current Medicinal Chemistry **9**(2): 138-161.

Hwang, Y. P. and H. G. Jeong (2010). "Ginsenoside Rb1 protects against 6-hydroxydopamine-induced oxidative stress by increasing heme oxygenase-1 expression through an estrogen receptor-related PI3K/Akt/Nrf2-dependent pathway in human dopaminergic cells." Toxicology and Applied Pharmacology **242**(1): 18-28.

Junghanns, J. U. and R. H. Müller (2008). "Nanocrystal technology, drug delivery and clinical applications." Int J Nanomedicine **3**(3): 295-309.

Junghanns, J. U. and R. H. Müller (2008). "Nanocrystal technology, drug delivery and clinical applications." International Journal of Nanomedicine **3**(3): 295-309.

Kakran, M., R. Shegokar, et al. (2012). "Fabrication of quercetin nanocrystals: comparison of different methods." European Journal of Pharmaceutics and Biopharmaceutics **80**(1): 113-121.

Kanaze, F. I., C. Gabrieli, et al. (2003). "Simultaneous reversed-phase high-performance liquid chromatographic method for the determination of diosmin, hesperidin and naringin in different citrus fruit juices and pharmaceutical formulations." Journal of Pharmaceutical and Biomedical Analysis **33**(2): 243-249.

Kanaze, F. I., E. Kokkalou, et al. (2004). "A validated solid-phase extraction HPLC method for the simultaneous determination of the citrus flavanone aglycones hesperetin and naringenin in urine." Journal of Pharmaceutical and Biomedical Analysis **36**(1): 175-181.

Kannan, K. and S. K. Jain (2000). "Oxidative stress and apoptosis." Pathophysiology **7**(3): 153-163.

Keck, C., S. Kobierski, et al. (2012). "Novel Top‐Down Technologies: Effective Production of Ultra‐Fine Drug Nanocrystals." Drug Delivery Strategies for Poorly Water-Soluble Drugs: 247-263.

Keck, C. M. (2006). Cyclosporine nanosuspensions optimized size characterisation and oral formulations. Dr. rer. nat. Dissertation, Freie Universität Berlin.

Keck, C. M. (2010). "Particle size analysis of nanocrystals: improved analysis method." International Journal of Pharmaceutics **390**(1): 3-12.

Keck, C. M. (2011). Nanocrystals and amorphous nanoparticles and method for production of the same by a low energy process. **Patent: EP2583672**.

Keck, C. M., Hanisch, J., Mauludin, R., Petersen, R. D., Müller, R.H. (2007). Rutin Drug Nanocrystals for Dermal Cosmetic Application. Annual Meeting of the American Association of Pharmaceutical Scientists, San Diego, USA

Keck, C. M., S. Kobierski, et al. (2008). "Second generation of drug nanocrystals for delivery of poorly soluble drugs: smartCrystals technology." Dosis **24**: 124-128.

Keck, C. M. and R. H. Müller (2006). "Drug nanocrystals of poorly soluble drugs produced by high pressure homogenisation." European Journal of Pharmaceutics and Biopharmaceutics **62**(1): 3-16.

Keck, C. M. and R. H. Müller (2013). "Nanotoxicological classification system (NCS) – A guide for the risk-benefit assessment of nanoparticulate drug delivery systems." European Journal of Pharmaceutics and Biopharmaceutics **84**(3): 445-448.

Kipp, J. E., J. C. T. Wong, et al. (2006). Microprecipitation method for preparing submicron suspensions. **Patent: US7037528**.

Kitagawa, S., Y. Tanaka, et al. (2009). "Enhanced skin delivery of quercetin by microemulsion." Journal of Pharmacy and Pharmacology **61**(7): 855-860.

Kobierski, S., K. Ofori-Kwakye, et al. (2009). "Resveratrol nanosuspensions for dermal application--production, characterization, and physical stability." Pharmazie **64**(11): 741-747.

Kohler, K., A. S. Santana, et al. (2010). "High pressure emulsification with nano-particles as stabilizing agents." Chemical Engineering Science **65**(10): 2957-2964.

Krause, K., K. Mäder, et al. (2001). Method for contrlled production of ultrafine microparticles and nanoparticles. **Patent: WO2001003670**.

Krause, K. P. and R. H. Müller (2001). "Production and characterisation of highly concentrated nanosuspensions by high pressure homogenisation." International Journal of Pharmaceutics **214**(1-2): 21-24.

Lai, F., E. Pini, et al. (2011). "Nanocrystals as tool to improve piroxicam dissolution rate in novel orally disintegrating tablets." European Journal of Pharmaceutics and Biopharmaceutics **79**(3): 552-558.

Lamson, D. W. and M. S. Brignall (2000). "Antioxidants and cancer, part 3: quercetin." Alternative medicine review : a journal of clinical therapeutic **5**(3): 196-208.

Lindfors, L., P. Skantze, et al. (2006). "Amorphous drug nanosuspensions. 1. Inhibition of Ostwald ripening." Langmuir **22**(3): 906-910.

Lu, F., S. H. Wu, et al. (2009). "Size effect on cell uptake in well-suspended, uniform mesoporous silica nanoparticles." Small **5**(12): 1408-1413.

Müller, R. H. and A. Akkar (2004). Nanocrystals of poorly soluble drugs. Encyclopedia of Nanosciecnce and Nanotechnology. H. S. Nalwa. Valencia, American Scientific Publishers. **2**.

Müller, R. H., B. H. Böhm, et al. (1999). "Nanosuspensions - Formulations for poorly soluble drugs with poor bioavailability - 2. Stability, biopharmaceutical aspects, possible drug forms and registration aspects." Pharmazeutische Industrie **61**(2): 175-178.

Müller, R. H., B. H. L. Böhm, et al. (1999). "Nanosuspensions - Formulations for poorly soluble drugs with poor bioavailability - 1st communication: Production and properties." Pharmazeutische Industrie **61**(1): 74-78.

Müller, R. H., R. Becker, et al. (1999). Pharmaceutical nanosuspensions for medicament administration as systemswith increased saturation solubility and rate of solution. **Patent: US005858410A**.

Müller, R. H., S. Gohla, et al. (2011). "State of the art of nanocrystals–special features, production, nanotoxicology aspects and intracellular delivery." European Journal of Pharmaceutics and Biopharmaceutics **78**(1): 1-9.

Müller, R. H. and C. M. Keck (2008). "Second generation of drug nanocrystals for delivery of poorly soluble drugs: smartCrystal technology." European Journal of Pharmaceutical Sciences **34**(1): S20-S21.

Müller, R. H., C. M. Keck, et al. (2008). Rutin smartCrystals: Bioactivity enhancement and stability against electrolytes. Annual Meeting of the American Association of Pharmaceutical Scientists, Atlanta, USA.

Müller, R. H., R. Shegokar, et al. (2011). "Nanocrystals: Production, Cellular Drug Delivery, Current and Future Products." Intracellular Delivery: Fundamentals and Applications **5**: 411-432.

Möschwitzer, J. and A. Lemke (2008). Method for the gentle production of ultrafine particles suspensions and ultrafine particles and the use thereof. **Patent: WO2006108637**.

Möschwitzer, J. and R. H. Müller (2006). "New method for the effective production of ultrafine drug nanocrystals." J Nanosci Nanotechnol **6**(9-10): 3145-3153.

Möschwitzer, J. and R. H. Müller (2006). "Spray coated pellets as carrier system for mucoadhesive drug nanocrystals." European Journal of Pharmaceutics and Biopharmaceutics **62**(3): 282-287.

Martin, L. J. (2001). "Neuronal cell death in nervous system development, disease, and injury (Review)." International Journal of Molecular Medicine **7**(5): 455-478.

Merisko-Liversidge, E. and G. G. Liversidge (2011). "Nanosizing for oral and parenteral drug delivery: a perspective on formulating poorly-water soluble compounds using wet media milling technology." Advanced Drug Delivery Reviews **63**(6): 427-440.

Merisko-Liversidge, E., G. G. Liversidge, et al. (2003). "Nanosizing: a formulation approach for poorly-water-soluble compounds." European Journal of Pharmaceutical Sciences **18**(2): 113-120.

Metodiewa, D., A. K. Jaiswal, et al. (1999). "Quercetin may act as a cytotoxic prooxidant after its metabolic activation to semiquinone and quinoidal product." Free Radical Biology and Medicine **26**(1-2): 107-116.

Mishra, P. R., L. Al Shaal, et al. (2009). "Production and characterization of Hesperetin nanosuspensions for dermal delivery." International Journal of Pharmaceutics **371**(1-2): 182-189.

Naoi, M., W. Maruyama, et al. (2000). "Apoptosis induced by an endogenous neurotoxin, N-methyl(R)salsolinol, in dopamine neurons." Toxicology **153**(1–3): 123-141.

Noyes, A. A. and W. R. Whitney (1897). "The rate of solution of solid substances in their own solutions." Journal of the American Chemical Society **19**(12): 930-934.

Okuda, S., N. Nishiyama, et al. (1998). "3-Hydroxykynurenine, an Endogenous Oxidative Stress Generator, Causes Neuronal Cell Death with Apoptotic Features and Region Selectivity." Journal of Neurochemistry **70**(1): 299-307.

Ossola, B., T. M. Kääriäinen, et al. (2009). "The multiple faces of quercetin in neuroprotection." Expert Opinion on Drug Safety **8**(4): 397-409.

Otsubo, Y. (1994). "Effect of Surfactant Adsorption on the Polymer Bridging and Rheological Properties of Suspensions." Langmuir **10**(4): 1018-1022.

Pedriali, C. A., A. U. Fernandes, et al. (2008). "The Synthesis of a Water-Soluble Derivative of Rutin as an Antiradical Agent." Química Nova **31**(8): 2147-2151.

Peltonen, L. and J. Hirvonen (2010). "Pharmaceutical nanocrystals by nanomilling: critical process parameters, particle fracturing and stabilization methods." Journal of Pharmacy and Pharmacology **62**(11): 1569-1579.

Petersen, R. (2008). Nanocrystals for use in topical cosmetic formulations and method of production thereof. **Patent: WO2008058755**.

Procházková, D., I. Boušová, et al. (2011). "Antioxidant and prooxidant properties of flavonoids." Fitoterapia **82**(4): 513-523.

Qi, W., D. Ding, et al. (2008). "Cytotoxic effects of dimethyl sulphoxide (DMSO) on cochlear organotypic cultures." Hearing Research **236**(1-2): 52-60.

Rice-Evans, C. (2001). "Flavonoid antioxidants." Current Medicinal Chemistry **8**(7): 797-807.

Rosen, M. J., Ed. (2004). Surfactants and Interfacial Phenomena, John Wiley & Sons, Inc.

Rothwell, J. A., A. J. Day, et al. (2005). "Experimental determination of octanol-water partition coefficients of quercetin and related flavonoids." Journal of Agricultural and Food Chemistry **53**(11): 4355-4360.

Rowe, R. C., P. J. Sheskey, et al. (2009). Handbook of Pharmaceutical Excipients. London, Pharmaceutical Press and American Pharmacists Association.

Sastry, P. S. and K. S. Rao (2000). "Apoptosis and the nervous system." Journal of Neurochemistry **74**(1): 1-20.

Scalia, S., R. Salama, et al. (2012). "Preparation and in vitro evaluation of salbutamol-loaded lipid microparticles for sustained release pulmonary therapy." Journal of Microencapsulation **29**(3): 225-233.

Sharma, O. P. and T. K. Bhat (2009). "DPPH antioxidant assay revisited." Food Chemistry **113**(4): 1202-1205.

Sinambela, P., B. M. Löffler, et al. (2013). Human In Vivo Study: Dermal Application of Rutin SmartCrystals® & Peptide-Loaded Liposomes to Decrease Skin Roughness. 40th Annual Meeting & Exposition of the Controlled Release Society, Hawaii, USA.

Sinambela, P., B. M. Löffler, et al. (2012). Antioxidant rutin nanocrystals for anti-aging treatment – an in vivo study. Annual Meeting of the American Association of Pharmaceutical Scientists, Chicago, USA.

Spencer, J. P., G. G. Kuhnle, et al. (2003). "Intracellular metabolism and bioactivity of quercetin and its in vivo metabolites." Biochemical Journal **372**(Pt 1): 173-181.

Suematsu, N., M. Hosoda, et al. (2011). "Protective effects of quercetin against hydrogen peroxide-induced apoptosis in human neuronal SH-SY5Y cells." Neurosci Lett **504**(3): 223-227.

Suhaj, M. (2006). "Spice antioxidants isolation and their antiradical activity: a review." Journal of Food Composition and Analysis **19**(6–7): 531-537.

Teeranachaideekul, V., V. B. Junyaprasert, et al. (2008). "Development of ascorbyl palmitate nanocrystals applying the nanosuspension technology." International Journal of Pharmaceutics **354**(1-2): 227-234.

U.S. Food and Drug Administration (2011). "Considering Whether an FDA-Regulated Product Involves the Application of Nanotechnology - Guidance for Industry."

Utesch, D., K. Feige, et al. (2008). "Evaluation of the potential in vivo genotoxicity of quercetin." Mutation Research/Genetic Toxicology and Environmental Mutagenesis **654**(1): 38-44.

Verri, W. A., F. T. M. C. Vicentini, et al. (2012). "Flavonoids as Anti-Inflammatory and Analgesic Drugs: Mechanisms of Action and Perspectives in the Development of Pharmaceutical Forms." Bioactive Natural Products, Vol 36 **36**: 297-330.

Wang, Q., A. Y. Sun, et al. (2009). "Neuroprotective effects of a nanocrystal formulation of sPLA(2) inhibitor PX-18 in cerebral ischemia/reperfusion in gerbils." Brain Research **1285**: 188-195.

Wang, Y. C. and K. M. Huang (2013). "In vitro anti-inflammatory effect of apigenin in the Helicobacter pylori-infected gastric adenocarcinoma cells." Food Chem Toxicol **53**: 376-383.

Wanpen, S., P. Govitrapong, et al. (2004). "Salsolinol, a dopamine-derived tetrahydroisoquinoline, induces cell death by causing oxidative stress in dopaminergic SH-SY5Y cells, and the said effect is attenuated by metallothionein." Brain Research **1005**(1–2): 67-76.

Xavier, C. R., C. Lima, et al. (2011). "Quercetin enhances 5-fluorouracil-induced apoptosis in MSI colorectal cancer cells through p53 modulation." Cancer Chemotherapy and Pharmacology **68**(6): 1449-1457.

Yan, S., B. Wu, et al. (2009). "Metabonomic characterization of aging and investigation on the anti-aging effects of total flavones of Epimedium." Molecular BioSystems **5**(10): 1204-1213.

Yuan, J. and B. A. Yankner (2000). "Apoptosis in the nervous system." Nature **407**(6805): 802-809.

Zhang, D., T. Tan, et al. (2007). "Preparation of azithromycin nanosuspensions by high pressure homogenization and its physicochemical characteristics studies." Drug Development and Industrial Pharmacy **33**(5): 569-575.

Zhang, M., S. G. Swarts, et al. (2011). "Antioxidant properties of quercetin." Advances in Experimental Medicine and Biology **701**: 283-289.

Zhang, Z. J., L. C. V. Cheang, et al. (2011). "Quercetin exerts a neuroprotective effect through inhibition of the iNOS/NO system and pro-inflammation gene expression in PC12 cells and in zebrafish." International Journal of Molecular Medicine **27**(2): 195-203.

Abbreviations

3-HK	3-hydroxykynurenine
6-OHDA	6-hydroxydopamine
AOC	antioxidative capacity
AD	Alzheimer’s disease
API	active pharmaceutical ingredient
BCS	Biopharmaceutics Classification System
CDs	cyclodextrins
CT	combination Technology
Da	dalton
DLS	dynamic light scattering
DMEM	Dulbecco’s Modified Eagle’s Medium
DMSO	dimethyl sulfoxide
DPPH	2,2-diphenyl-1-picrylhydrazyl
EDTA	ethylenediaminetetraacetic acid
FBS	fetal bovine serum
FDA	US Food & Drug Administration
g	gram
h	hour
KRL	Kit Radicaux Libres
HD	Huntington's disease
HPH	high pressure homogenization
HPLC	high performance liquid chromatography

IPAM	Institute for Preventive and Aesthetic Medicine
LD	laser diffractometry
min	minute
mg	milligram
ml	milliliter
mp.	melting point
mV	millivolts
mw.	molecular weight
NCS	Nanotoxicological Classification System
nm	nanometer
PBS	phosphate buffered saline
PCS	photon correlation spectroscopy
PD	Parkinson’s disease
PdI	polydispersity index
PXRD	powder X-ray diffraction
ROSs	reactive oxygen species
rpm	revolutions per minute
µm	micrometer
SAL	(±)salsolinol
SDS	sodium dodecyl sulfate
SPF	sun protection factor
UHS-R/S	ultra-high speed rotor/stator
UV	ultraviolet
WBM	wet bead milling

w/w	weight/weight
ZP	zeta potential

List of publications

Paper

1. Rainer H. Müller, **Run Chen**, Cornelia M. Keck. smartCrystals for consumer care & cosmetics: enhanced dermal delivery of poorly soluble plant actives [J]. Household and Personal Care Today, 2013, 8(5): 18-23

Proceeding

1. **Chen, R.**, Prost, M., Greiner, L., Müller, R. H., Keck, C. M., Antioxidant Capacity of Tailor-made Quercetin Nanocrystals with KRL Test, Abstract ID 100409, #827, 40th CRS Annual Meeting & Exposition, Honolulu, 21-24 July, 2013
2. Müller, R. H., **Chen, R.**, Keck, C. M., ARTcrystals® – Nanocrystal Production & Physical Long-Term Stability, #675, 40th CRS Annual Meeting & Exposition, Honolulu, 21-24 July, 2013
3. Zhang, Y., **Chen, R.**, Keck, C. M., Müller, R. H., Intravenous Rutin Nanocrystals with Potential Use for Alzheimer Treatment, #902, 40th CRS Annual Meeting & Exposition, Honolulu, 21-24 July, 2013
4. **Chen, R.**, Kumanova, Ö., Keck, C. M., Müller, R. H., ART nanocrystals - a novel simple method for the production of nanocrystals in industrial scale, podium proceeding, #65, 39th CRS Annual Meeting & Exposition, Québec City, 15-18 July, 2012
5. Harden, D., **Chen, R.**, Müller, R. H., Keck, C. M., Zeta potential measurements of high concentrated fish oil nanoemulsions, #662, 39th CRS Annual Meeting & Exposition, Québec City, 15-18 July, 2012

Abstracts

1. **Chen, R.**, Romero, G. B., Keck, C. M., Müller, R. H., Reproducibility of smartCrystal technology for large scale production of cosmetic hesperidin nanocrystals. AM-13-1626, 2013 AAPS Annual Meeting & Exposition, San Antonio , 10-14 November, 2013

2. **Chen, R.**, Prost, M., Durand, P., Greiner, L., Müller, R. H., Keck, C. M., Increased kinetic solubility and antioxidant capacity of tailor-made quercetin nanocrystals . AM-13-1638, 2013 AAPS Annual Meeting & Exposition, San Antonio , 10-14 November, 2013

3. **Chen, R.** Prost, M., Greiner, L., Müller, R. H., Keck, C. M., Size-dependent Antioxidant Capacity of Tailor-made Quercetin Nanocrystals: a quick look from KRL Test. I-51, 7th Symposium of Polish-German on Pharamceutical Science, Gdańsk , 24-25 May, 2013

4. **Chen, R.**, Li, X., Müller, R. H., et al., Improvement of Kinetic Solubility of Tailor-made Quercetin Nanocrystals. S35. CRS German Chapter Annual Meeting, Ludwigshafen, 21-22 March, 2013

5. **Chen, R.**, Sauer, M., Durand, P., et al., Rutin Nanocrystals: Production, Antioxidative Capacity, and Neuroprotection. S36. CRS German Chapter Annual Meeting, Ludwigshafen, 21-22 March, 2013

6. Li, X., **Chen, R.**, Baisaeng, N., Müller, R. H., Keck, C. M. (2013) Surfactants for the formulation of NLC: Effects on size and physical stability, S38. CRS German Chapter Annual Meeting, Ludwigshafen, 21-22 March, 2013

7. Peters, D., Harden, D., Schmidt, C., **Chen, R.**, Müller, R. H., Keck, C. M., Antioxidant capacity of omega 3 fatty acids – improvement by nanoemulsification, M1252, AAPS Annual Meeting, Chicago, 14-18 October 2012

8. Romero, G. B., **Chen, R.**, Müller, R. H., LBL coating of nanocrystals – development of industrially feasible process, R6072, AAPS Annual Meeting, Chicago, 14-18 October 2012

9. **Chen, R.**, Kumanova, Ö., Keck, C. M.,et al., ART nanocrystals: a novel combinational technology to produce drug nanocrystals - more efficient and economical. AM-12-1638, 2012 AAPS Annual Meeting & Exposition, Chicago, 14-18 October 2012

10. **Chen, R.**, Wszelaki, N., Melzig, M. F., et al., Tailor-made production of quercetin and rutin nanocrystals for investigating the correlation between the size and effect to cell. Tagungsband 145, Jahrestagung der Deutschen Pharmazeutischen Gesellschaft (DPhG), Greifswald, 10-13 October, 2012

11. **Chen, R.**, Wszelaki, N., Melzig, M. F., et al., Production, characterization and neuro-effect of quercetin nanocrystals: Correlation between the size and cell penetrating. Tag der Pharmazie, DPhG Landesgruppe Berlin-Brandenburg, Berlin, 6. Juli 2012

12. **Chen, R.**, Kumanova, Ö., Keck, C. M., ART-Crystals: a new method for the production of nanocrystals. P2-9, CRS German Chapter Annual Meeting, Würzburg, 29-30 March, 2012
13. **Chen, R.**, Müller, R. H., Keck, C. M., LBL^{Plus} - nanocrystals with enhanced stability in body fluids, P2-11, CRS German Chapter Annual Meeting, Würzburg, 29-30 March, 2012
14. **Chen, R.**, Müller, R. H., Keck, C. M., Antioxidative nanocrystals: correlation between particle size and physico-chemical properties. P16, CRS German Chapter Annual Meeting, Jena, 15-16 March, 2011

Curriculum Vitae

For reasons of data protection,

the curriculum vitae is not published in the electronic version

For reasons of data protection,

the curriculum vitae is not published in the electronic version

For reasons of data protection,

the curriculum vitae is not published in the electronic version

Acknowledgements

First of all I appreciate the supervision from Prof. Dr. Cornelia M. Keck and Prof. Dr. Rainer H. Müller during my research stay in our group. Their guidance and suggestion in scientific idea, practical work and academic writing are of great help. The more important thing is their attitudes towards science and innovation influence me a lot.

I would like to thank China Scholarship Council for the financial support to my three-year doctoral study in Freie Universität Berlin.

I also thank the collaborators in my research:

Dr. Natalia Wszelaki in Prof. Dr. Matthias F. Melzig's group, FU Berlin;

Mr. Özcan Kumanova from ART Prozess- & Labortechnik GmbH & Co. KG, Germany;

Dr. Michel Prost and Dr. Philippe Durand in LARA SPIRAL SA and KIRIAL INTERNATIONAL limited, France.

Without their help my research would be difficult to proceed.

I would like to thank Dr. Wolfgang Mehnert, Dr. Lothar Schwabe, Ms. Gabriela Karsubke, Ms. Corinna Schmidt, Ms. Inge Volz and Mr. Alfred Protz for their help and advice.

I wish to thank the lab mates (Daniel, Daniela, Add, Jing, Lee) for their kind help in lab affairs and excellent daily academic talks.

Thanks to Sung-Min, Luisa and Sven for their help on my “Zusammenfassung”.

I would like to thank the Chinese lunch group: Hedy, Tina, Echo, Tao for the good energy-refilling and brainstorm in the lunch break of everyday.

Finally, I would like to thank my wife for her constant accompanying, my parents for their endless support and my family members for all the encouragement.